DEVELOPMENTAL FUNCTIONS OF MIR156 AND MIR157 IN *ARABIDOPSIS*

JIA HE

A DISSERTATION

in

Biology

Presented to the Faculties of the University of Pennsylvania

in

Partial Fulfillment of the Requirements for the

Degree of Doctor of Philosophy

2017

Supervisor of Dissertation

_____

Scott Poethig

John H. and *Margaret B. Fassitt* Professor

Graduate Group Chairperson

_____

Michael Lampson, Ph.D., Associate Professor of Biology

Dissertation Committee

Brian D. Gregory (Chair), Ph.D., Associate Professor of Biology

Kimberly Gallagher, Ph.D., Associate Professor of Biology

Thomas A. Jongens, Ph.D., Associate Professor of Genetics

Doris Wagner, Ph.D., Professor of Biology

ACKNOWLEDGMENT

First and foremost, I would like to thank my advisor, Professor Scott Poethig, for his guidance and influence throughout my doctoral study. He is always willing to share his insights of any research topics. He exemplifies how science is done with his knowledge, passion and dedication. When Ph.D. is a goal in my career, he doesn't push me there but shows me how to reach that goal, and more importantly, how to find the next goal in my life.

I would like to thank the current and past members of the Poethig lab for all the helpful discussions and the scientific atmosphere throughout the years.

I would also like to thank members of my committee. Dr. Brian Gregory, Dr. Kimberly Gallagher, Dr. Thomas Jongens and Dr. Doris Wagner have provided very helpful suggestions and critiques, as well as encouragement over the past few years.

Last but not the least, I would like to thank my family, especially my parents and my girlfriend, for all their love and unconditional support. They helped me develop my personality and know myself better.

ABSTRACT

DEVELOPMENTAL FUNCTIONS OF MIR156 AND MIR157 IN *ARABIDOPSIS*

Jia He

Scott Poethig

Leaves produced at different times of shoot development are often morphologically distinct. Some of these traits change gradually throughout shoot development, others change early in shoot development and are then expressed more-or-less uniformly, while still others are present at one stage of development and absent at a different stage. These latter two patterns allow the shoot to be divided into several discrete phases, the transition between which is termed "vegetative phase change"

Although it is clear that miR156, and possibly miR157, regulate many of the changes that occur during shoot development through repressing *SQUAMOSA PROMOTOR BINDING PROTEIN-LIKE* (*SPL*) transcription factors, the function of these miRNAs at specific times in development and in specific leaves is poorly understood. How these miRNAs quantitatively regulate *SPL*s is also unclear. To address these questions, we characterized the morphological and molecular phenotypes of loss-of-function mutations in MIR156 and MIR157 genes, and measured the absolute amount of miR156 and miR157 in successive leaf primordia. We also quantified the effect of varying miR156/miR157 levels on the RNA and protein abundance of their targets. Our results demonstrate that miR156 and miR157 are functionally distinct, and mediate transcript cleavage and translational repression to different degrees at different *SPL* genes. We also show that variation in the level of miR156/miR157 only has a significant effect on *SPL* gene expression when these miRNAs are present at relatively low levels. These results provide a foundation for detailed studies of the molecular mechanism of

miR156/miR157 activity, and their role in shoot morphogenesis. This knowledge also inspired us to perform a sensitized mutant screen using miR157 mutants as a genetic background. This screen identified the B3 domain transcription factor *VAL*s as regulators of miR156 during vegetative development. *val* mutations led to increased miR156 abundance as a result of elevated *pri-miR156A* and *pri-miR156C* transcript levels, accompanied by reduced H3K27me3 at the *MIR156A* and *MIR156C* loci.

TABLE OF CONTENTS

LIST OF TABLES

LIST OF FIGURES

1. Introduction

1.1 Terminology and definition of vegetative phase change

All organisms go through more or less distinct developmental stages during their lifespan. Unlike most animals, plants establish new structures, organs and increase in complexity during post-embryonic development, till they senesce and die. The post-embryonic development of higher plants involves transitions that happen at predictable times that we can divide it into three phases: juvenile vegetative phase, adult vegetative phase and reproductive phase (Poethig, 1990). The vegetative to reproductive transition (reproductive phase change) has been studied most extensively. During reproductive phase change, the vegetative shoot apical meristem (SAM) transitions to an inflorescence meristem, which goes on to develop the floral meristem responsible for producing floral structures (Huijser & Schmid, 2011). However, for a long time the developmental transitions that occur during the vegetative stage prior to the acquisition of reproductive competence and floral induction have been largely ignored.

Hildebrand (Hildebrand, 1875) and Goebel (Goebel, 1889) were the first to conceptually divide shoot development into juvenile and adult stages. Goebel noted that using various traits, such as leaf shape, the ability to produce adventitious roots, branching orientation and reproductive competence, shoot development can be divided into juvenile and adult stages. He used the term “heteroblasty” to refer to the significant morphological changes that occur in some species, and “homoblasty” to describe the more moderate changes in other plants. More recently, the term heteroblasty has acquired a broader meaning, and is now used to refer to any morphological variation along the whole shoot (Poethig, 2013; Zotz, Wilhelm, & Becker, 2011).

While the pattern of morphological and physiological traits along the shoot can be affected by many factors, some changes happen at a predictable time preceding flowering, and are irreversible in natural conditions. These changes can be used as criteria for distinguishing the juvenile vegetative state and the adult vegetative state. Leaf shape is one of the major readouts of vegetative phase change. A classic example is found in *Acacia* species native to Australia (Hildebrand, 1875) (Goebel, 1889). These species produce bipinnately compound leaves in early shoot development but later begin producing simple leaves called phyllodes. The transition between the two developmental states is often accompanied by the production of leaves of intermediate morphology, which have bipinnate leaflets and a phyllodinous portion co-existing in one leaf (Wang et al., 2011)(Figure 1.1A). In herbaceous plants such as *Arabidopsis thaliana*, leaf shape also varies throughout shoot development. Under long days (16h light: 8h dark, LD) at 22ºC, leaf 1 and 2 are round and small with a smooth margin. Starting from leaf 3, leaves become more and more elongated and have a sharper leaf base angle, with more serrated leaf margins (Figure 1.1B). Unlike in *Acacia*, these leaf shape changes are gradual and there is no clear demarcation between stages.

Besides leaf shape, there are other important species-specific leaf features that distinguish the juvenile phase from the adult phase. In maize (*Zea mays*) for example, juvenile leaves have a thin cuticle (~1µm), circular epidermal cells (in cross-section), epicuticular wax and no epidermal hairs, while adult leaves have a thick cuticle (~3 µm), rectangular epidermal cell shape, epidermal hairs and no epicuticular wax (Poethig, 1990). In *Arabidopsis*, the pattern of trichome production has been established as a reliable marker for phase change. Leaves produced early in development (juvenile leaves) have trichomes on their adaxial (upper) surface but lack trichomes on their

abaxial (lower) side; leaves produced later (adult leaves) have trichomes on both surfaces; leaves in the inflorescence (bracts) have trichomes on the abaxial side but few or no trichomes on their adaxial surface (Telfer, Bollman, & Poethig, 1997). This discovery greatly facilitated the analysis of the molecular mechanisms underlying vegetative phase change because it allowed for easy and reliable mutant screens.

Figure 1.1 Leaf shape changes through vegetative development.

A. Morphology of the first 8 leaves of A. colei. J=juvenile, T=transition, A=adult. (Wang et al., 2011)

B. Heteroblasty of *Arabidopsis* thaliana showing the leaf shape changes during its vegetative development.

1.2 Molecular mechanisms of vegetative phase change

For a long time vegetative phase change was studied mainly in woody plants because of the prolonged, stable phases and the easily assayed qualitative morphological changes (Zimmerman, Hackett, & Pharis, 1985). However the long life cycle and limited genetic tools in these species made it nearly impossible to identify the molecular mechanisms underlying vegetative phase change. The advances in maize genetics made it an excellent species for phase change studies. The discovery that *Corn grass* (*Cg*), *Teopod1* (*Tp1*), *Teopod2* (*Tp2*) and *Teopod3* (*Tp3*) are heterochronic mutations that promote juvenile phase identity provided first evidence that phase change is a genetically controlled endogenous developmental process (Poethig, 1988, 1990; Whaley & Leech, 1950). However, the nature of these genes was not clear until decades later because of the technical difficulties in cloning these genes.

The discovery that abaxial trichomes could be used as a marker for adult leaf identity in *Arabidopsis* (Telfer et al., 1997), opened the way for forward genetics screens for mutations affecting vegetative phase change in this species. *HASTY* (*hst*) was one of the first genes identified in these screens. Loss-of-function mutations of *HASTY* are precocious, showing an earlier appearance of abaxial trichomes (Telfer & Poethig, 1998). Subsequent cloning of the gene revealed that it was the *Arabidopsis* ortholog of the importin β-like nucleocytoplasmic transport receptors exportin 5 in mammals and MSN5 in yeast (Bollman et al., 2003). HASTY was subsequently demonstrated to be responsible for stabilizing miRNAs in the nucleus; the loss of HASTY resulted in decreased accumulation of many miRNAs (M. Y. Park, Wu, Gonzalez-Sulser, Vaucheret, & Poethig, 2005). Similarly, *SERRATE* (*SE*), a gene found to promote

juvenile traits, was demonstrated to be a nuclear regulator of primary miRNA processing (Clarke, Tack, Findlay, Van Montagu, & Van Lijsebettens, 1999; Grigg, Canales, Hay, & Tsiantis, 2005; Li Yang, Liu, Lu, Dong, & Huang, 2006). Genes involved in post-transcriptional gene silencing (PTGS, also known as RNAi) were also found in screens for vegetative phase change phenotypes (Morel et al., 2002; Peragine, Yoshikawa, Wu, Albrecht, & Poethig, 2004). The nature of these genes pointed to the possibility that small RNAs may play crucial roles in vegetative phase change.

The concept of small RNAs regulating developmental transitions wasn't new. miRNAs were first identified in *Caenorhabditis elegans* as regulators of the juvenile-to-adult transition. lin-4 and let-7 are temporally expressed miRNAs that increase in abundance at different larval stages to repress target genes that promote juvenile larval fate (Lee, Feinbaum, & Ambros, 1993; Pasquinelli & Ruvkun, 2002; Reinhart et al., 2000; Wightman, Ha, & Ruvkun, 1993). Several miRNAs were then found to be associated with developmental programs in *Arabidopsis* (Achard, Herr, Baulcombe, & Harberd, 2004; Aukerman & Sakai, 2003; Chen, 2004; Schwab et al., 2005). miR172, apart from its roles in flowering, was also linked to juvenile-to-adult transition in maize as it targets *Glossy15* (*Gl15*) which is required for juvenile epidermal traits (Evans, Passas, & Poethig, 1994; Lauter, Kampani, Carlson, Goebel, & Moose, 2005; Moose & Sisco, 1994).

This evidence eventually led to the discovery of miR156 as a regulator of vegetative phase change (Chuck, Cigan, Saeteurn, & Hake, 2007; Wu & Poethig, 2006). When miR156 was over-expressed under a strong constitutive promoter in *Arabidopsis*, plants exhibited severely prolonged juvenile phase, while the depletion of miR156 by target mimicry caused plants to skip their juvenile phase (Franco-Zorrilla et al., 2007; Wu et al.,

2009; Wu & Poethig, 2006). miR156 is an ancient miRNA that exists in all land plants (M. J. Axtell & Bowman, 2008). Like other plant miRNAs, the miR156 primary RNA is transcribed by RNA polymerase II, and is protected by the nuclear mRNA cap-binding complex (Gregory et al., 2008) (Z. Xie et al., 2005). The primary-miRNA is then processed into miRNA/miRNA* double strand RNAs in the nucleus by a protein complex consisting of DICER-LIKE1 (DCL1), HYPONASTIC LEAVES1 (HYL1), and SERRATE (SE) and other factors (Kurihara, Takashi, & Watanabe, 2006; W. Park, Li, Song, Messing, & Chen, 2002; Reinhart, Weinstein, Rhoades, Bartel, & Bartel, 2002; Rogers & Chen, 2013; Vazquez, Gasciolli, Crete, & Vaucheret, 2004; Z. Xie et al., 2004; Li Yang et al., 2006). The miRNA/miRNA* duplex is stabilized by HUA ENHANCER (HEN1) through methylation on its 3' ends, and is then exported from the nucleus to the cytoplasm by HASTY and other unknown factors (M. Y. Park et al., 2005; B. Yu et al., 2005). The mature guide strand of a miRNA is then separated from the passenger strand and sorted to different ARGONAUTE (AGO) proteins according to the 5' nucleotide (Shijun Mi et al., 2008). The AGO protein serves as a central component of the RNA-induced silencing complex (RISC), and is associated with HEAT SHOCK PROTEIN90 (HSP90) and cyclophilin 40 (Iki, Yoshikawa, Meshi, & Ishikawa, 2012; Smith et al., 2009). The RISC complex binds to target mRNAs through complementarity with the associated mature miRNA, and silences the target gene by either transcript cleavage or translational repression.

miR156 targets a subset of the *SQUAMOSA PROMOTER BINDING PROTEIN LIKE* (*SPL*) genes (Reinhart et al., 2002; Rhoades et al., 2002). In the first study demonstrating miR156's role in promoting juvenile identity (Wu & Poethig, 2006), *SPL3* was shown to be repressed by miR156. Over-expression of *SPL3* genomic sequences

resulted in no significant phenotype due to the efficient repression from miR156. Over-expression lines containing a mutated version of *SPL3*—where the miR156 target site sequence was modified to prevent the binding of miR156—had strong precocious phase change phenotypes. Follow-up studies further revealed a more complete regulatory pathway involving miR156 target *SPL9* and a downstream miRNA, miR172. As plants transition into the adult phase, the reduction of miR156 relieves its repression of *SPL9* and other *SPL* genes, resulting in the appearance of adult phase phenotypes that are directly related to those *SPL*s. In parallel, *SPL9* promotes the expression of miR172, which targets *AP2*-like genes such as *TOE1* and *TOE2*, leading to early flowering (Wang, Czech, & Weigel, 2009; Wu et al., 2009).

Details of the miR156-SPL module, especially the functions of each *SPL*, have been characterized recently. Of the 10 *SPL* genes that are targeted by miR156, *SPL2, SPL9*, *SPL10, SPL11, SPL13* and *SPL15* contribute to both the juvenile-to-adult transition and the vegetative-to-reproductive transition, as demonstrated by their loss-of-function mutant phenotypes (Xu, Hu, Zhao, et al., 2016). However, loss-of-function mutations in *SPL3*, *SPL4* and *SPL5* did not cause any significant phase change phenotypes. This study also raises questions about the response pattern of individual *SPL*s to miR156 changes. The temporal expression patterns of *SPL* transcripts do not always reflect miR156 reduction, which indicates that miR156 may regulate *SPL* genes through translational repression besides transcript cleavage. Interestingly, when *Arabidopsis* AGO1-RISC silencing machinery was assembled *in vitro*, *SPL13* was shown to be regulated by translational repression in addition to target cleavage (Iwakawa & Tomari).

With the discovery of miR156 as a master regulator of vegetative phase change, finding the factors responsible for the temporal expression of miR156 became a key goal. The

question of where these endogenous signals act had been worked on well before the molecular mechanisms of phase change was revealed. Wiltshire and Reid (1992) showed in *Eucalyptus tenuiramus* that the node where vegetative phase change occurs is strongly correlated with the total number of nodes produced before the transition, but not the age of the shoot. It also more highly correlated with the cumulative amount of light received by the shoot, than with day length or temperature. These results suggested that the factors regulating phase change are tightly linked to leaf number and light quantity. These investigators further ruled out roots as a source of regulatory factors by reciprocal grafting *E. tenuiramus and E. risdonii*, which have very different patterns of vegetative phase change.

An important but often overlooked study of this topic in maize provided insights into the role of the SAM and leaf primordia in vegetative phase change. Orkwiszewski and Poethig cultured maize shoot apices with adult leaf primordia and found that all of these adult leaf primordia could be at least partially rejuvenated, whereas uninitiated leaves later developed as either transitional leaves or adult leaves. The SAM, on the other hand, remained in the adult phase as the cultured plants produced same number of leaves as soil-grown plants (Orkwiszewski & Poethig, 2000). This experiment suggested that certain factors could regulate leaf identity independently of the SAM's innate time keeping mechanism.

The source of these factors was investigated by Yang and colleagues through leaf ablation experiments in *Arabidopsis*. They discovered that phase change occurred normally in plants lacking root system or cotyledons but was delayed by leaf ablation which is accompanied with an increased level of miR156 (L. Yang, Conway, & Poethig, 2011). This result implicated leaves as the source of the factors regulating phase

change. Follow-up studies revealed that sugar accelerates vegetative phase change and represses miR156 expression. In particular, it was shown that mutations in the chlorophyll synthesis gene, *ch1*, prolonged the juvenile phase and increased miR156 abundance. When supplemented with glucose or sucrose in whole seedlings or isolated leaf primordia, or to petiole stubs on defoliated seedlings, vegetative phase change was accelerated in both WT and *ch1* mutant. The repressive effect of sugar on miR156 was mitigated by mutations in *HEXOKINASE1* (*HXK1*), a regulator of glucose signaling in *Arabidopsis*. However the mutation does not affect the temporal expression pattern of miR156. These results suggested that sugar is an endogenous cue for phase change partially via *HXK1* pathway (L. Yang, Xu, Koo, He, & Poethig, 2013; S. Yu et al., 2013).

Our understanding of the regulation of miR156 was pushed forward by the recent discovery of epigenetic regulation of phase change. The temporal decrease of miR156 abundance is largely attributed to the decline of *miR156A* and *miR156C*, which is correlated with an increased amount of H3K27me3 at these loci. H3K27me3 is the product of Polycomb Repressive Complex 2 (PRC2), which was first identified in Drosophila, where it consists of four subunits, Enhancer of Zeste [E(z)], Suppressor of Zeste12 (Su(z)12), Extra sex combs (ESC), and p55. One of the three genes encoding the E(z) homologue in *Arabidopsis* – *SWINGER* (*SWN*) was found to be crucial in the epigenetic regulation of miR156. The loss of *SWN*, especially when combined with a *PICKLE* (*PKL*) loss-of-function mutation, resulted in decreased H3K27me3 at *miR156A* and *miR156C*, leading to increased miR156 abundance and prolonged vegetative phase (Xu, Hu, Smith, & Poethig, 2016). One of the unanswered questions is how PRC2 participates in the temporal regulation of *miR156A* and *miR156C*. One possibility is that a temporal change in H3K27ac at these loci antagonizes PRC2 binding. Another

possibility is that DNA-binding proteins, such as transcription factors, recruit PRC2 to these loci in a temporal manner.

1.3 Questions

Our understanding of vegetative phase change has been largely based on manipulations of miR156 abundance to extreme values. For example, over-expression of a miR156 target site mimic (MIM156) effectively reduces miR156 abundance/activity to very low levels and produces adult leaves starting at the first leaf position. However, the quantitative correlation between miR156 and phase change has not been established. This is of vital importance as it completes our view on how miR156 abundance translates to vegetative phase change phenotypes, and serves as the foundation for our quantitative understanding of the miR156-SPLs module. In Chapter 2&3 of this thesis, I will address this question and establish a quantitative framework for how miR156 and miR157, a related miRNA, regulate vegetative phase change through their targeted *SPL* genes.

Another fundamental question is how developmental timing is measured. With the discovery of miR156 as the master regulator of phase change, this question becomes more specific: how is miR156 is regulated? In Chapter 4, I will demonstrate that the B3 domain transcription factors, *VAL1* and *VAL2*, regulate the temporal expression of miR156 by promoting the deposition of H3K27me3.

Lastly, identifying new genetic variations that regulate phase change has been a challenge since mutations from various kinds of mutagenesis are getting closer to

saturation. Natural genetic variation serves as an additional resource for our study of the genetic basis of phase change. In Chapter 5, I describe the wide range of phenotypic variation in phase change among ecotypes of *Arabidopsis*, and my effort to map a QTL controlling this variation utilizing Traffic Lines.

2. Genetic analysis of miR156 and miR157

2.1 Abstract

Vegetative phase change is regulated by a decline of the related miRNAs miR156 and miR157 and the consequent increase in the expression of their targets, *SQUAMOSA PROMOTOR BINDING PROTEIN-LIKE* (*SPL*) genes. A major unanswered question is how the gradual decline in these miRNAs produces qualitative phenotypic changes during phase transitions (seedling-to-juvenile and juvenile-to-adult), which was complicated by the fact that miR156 and miR157 are encoded by multiple loci in *Arabidopsis*. To start answering this question we performed detailed analysis of a collection of miR156 and miR157 loss-of-function mutants for their effects on vegetative phase change. We then measured the detailed temporal expression patterns of these miRNAs and compared their abundances over time. These experiments revealed that *miR156A*, *miR156C*, *miR157A* and *miR157C* are the major contributors to the mature miR156/miR157 pool. miR156 and miR157 have different temporal decline rate, and are functionally different. miR156 regulates both early and late transitions of vegetative development, with a non-linear mode of action. Although miR156 is less abundant than miR157 it has a more significant impact on early vegetative morphology than miR157, which can be partially explained by miR156's higher loading efficiency onto AGO1 than miR157.

Contributions: Matthew R. Willmann from the Scott Poethig Lab and Kevin McCormick from the Blake C. Meyers Lab performed the small RNA sequencing. Tieqiang Hu generated the *miR156b* Talen mutant.

2.2 Background

During post-embryonic development, plants experience coordinated changes in leaf morphology, growth rate, branching patterns and disease resistance and eventually obtain reproductive competence. These changes take place at predicted time in vegetative development, and involve a combination of quantitative and qualitative changes that allow us to divide this process into several phases; the transition between these phases is termed vegetative phase change (Poethig, 1990) (Poethig, 2013). miR156 is the master regulator of vegetative phase change in *Arabidopsis:* over-expression of miR156 prolongs the juvenile phase while depletion of miR156 by target mimicry causes plants to skip their juvenile phase (Wu & Poethig, 2006*)* (Wu et al., 2009). miR156 has also been shown to regulate vegetative phase change in several other species (Chuck et al., 2007; Fu et al., 2012; Wang et al., 2011; K. Xie, Wu, & Xiong, 2006). miR157 differs from miR156 by 3 nucleotides and was indicated to have similar functions to miR156 in *Torenia fournieri* as the over-expression of *miR157B* resulted in a high degree of branching with small leaves (Shikata, Yamaguchi, Sasaki, & Ohtsubo, 2012). However its detailed function and expression pattern have not been well characterized. Current understanding of the temporal expression pattern of miR156 suggests that miR156 drops quickly very early in vegetative development and then declines at a slower rate (Xu, Hu, Smith, et al., 2016). However, it is still unknown how this expression pattern correlates with the qualitative and quantitative changes in leaf morphology that occur during vegetative development.

Mutant screens in *Arabidopsis* have identified a number of precocious mutants with reduced miR156 abundance. However, all of these represent mutations in general

regulators of miRNA biosynthesis/processing (Wu & Poethig, 2006*)* (Wu et al., 2009), not mutations in MIR156 or MIR157 genes. This observation suggests that the majority of mature miR156 is produced by more than one locus. The availability of T-DNA insertion mutations in MIR156 and MIR157 genes made it possible to analyze the contribution of each of these genes to the total pool of miR156/miR157, as well as the function of these genes in vegetative phase change.

2.3 Results

2.3.1 miR156 and miR157 increase as the leaf expands

In vegetative phase change studies, there has been no consensus on the type and developmental stage of the tissues used for miR156/miR157 quantification. Common types of tissues include whole seedlings from different time points, shoot apices with leaf primordia at manageable sizes from different time points, or leaf series at a given time. The importance of tissue type has been overlooked. Experiments in maize suggest that phase identity is determined after leaf initiation, and that leaf identity is specified independently of the phase identity of the shoot apical meristem (SAM) (Irish & Karlen, 1998; Orkwiszewski & Poethig, 2000). In *Arabidopsis*, it was demonstrated that phase change occurs normally in the absence of the root system and cotyledons. However, leaf ablation caused delayed phase change due to elevated miR156 (L. Yang et al., 2011). These results suggest that young leaf primordia are the most relevant tissue for studies of vegetative phase change. When whole seedlings are used, the high abundance of miR156 in the cotyledons which doesn't contribute to leaf phase identity will inevitably skew the analysis. When leaf series are collected at the same time, the age of the

leaves are different, so is the degree of leaf expansion. It is thus important to know if the miR156/miR157 level in expanded leaves can reflect its abundance in young leaf primordia. As shown in Figure 2.1, leaf primordia from the same leaf positions were harvested at different time points. Northern blotting and qRT-PCR were used to quantify the relative miR156 and miR157 levels from different samples. It is clear that miR156 and miR157 increases as leaf expands. Thus we decided to use leaf primordia ~1mm in length as the default tissue type in our analysis.

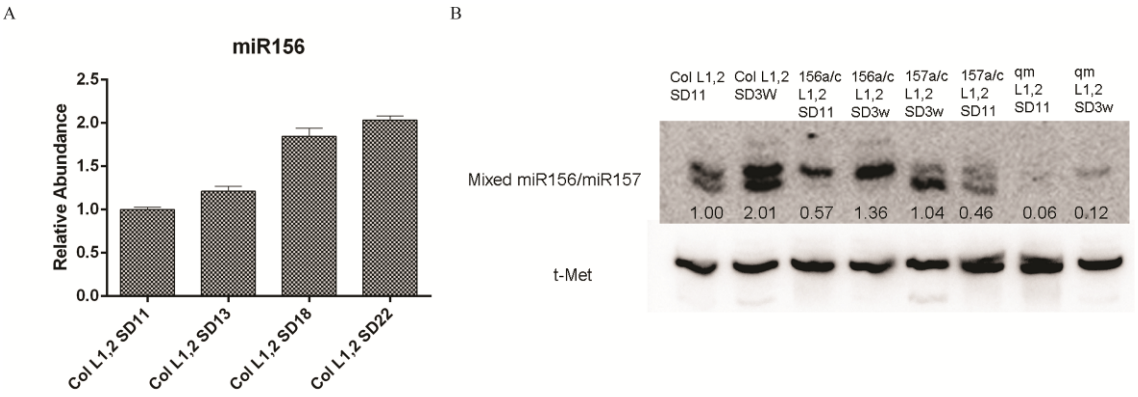

Figure 2.1 miR156/miR157 increase as leaves expand

A. qRT-PCR measurement of miR156 in Col leaf 1&2 at different time points.

B. Northern analysis of miR156 and miR157 in Col, *miR156a miR156c*, *miR157a miR157c* and *miR156a miR156c miR157a miR157c* genetic backgrounds.

2.3.2 *miR156A* and *miR156C*, *miR157A* and *miR157C* are the major contributors to the mature miR156 and miR157.

In *Arabidopsis*, miR156 is encoded by 8 genes and miR157 is encoded by 4 genes. Sequencing of small RNAs from the shoot apices of 11-day-old FRI FLC and FRI *flc-3* seedlings grown in LD revealed 6 transcripts that map to one or more of these loci. The most abundant miR156-related transcript was 20 nt in length, and maps to *MIR156A, B, C, D, E,* and *F*. A 21 nt miR156 transcript containing an additional 5' U was present at much lower levels, and maps uniquely to *MIR156D*. Transcripts derived from *MIR156G* and *MIR156H* were present at even lower levels. The most abundant miR157 transcript was 21 nt, and maps to *MIR157A*, *B*, and *C*; this transcript was about 50% more abundant than miR156. A transcript that maps uniquely to *MIR157D* was present at a very low level.

To determine the source of these transcripts, we identified T-DNA insertions in *MIR156A*, *MIR156C*, *MIR156D*, *MIR157A*, and *MIR156C*, and used site-directed mutagenesis to produce mutations in *MIR156B* in a *miR156c* background. RT-qPCR analysis of the T-DNA alleles demonstrated that they eliminate or greatly reduce the primary transcripts of the affected genes (Figure 2.2). The amount of miR156 and miR157 in these stocks was assessed by hybridizing RNA blots with probes for miR156, miR157, and a combination of both probes. Although the miR156 and miR157 probes cross-hybridize to some extent, the effect of *mir156* and *mir157* mutations on these hybridization patterns made it possible to determine the source of the signal.

We initially examined the effect of these mutations on miR156 and miR157 levels in 11-day-old seedlings grown in long days (16 hrs light: 8 hrs dark). In Col, the miR156 probe hybridized to 20 nt and 21 nt transcripts, with the 20 nt transcripts being more abundant than the 21 nt transcript. Consistent with previous results (L. Yang et al., 2013), the abundance of the 20 nt transcript was reduced by approximately 40% in both *miR156a-2* (hereafter, *mir156a*) and *miR156c-1* (hereafter, *mir156c*), and by greater than 80% in the *miR156a,c* double mutant. These genes are therefore the major source of the 20 nt miR156 transcript. By itself, *mir156d* had no obvious effect on abundance of the 20 nt or 21 nt transcript, but the effect of this mutation was apparent in *mir156a/c/d mi157a/c*, which had slightly fewer 21 nt transcripts than *miR156a/c mir157a/c*. *mir156a/b/c/d* was essentially indistinguishable from *mir156a/c.* These results demonstrate that *MIR156D* produces a 21 nt transcript that is present at low levels in 11 day-old seedlings, and that *MIR156B* makes little contribution to the pool of miR156 at this stage of development.

The miR157 probe hybridized to 21 nt and 20 nt transcripts. The 20 nt transcripts were absent in *miR156a/c*, and thus correspond to miR156. *miR157c-1* (*mir157c*) had less than 40% of the wild-type level of the 21 nt transcript. The effect *miR157a-1* (*mir157a*) on this transcript was not obvious in the single *mir157a* mutant but was apparent in *miR157a/c*, which had lower levels of this 21 nt transcript than *mir157c*. Thus, *MIR157C* is the major source of miR157 whereas *MIR157A* makes a significant but much smaller contribution.

Hybridization with a 1:1 mixture of miR156/miR157 probes revealed that 21 nt. miR156/miR157 transcripts are more abundant than 20 nt miR156 transcripts in 11 day-old seedlings. To ensure that this result was not attributable to a difference in the hybridization efficiency of the miR156 and miR157 probes, we hybridized blots with 1:3

mixture and 3:1 mixture of the mir156 and miR157 probes, and obtained the same result. The 21 nt transcripts were significantly reduced in *mir157a/c* and are therefore derived primarily from *MIR157A* and *MIR157C*. These results are consistent with the results obtained by RNA sequencing (Figure 2.2A), and demonstrate that miR157 is more abundant than miR156 in 11-day-old seedlings.

To determine if the expression pattern of these genes changes during shoot development, we examined miR156 and miR157 levels in leaf primordia (LP) 1,2 and 3,4 from plants grown in short days (SD; 10hr light: 14hr dark). RNA was isolated from primordia that were less than 1 mm in length, and analyzed by Northern blotting using mixed miR156/miR157 probes (Figure 2.2C). In Col, miR156 was less abundant than miR157 in LP1,2, and the ratio between these transcripts was even greater in LP3,4. This result suggests that miR156 declines more rapidly than miR157 during shoot development. *mir156a* and *mir156c* reduced miR156 by approximately the same amount in LP1,2, but *mir156c* had a more significant effect than *mir156a* on miR156 levels in LP3,4. This result is consistent with the observation that the primary transcript of *MIR156C* decreases more slowly than the primary transcript of *MIR156A* (Xu et al, 2016), and demonstrates that *MIR156C* makes a larger contribution to the production of miR156 in LP3,4 than *MIR156A*. *mir157c* produced a significant reduction in the level of miR157 in LP1,2 and LP3,4, and is the major source of MIR157 in these leaves. Indeed, the 21 nt band visible in *miR156c* and *mir156a,c* is attributable to *MIR156D*, not to *MIR157B*, because it is present in *mir156a/c mir157a/c* but absent in *mir156a,c,d mir157a/c*.

A

Genes	Sequence (5' to 3')																			FRI FLC (11d)	FRI flc-3 (11d)
MIR1566A,B,C,D,E,F		U	G	A	C	A	G	A	A	G	A	G	A	G	U	G	A	G	C	A	C	109,162	98,922
MIR156D	U	U	G	A	C	A	G	A	A	G	A	G	A	G	U	G	A	G	C	A	C	12,372	22,728
MIR156G		C	G	A	C	A	G	A	A	G	A	G	A	G	U	G	A	G	C	A	C	70	78
MIR156H	U	U	G	A	C	A	G	A	A	A	A	G	A	G	A	G	A	G	C	A	C	42	50
MIR157A,B,C	U	U	G	A	C	A	G	A	A	T	A	G	A	G	A	G	A	G	C	A	C	149,785	148,227
MIR157D	C	U	G	A	C	A	G	A	A	T	A	G	A	G	A	G	A	G	C	A	C	87	128

B

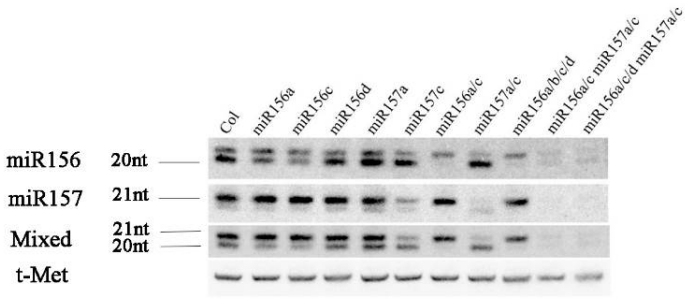

C

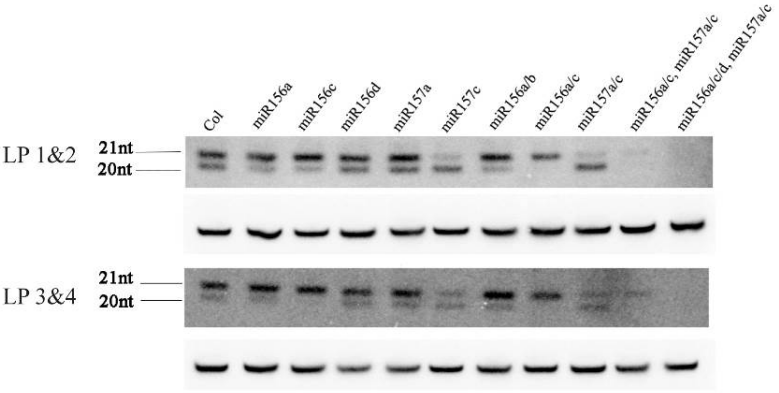

D

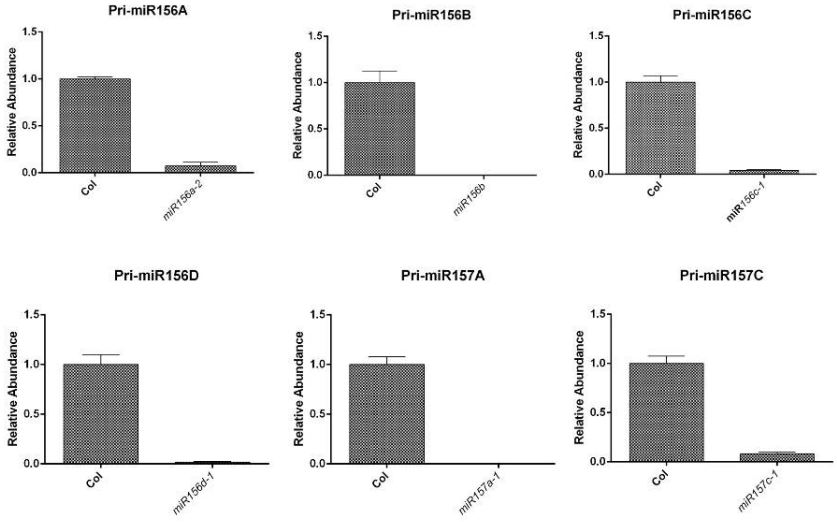

Figure 2.2 *miR156A*, *miR156C*, *miR157A* and *miR157C* contribute to the majority of mature miR156 and miR157 pool.

(A) Small RNA sequencing from the shoot apices of 11-day-old FRI FLC and FRI *flc-3* seedlings grown in LD revealed 6 transcripts that map to one or more of these loci.

(B) Northern blotting of various miR156, miR157 mutants using 11day old seedlings grown under LD 22C conditions. A single *miR156A* or *miR156C* mutation reduces the mature miR156 pool by 40%-50% and the *miR156a/miR156c* double mutant has <20% miR156 left compared to WT. A single miR157C mutation depleted most of the miR157 mature miRNA and adding the *miR157A* mutation further decreases miR157 level to <20% of the WT. In higher order mutants *miR156a/c miR157a/c* or *miR156a/c/d miR157a/c*, the remaining miR156/miR157 pool is < 10% of the WT.

(C) Northern blotting of various miR156, miR157 mutants using young leaf primordia 1&2 or 3&4 under 22C SD conditions. The blots were hybridized with 1:1 mixed miR156 and miR157 probes. The samples were harvested at similar developmental stages of the corresponding leaves (young leaf primordia <1mm in length). Similar results were obtained as in Figure 2.2B.

(D) qRT-PCR measures the primary transcript of the mutated gene compared to WT. Mutants used in the study of miR156/miR157 are null mutants or close-to-null mutants.

2.3.3 The abundance and different temporal expression patterns of miR156 and miR157

Vegetative phase change involves both rapid qualitative changes and more gradual quantitative changes in plant morphology (Telfer et al., 1997). In plants grown in SD to delay flowering, the first two rosette leaves are small and round, lack serrations and abaxial trichomes. Leaves 3 and 4 are significantly larger than leaves 1 and 2, but also have round leaf blades with no serrations and no abaxial trichomes. Leaves 5 through 9 are larger, more elongated, and more serrated than the first four leaves, but also lack abaxial trichomes. Abaxial trichome production begins at leaf 8 or 9, and is accompanied by a subtle but highly reproducible decrease in the angle of the leaf base and by the production of more prominent serrations. Transgenic plants over-expressing miR156 or a miR156 target site mimic have demonstrated that these traits are regulated by miR156 and/or miR157 (Wang et al., 2009; Wu et al., 2009), but how normal variation in the abundance of these miRNAs produce these morphological changes, is unclear.

To address this question, we first compared the abundance of miR156 and miR157 in successive leaf primordia using RT-qPCR. As shown in Figure 2.2, miR156 and miR157 decreased significantly from LP1,2 to LP3,4, and then declined more gradually. LP3,4 had 25% of the amount of miR156 present in LP1,2, whereas leaf 9 had approximately 12% of this amount. miR157 declined more slowly, and to a lesser extent. LP 3&4 had approximately 50% of the amount of miR157 present in LP1,2 and LP9 had about 25% of this amount. To measure the absolute amounts of these miRNAs, we synthesized miR156 and miR157 RNA and produced serial dilutions of these molecules in 600ng/µl E.coli RNA. RT reactions were performed on these standards and 600ng total RNA from

LP 1&2, and the abundance of miR156 and miR157 was then measured using qPCR. A standard curve was produced by plotting the concentrations of the miR156 and miR157 standards against 2^{-ct} of the corresponding PCR reaction. The 2^{-ct} value of the LP1&2 sample was then fitted to the standard curve, and the concentration of miR156 or miR157 was calculated using linear regression. We then used this information and the results of the experiment shown in Figure 2B to calculate the absolute amount of miR156 and miR157 in other leaf primordia (Figure 2C). This experiment revealed that miR156 is present in LP 1&2 at a concentration of $(2.0 \pm 0.1) \times 10^5$ copies per ng total RNA, whereas miR157 is present at a concentration of $(2.5 \pm 0.2) \times 10^5$ copies per ng total RNA (Figure 2B). miR156 subsequently declines to approximately 2.6×10^4 copies per ng total RNA in LP9, whereas miR157 declines to 6.1×10^4. These results suggest that the developmental transition that occurs between leaves 1 and 2 and leaves 3 and 4 is the result of a major decline in the level of miR156 and miR157, whereas that morphological transitions that occur later in shoot development arise from much smaller changes in the abundance these miRNAs.

To test this hypothesis and determine if miR156 and miR157 have specific functions in shoot development we characterized the phenotypes of *mir156* and *mir157* mutants. *miR156a* and *miR156c* accelerated abaxial trichome production by about 1 leaf in LD, but had little or no effect on abaxial trichome production in SD. Neither mutation had an obvious effect on leaf shape or size in either LD or SD. The *mir156a, c* double mutant had a much stronger phenotype. Under LD, these plants produced abaxial trichomes about 2 leaves earlier than Col, and in SD they produced abaxial trichomes 3 leaves earlier than Col. Furthermore, the first two leaves of this double mutant were larger and

more elongated than wild-type leaves, and resembled leaves 3 and 4 in wild-type plants. Subsequent rosette leaves were also larger and had a narrower leaf base than normal. LP1&2 of *mir156a* and *mir156c* have about 60% of the wild-type level of miR156, whereas LP1&2 of *mir156a,c* have about 20% of the wild-type level of miR156. The observation that leaves 1&2 of *mir156a* and *mir156c* are indistinguishable from wild-type leaves whereas leaves 1&2 of *mir156a,c* are morphologically similar to leaves 3&4 in wild-type plants therefore suggests that the transition between leaves 1&2 and leaves 3&4 requires an 80% decrease in the level of miR156. This conclusion is supported by the observation that wild-type LP3&4 have 20-25% of the amount of miR156 present in LP1&2, i.e., approximately the same amount as LP1&2 in *miR156a,c*.

Although miR157 is significantly more abundant than miR156 at all stages of shoot development, a reduction in the level of this miRNA had very little effect on shoot morphology. When comparing *miR156* to *miR157* mutants—especially *miR156a/c* versus *miR157a/c,* where the mature miR156 and miR157 pool is largely reduced—we noticed that *miR156a/miR156c* had much stronger precocious phenotype than *miR157a/miR157c*. *miR156a/miR156c* had earlier appearance of abaxial trichomes than *miR157a/miR157c* in both SD and LD conditions (Figure 2.3), and more importantly, showed an adult-like leaf size and shape in leaf 1&2 (Figure 2.4). When we further compared the phenotype of *miR156a/miR156c* to the quadruple mutant *miR156a/miR156c miR157a/miR157c*, we observed a dramatic enhancement of the precocious phase change phenotype. Leaf 1&2 from the quadruple mutant showed strong adult leaf characteristics such as increased size, elongated leaf shape, serrated leaf margin and abaxial trichome (Figure 2.3, Figure 2.4). These results suggest that

miR156 and miR157 both function to promote juvenile identity, while miR156 is more important than miR157 in early development. When miR156 level is low, the reduction of miR157 can lead to severe precocious phase transitions.

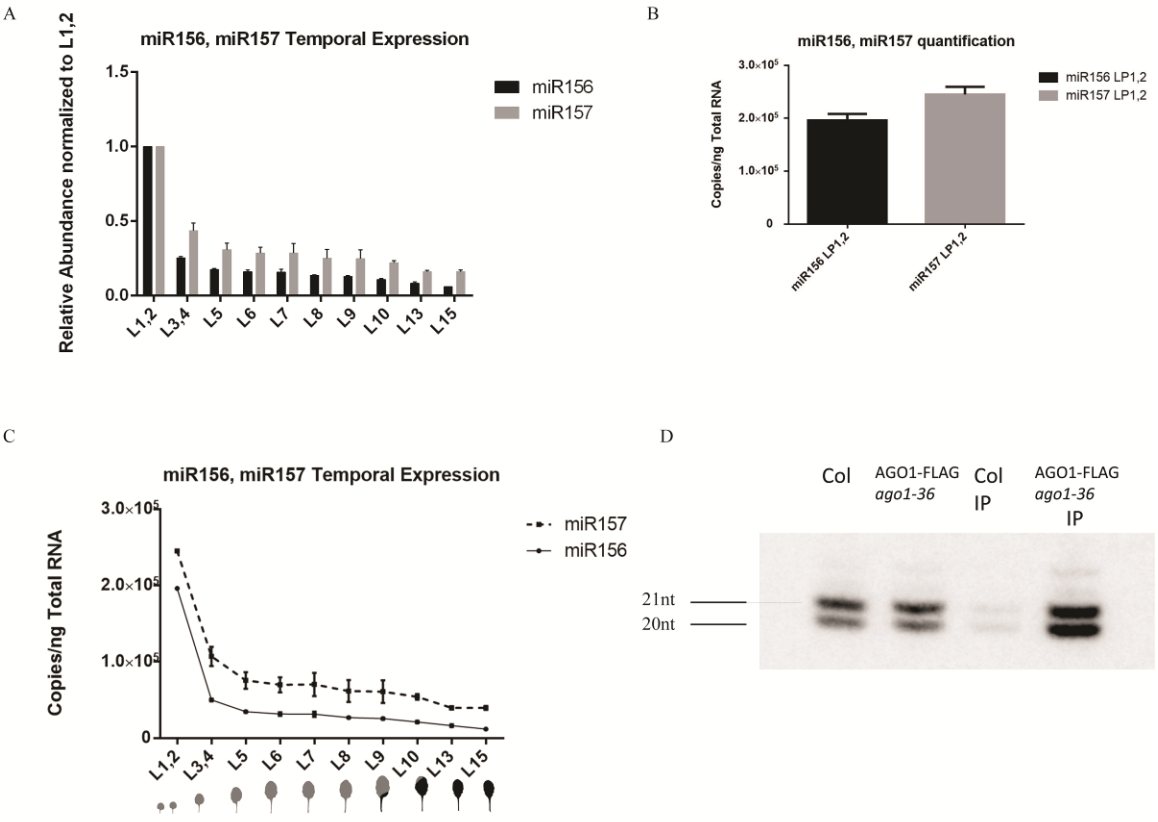

Figure 2.3 miR157 is more abundant than miR156, with a slower decline rate.

(A) Temporal expression patterns of miR156 and miR157, normalized to the levels in Col LP 1&2.

(B) Quantification of the molecule copy number of miR156 and miR157 in young leaf primordia 1&2, 22C SD condition. miR157 is ~20% more abundant than miR156.

(C) Temporal expression patterns of miR156 and miR157. miR156 and miR157 both decline with time, however, miR157 has a slower decline rate.

(D) Immunoprecipitation (IP) was performed in Col and AGO1-FLAG/ *ago1-36* using FLAG antibody. Small RNAs were extracted from both the IP and non-IP factions of Col and AGO1-FLAG/ *ago1-36*. Northern Blotting of these samples probed with mixed miR156/miR157 probes revealed that miR156 is more abundant than miR157 in AGO1-FLAG/ *ago1-36* IP fraction while miR157 is more abundant in the non-IP fraction.

	Long Day			Short Day	
	JLN	n		JLN	n
Col	5.9±0.7	9	Col	9.4±0.6	22
miR156a	4.9±0.9[a,c]	11	*miR156a*	8.3±1.0[a,d]	24
miR156c	4.9±0.6[a,c]	12	*miR156c*	9.6±0.5[b,d]	10
miR156d	6.3±0.7[b,c,d]	8	*miR156d*	9.4±1.4[b,d]	21
miR157a	5.8±0.9[b,c,d]	9	*miR157a*	9.2±0.9[b,d]	21
miR157c	5.2±0.6[a,c]	10	*miR157c*	7.7±1.3[a,c]	22
miR156a/c	4±0.6[a,d]	12	*miR156a/b*	8.7±0.8[a,c,d]	20
miR157a/c	4.8±0.6[a,c]	11	*miR156a/c*	6.4±0.7[a,d]	17
miR156a/b/c/d	4±0[a,d]	6	*miR157a/c*	7.2±0.8[a,c]	19
miR156c/d miR157a/c	3.1±0.6[a,c,d]	9	*miR156a/b/c/d/*	5.6±0.6[a,c,d]	13
miR156a/c miR157a/c	1.6±0.7[a,c,d]	14	*miR156a/c miR157c*	4.7±0.7[a,c,d]	19
miR156a/c/d miR157a/c	0.4±0.8[a,c,d]	5	*miR156a/c miR157a*	6.1±1.1[a,d]	13
			miR156c/d, miR157a/c	4.7±0.5[a,c,d]	10
			miR156a/c miR157a/c	2.2±0.7[a,c,d]	11
			miR156a/c/d miR157a/c	2.0±0.2[a,c,d]	24

a: significantly lower than Col
b: non-significant compared to Col
c: significantly different to miR156a/c
d: significantly different to miR157a/c

Table 2.1 miR156 and miR157 mutants show various degrees of phase change phenotypes in trichome production.

The table shows the t-test statistics of Juvenile leaf number defined by the latest leaf without abaxial trichomes. ± represents standard deviation.

2.3.4 Phase change phenotypes correlate with miR156 in a non-linear fashion

Vegetative phase change involves both gradual quantitative changes and rapid qualitative changes in plant morphology. How variation in the abundance of miR156 and miR157 produce this complex pattern is still unclear. To determine the relationship between the abundance of these miRNAs and organ identity, we characterized the phenotype of loss-of-function mutations in these genes. Juvenile leaves are relatively small in size, and have a round leaf blade with few or no serrations and no abaxial trichomes, whereas adult leaves are larger, and have elongated, serrated leaves with trichomes on their abaxial surface (Telfer et al., 1997). *miR156a* and *miR156c* each reduce the level of miR156 in LP 1&2 by about 40%, accelerate abaxial trichome production by about 1 leaf in LD, but have a smaller effect— if any—on abaxial trichome production in SD. Neither mutation had an obvious effect on leaf shape. When miR156A and miR156C are mutated at the same time, which represents a ~80% reduction of mature miR156 in leaf 1&2 compared to Col, we observe a strong precocious phenotype including early abaxial trichome, elongated leaf shape and early appearance or serrations on leaf margin. Interestingly, leaf 1&2 of the miR156a/miR156c double mutant start to display some characteristics of transitional leaves, resembling leaf 3&4 in Col. This correlates with the temporal expression pattern of miR156 in Col that in leaf 3&4 miR156 is reduced to 20%~25% of that in leaf 1&2.

These results suggest that miR156 regulates both early and late transitions in vegetative development, with a non-linear mode of action. In cases where miR156 is reduced significantly but not below a critical value, it has relatively little effect on vegetative development. These data also demonstrate that miR156 and miR157 are functionally

distinct, and that variation in their abundance only has phenotypic consequences when they are present at a relatively low level.

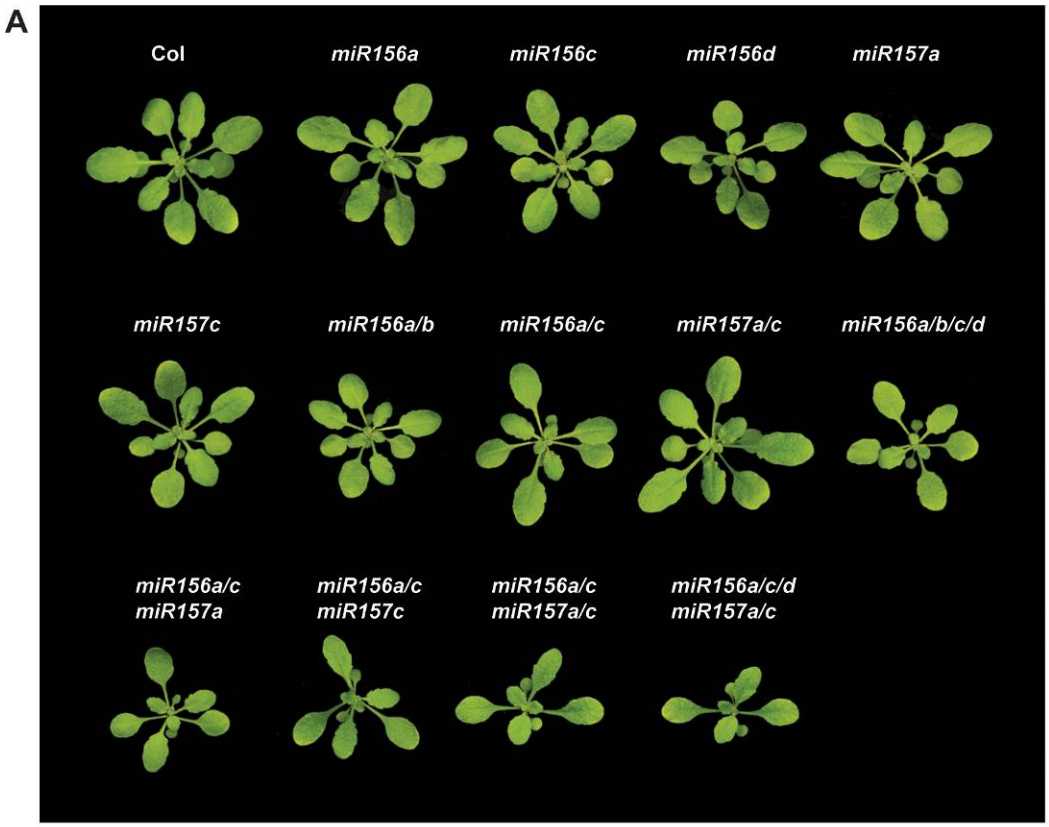
A
Col
miR156a
miR156c
miR156d
miR157a
miR157c
miR156a/b
miR156a/c
miR157a/c
miR156a/b/c/d
miR156a/c miR157a
miR156a/c miR157c
miR156a/c miR157a/c
miR156a/c/d miR157a/c

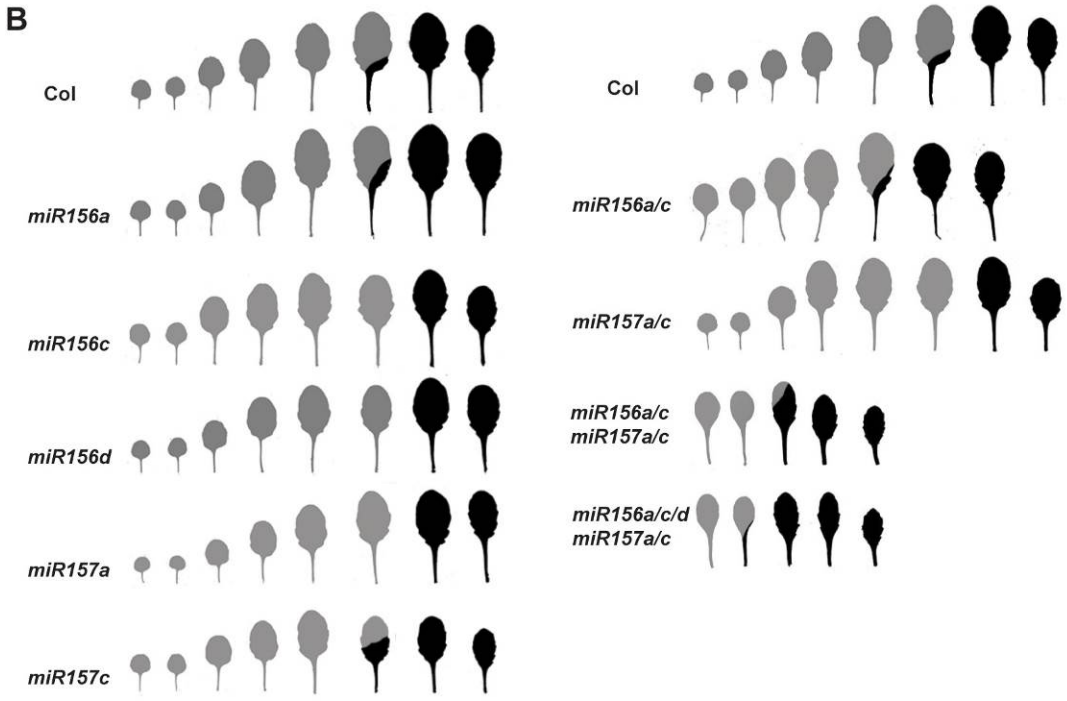
B
Col
miR156a
miR156c
miR156d
miR157a
miR157c
Col
miR156a/c
miR157a/c
miR156a/c miR157a/c
miR156a/c/d miR157a/c

Figure 2.4 Heteroblasty of miR156 and miR157 mutants grown under 22C SD conditions.

(A) An aerial view of the rosette leaves of a collection of miR156 and miR157 mutants grown under 22C SD conditions.

(B) Heteroblasty of Col in comparison to single and multiple mutants. The leaf shape phenotypes of single miR156 and miR157 mutants are very close to that of Col. m*iR156a/miR156c* shows stronger adult leaf shape phenotypes than *miR157a/miR157c*. In higher order mutants, the precocious phenotypes become much more severe.

2.3.5 miR156 and miR157 are loaded onto AGO1 with different efficiency

The above results suggested that miR156 is functionally more important than miR157 in early development, although miR157 is more abundant. Previously we showed that when miR156 is reduced, a reduction in the level of miR157 can lead to striking precocious phase transitions. However the precocious phenotype of *miR157a/miR157c* is not as strong as the phenotype of *miR156a/miR156c*, suggesting miR157 is not as important as miR156 for vegetative phase change. This raises the question of why the more abundant miRNA is less important for phase change. miRNAs with a 5' terminal uridine, as in miR156 and miR157, are predominantly loaded onto AGO1 (S. Mi et al., 2008). We therefore tested if miR156 and miR157 are loaded onto AGO1 with similar efficiency. Immunoprecipitation was performed on Col and AGO1-FLAG/ *ago1-36* using a FLAG antibody. Small RNAs were then extracted from the IP products, and also from Col and AGO1-FLAG/ *ago1-36* non-IP tissue. Northern blots of these samples probed with a mixed miR156/miR157 probe revealed that miR156 is more abundant than miR157 in AGO1-FLAG/ *ago1-36* IP fraction while miR157 is more abundant in the non-

IP fraction (Figure 2.3D). This result indicates that although miR157 is more abundant in whole tissue, there is more miR156 loaded onto AGO1.

2.3.6 The function of miR156 and miR157 in the endogenous flowering pathway

After the quick decline in abundance during early vegetative development, miR156 and miR157 are present at a lower but significant level throughout development. However their functions in late development have not been determined. Since miR156 regulated *SPL* genes have been reported to promote flowering under non-photoinductive conditions (Hyun et al., 2016; Wang et al., 2009; Xu, Hu, Zhao, et al., 2016), we are curious to explore the role of miR156 and miR157 in this process. We measured the flowering time phenotypes of our collection of miR156 and miR157 mutants under SD conditions. Surprisingly, as shown in Figure 2.5, miR156 and miR157 mutations have very small impact on flowering time under SD conditions. Even in *miR156a/c miR157a/c* we observed similar flowering time, as measured by visible flower buds formation, to Col and other miR156 or miR157 mutations. This is strikingly different to the effects of those mutations on vegetative phase change traits such as abaxial trichome production or leaf shape.

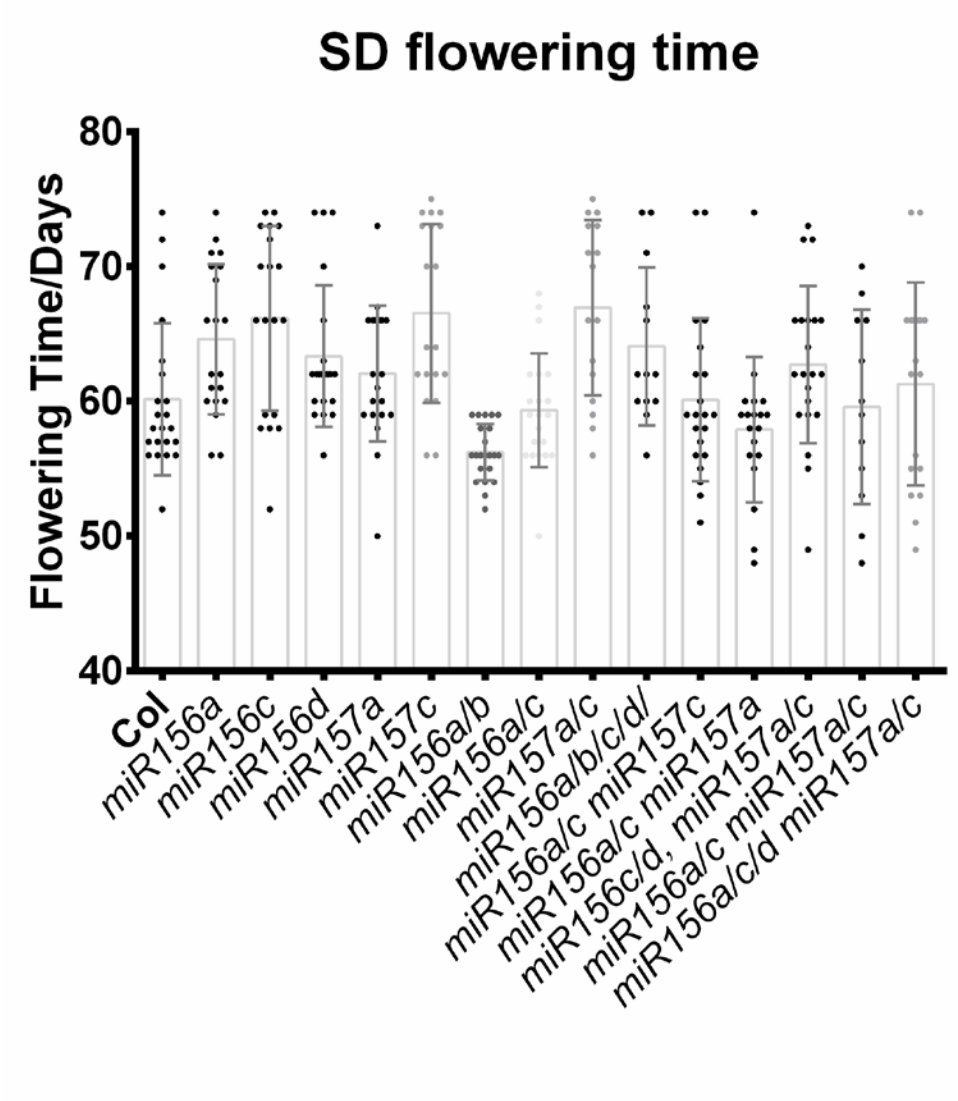

Figure 2.5 Flowering time of miR156 and miR157 mutants compared to Col under SD 22C conditions.

In miR156 and miR157 mutants including higher order mutants, there was no dramatic changes in flowering time. Each dot represents a single data point. Error bar showing standard deviation.

2.4 Discussion

2.4.1 miR156 and miR157 levels increase as leaves expand

The observation that miR156 and miR157 increase with leaf expansion demonstrates the importance of selecting developmentally matched samples in studies of vegetative phase change. The identity of the leaves are determined after leaf initiation, as demonstrated in maize that juvenile and adult regions of maize transitional leaves did not become clonally distinct until after the primordium is 700 µm in length (Orkwiszewski & Poethig, 2000). To better reflect the actual physiology and molecular network in the critical developmental stage of leaf identity determination, we tried to collect leaf primordia at the smallest size manageable, which is ~ 1mm in length. In this way we are comparing leaf primordia of different leaves at their same developmental stages (which also represents different time points along the whole shoot development).

We also measured miR156 and mR157 in expanded leaf series harvested at the same time. Their relative abundances do show a decline pattern similar in leaf primordia (Figure 2.6). In cases where harvesting leaf primordia is technically difficult, using expanded leaves to compare the relative abundance of these miRNAs from different genetic backgrounds could also provide valuable information.

miR156 and miR157's expression pattern with leaf expansion also poses a question to the function of these miRNAs in expanded leaves. miR156 has been reported to respond to various stresses in a number of species (Cui, Shan, Shi, Gao, & Lin, 2014; Hsieh et al., 2009; Zhao, Jiang, Zhang, & Su, 2012). It is possible that miR156 and miR157 serve multiple roles in expanded leaves that require a higher abundance of these molecules.

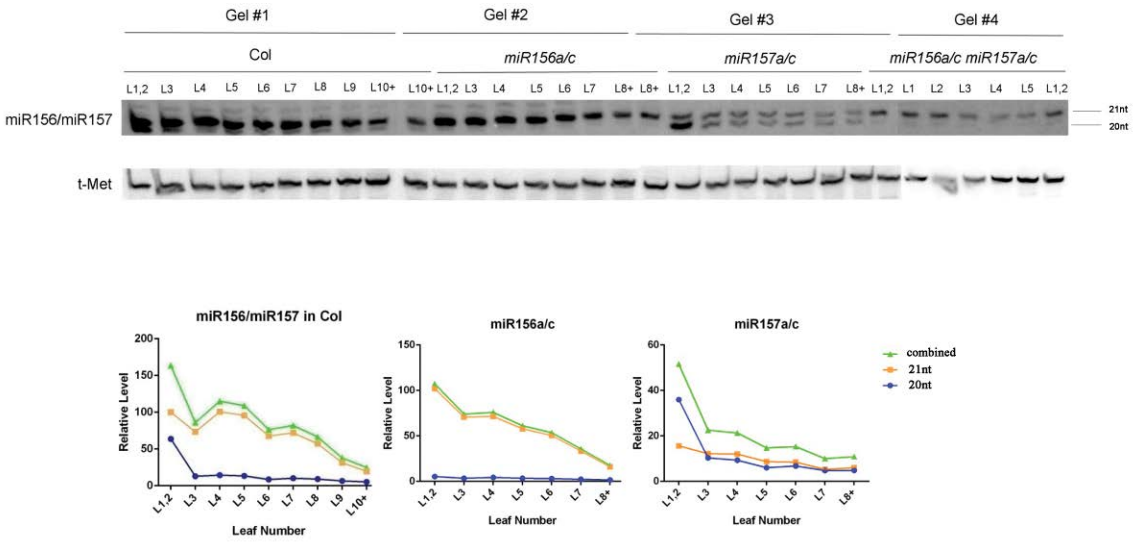

Figure 2.6 Northern blots show the expression patterns of miR156 and miR157 in expanded leaf series.

Northern blots measuring miR156 and miR157 in Col, *miR156a/miR156c*, *miR157a/miR157c* and *miR156a/miR156c miR157a/miR157c* expanded leaf series using 1:1 mixed probes.

2.4.2 miR156/miR157 mutants lines as sensitized genetic background for mutant screening

As illustrated by the subtle or insignificant phenotypes of *miR156a* or *miR156c* single mutants, mutations that result in moderate changes in miR156 abundance/activity are rarely noticeable from mutant screening. In fact, mutant screens for aberrant phase change timing yielded a large number of mutations involved in miRNA biogenesis/processing pathways or general miRNA activity. In order to uncover regulators or cis regulatory elements of miR156, a sensitized genetic background is required. *miR157a/miR157c* is suitable for this purpose. *miR157a/ miR157c* by itself has mild phase change phenotypes in terms of abaxial trichome production and leaf shape. When miR156 level is reduced ~50% in this background, as in *miR156a/ miR157a/miR157c* or *miR156c/ miR157a/miR157c* triple mutants, we can observe prominent precocious phenotypes from leaf shape, without even counting trichome.

An EMS mutagenesis was performed using *miR157a/miR157c* as the genetic background. Roughly 10,000 *miR157a/miR157c* seeds were mutagenized by EMS and grew under standard conditions. Selfed seeds from approximately every 150 M1 plants were harvested in bulk. M2 seeds were planted and screened for precocious or late phase change phenotypes. Mutants of interest were then harvested individually. To determine whether miR156 was specifically affected in those mutants, qPCR were performed to quantify the fold change of miR156 and other miRNAs (miR159, miR166 or miR167). According to the miRNA level pattern, mutants could be sorted into four categories. 1) miRNA level in general is not changed. 2) miR156 and other miRNAs are reduced. 3) miR156 and other miRNAs are elevated. 4) miR156 is reduced while other

miRNAs remain unchanged. More details of the mutant screen will be discussed in Chapter 6 Future directions.

2.4.3 Function of miR156 and miR157 in reproductive competence

miR156 regulated *SPL* genes have been reported to promote flowering under non-photoinductive conditions (Hyun et al., 2016; Wang et al., 2009; Xu, Hu, Zhao, et al., 2016). These results are related to a long-standing question in shoot maturation, concerning the relationship between vegetative phase change and reproductive competence and whether they are regulated by the same mechanisms. The Poethig lab have argued that these developmental transitions are regulated independently (Poethig, 1990). The phenotypes of plants overexpressing miR156 or miR156 target mimicry provided strong evidence for this argument. In Col, when miR156 is overexpressed, vegetative phase change is strongly delayed but the flowering time is only slightly delayed. On the other hand, when miR156 is depleted by the overexpression of miR156 target mimicry, vegetative phase change is dramatically accelerated while flowering time is only slightly affected. Our analysis of the flowering time of miR156 and miR157 mutations under SD conditions also showed that flowering time is hardly affected by the reduction of these miRNAs. These results suggested that other inputs on *SPL* genes, such as photoperiod, have strong regulatory roles when miR156 and miR157 are relatively low in abundance.

One thing to note about these results is that Col is an ecotype with a non-functional allele of *FRIGIDA* (*FRI*) which results in low levels of *FLOWERING LOCUS C* (*FLC*) that allows for early flowering under inductive conditions. To have a more complete view of

how miR156 and miR157 affect flowering, it will also be important to carry out the analysis in a genetic background with functional FRI and FLC.

Reproductive competence could be practically defined as the ability of plants to respond to flowering inducing cues. One way to measure reproductive competence is to assay flowering time in response to photoperiod changes. Mutants and WT seeds can be germinated and grown under SD conditions, and then transferred to LD conditions at different time points, exposed to the photo-inductive environment for a fixed period of time and then returned to SD. Flowering time of each genotype will then be measured. Preliminary data from my colleague Jainfei Zhao using our existing miR156 and miR157 mutations to measure reproductive competence supports the argument that reproductive competence is also regulated by miR156-independent pathway(s).

3. The quantitative relationship between miR156/miR157 and *SPL*s

3.1 Abstract

Vegetative development in plants can be divided into several discrete phases based on coordinated morphological and physiological changes that occur at predictable times in shoot growth. The transition between these phases is termed vegetative phase change. Vegetative phase change is regulated by a decline in the related miRNAs miR156 and miR157 and the consequent increase in the expression of their targets, *SQUAMOSA PROMOTOR BINDING PROTEIN-LIKE* (*SPL*) genes. A major unanswered question is how the gradual decline in these miRNAs produces the qualitative phenotypic changes that occur during phase transitions (seedling-to-juvenile and juvenile-to-adult). To answer this question we characterized the effects of miR156 and miR157 reduction on *SPL* transcript abundance and discovered a wide range of responses from different *SPL* transcripts. Quantitative analysis of the effect of miR156 on the RNA and protein levels of *SPL9* and *SPL13* indicates that miR156 regulates *SPL13* mainly by promoting its translational repression, but regulates *SPL9* via both transcript cleavage and translational repression. Variation in the abundance of miR156/miR157 has no effect on the expression of *SPL9* and *SPL13* when these miRNAs are present at high levels, but has a major effect on the expression of these genes when the level of miR156/miR157 is relatively low. The non-linear response of *SPL* gene expression to variation in the abundance of miR156/miR157 provides a molecular mechanism for the rapid, qualitative changes in shoot morphology that occur during vegetative phase change.

Contributions: Mingli Xu performed *in situ* hybridization of *SPL*s in Col and *miR156a/miR156c miR157a/miR157c* quadruple mutant background. Li Yang constructed the original Indmim156 line.

3.2 Background

Vegetative phase change is regulated by the temporal reduction of miR156 and the related miRNA miR157, and the consequent increase of *SPL* gene expression. 10 members of the *SPL* gene family in *Arabidopsis* are targeted by miR156/miR157 (Reinhart et al., 2002; Rhoades et al., 2002). These genes are grouped into 5 clades based on the amino acid sequence of their DNA binding domain (Riese, Hohmann, Saedler, Munster, & Huijser, 2007; K. Xie et al., 2006). The function of these and related *SPL* genes have been investigated using different approaches in different species. The most common approach has been to analyze the phenotype of lines over-expressing these genes (Stief et al., 2014; Usami, Horiguchi, Yano, & Tsukaya, 2009; Wang et al., 2009; Wu et al., 2009; Wu & Poethig, 2006; Yamaguchi et al., 2009). While this approach provides evidence that different *SPL*s are involved in various aspects of phase change, flowering time or root development, these over-expression phenotypes may have little to do with the normal function of these genes. A recent detailed loss-of-function analysis of miR156-targeted *SPL*s demonstrated that *SPL2*, *SPL9*, *SPL10*, *SPL11*, *SPL13* and *SPL15* contribute to both vegetative phase change and the vegetative to reproduction transition, while *SPL3*, *SPL4*, *SPL5* do not play major roles in vegetative phase change (Xu, Hu, Zhao, et al., 2016). It also showed that in *Arabidopsis*, miR156 declines dramatically early in vegetative development, and then decreases at a much slower rate. During this period, the transcript levels of some of its targets increase significantly, whereas other target transcripts change very little (Xu, Hu, Smith, & Poethig, 2016). This variation suggests that these targets either have different degrees of sensitivity to miR156, or that miR156 regulates different genes by different

mechanisms. The contrast between the expression pattern of miR156/miR157 and the expression patterns of their targets also raises the question of how graded variation in miR156/miR157 leads to discrete changes in cell fate and organ identity. With our collection of miR156 and miR157 mutations, it is possible to obtain a quantitative view of how different SPLs respond to fluctuations of miR156 and miR157 and provide insights into this fundamental question in vegetative phase change.

3.3 Results

3.3.1 *SPL*s transcripts levels are differentially responsive to the reduction of miR156/miR157

SPL genes are targets of miR156/miR157 and are important in the juvenile-to-adult transition as well as in the vegetative-to-reproductive transition (Gandikota et al., 2007; Wang et al., 2009; Wu et al., 2009; Wu & Poethig, 2006). Specifically, *SPL2*, *SPL9*, *SPL10*, *SPL11*, *SPL13* and *SPL15* contribute to both vegetative phase change and the vegetative to reproduction transition while *SPL3*, *SPL4*, *SPL5* do not play major roles in vegetative phase change (Xu, Hu, Zhao, et al., 2016). Understanding the spatiotemporal expression patterns of these *SPL*s and how they respond to miR156/miR157 will provide insights into how variation in the level of these miRNAs produces the morphological patterns associated with vegetative phase change.

In situ hybridization was performed on 3-week-old Col and *miR156a/miR156c miR157a/miR157c* shoot apices (Figure 3.1). Slides were incubated for the same amount of time to enable comparisons between the expression levels of different *SPL*

genes. *SPL3*, *SPL9*, *SPL13* and *SPL15* transcripts were uniformly expressed in the shoot apical meristem and leaf primordia of wild-type plants, and were slightly, but consistently, elevated in the shoot apices of quadruple mutants. *SPL2*, *SPL10* and *SPL11* transcripts were undetectable in wild-type, but were present at high levels in the shoot apical meristem and leaf primordia of the quadruple mutant. *SPL4*, *SPL5* and *SPL6* transcripts were undetectable in both wild-type and in quadruple mutant plants. *SPL3*, *SPL9*, *SPL13* and *SPL15* transcripts are thus more abundant in the vegetative shoot apex than other *SPL* transcripts, and are relatively insensitive to variation in the amount of miR156/miR157. The low expression of *SPL2*, *SPL10* and *SPL11* is attributable to the sensitivity of these transcripts to degradation by miR156/miR157 because all three transcripts were undetectable in wild-type plants but accumulated to high levels in plants lacking *miR156A*, *miR156C*, *miR157A* and *miR157C*. On the other hand, our inability to detect *SPL4*, *SPL5* and *SPL6* in wild type shoot apices is attributable to their low rate of transcription because these transcripts were undetectable even in this quadruple mutant.

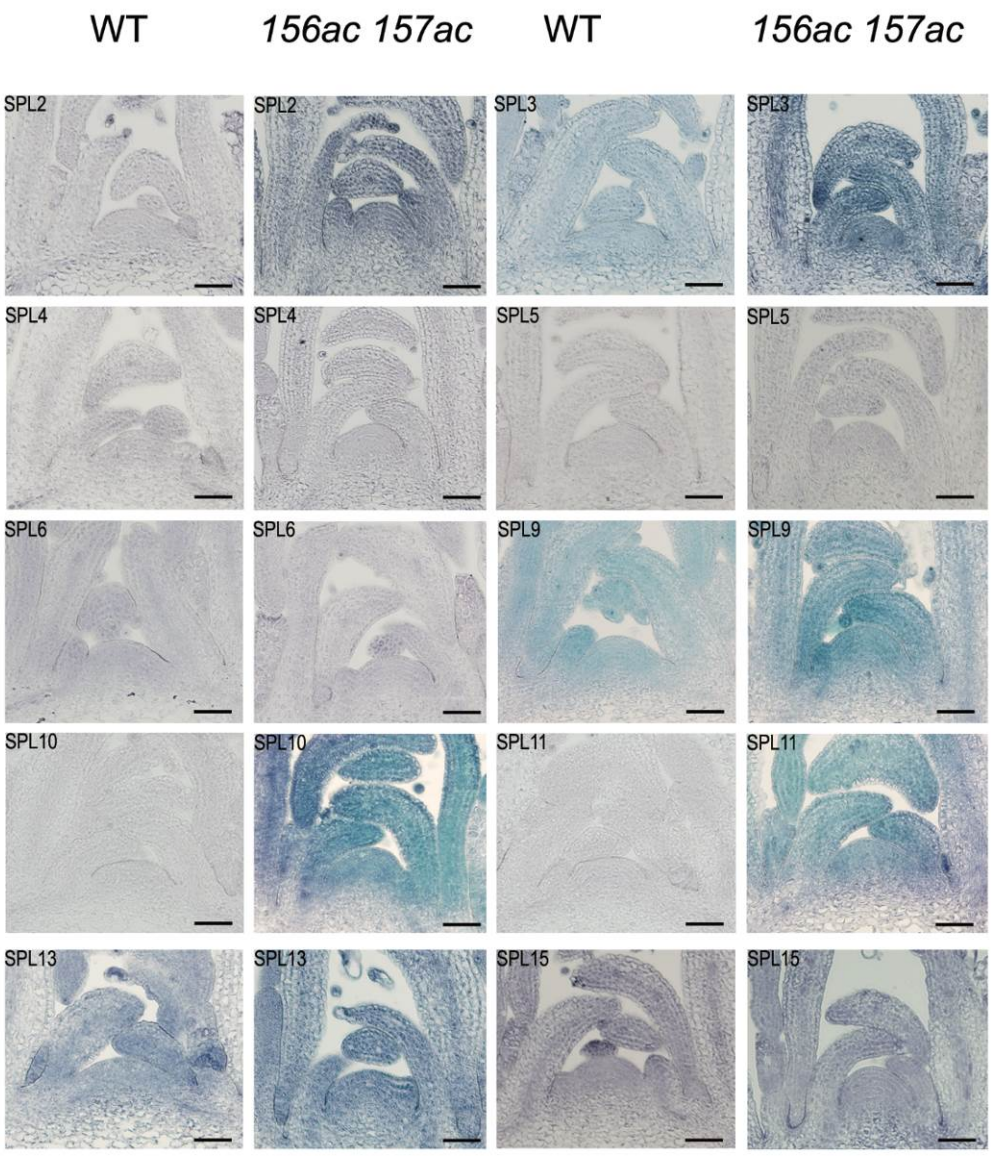

Figure 3.1 *In situ* hybridization of *SPL*s in Col and *miR156a/miR156c miR157a/miR157c* background.

In Col, *SPL3*, *SPL6*, *SPL9*, *SPL13* and *SPL15* transcripts are present in the shoot apices and young leaf primordia while other SPL transcripts levels are low or undetectable. In the *miR156a/miR156c miR157a/miR157c* quadruple mutant, increased staining patterns, though not to the same degree, are observed. *SPL10* and *SPL11* transcripts, though not detectable in Col, become highly visible in the *miR156a/miR156c miR157a/miR157c* quadruple mutant.

A previous study showed that the decline in miR156 is not associated with a major increase in most *SPL* transcripts in shoot apices, suggesting that translational repression may be an important component of miR156 function (Xu, Hu, Zhao, et al., 2016). To obtain a more quantitative picture of how *SPL* transcripts respond to miR156/miR157, qRT-PCR was performed on the primordia of leaves 1&2 and leaves 3&4 in Col, *miR156c*, *miR157c*, *miR156a/miR156c*, *miR157a/miR157c*, *miR156a/miR156c miR157a/miR157c*, *miR156a/miR156c/miR156d miR157a/miR157c* genotypes grown under 22ºC SD conditions (Figure 3.2). Consistent with the evidence that SPL transcripts do not increase dramatically in association with the decrease in miR156 during shoot development (Xu, Hu, Zhao, et al., 2016), we did not observe large changes in the transcripts of most *SPL* genes in the single *miR156c* and *miR157c* mutants (Figure 3.2). *SPL* genes responded differentially to further reductions in miR156/mir157 however. *SPL3* transcripts were particularly responsive to miR156, increasing about 4-fold in *mir156c,* and 5-to-6-fold in *mir156a/c.* By themselves, *miR157c* and *miR157a* did not have a dramatic effect on the abundance of *SPL3*, but the *mir156a/c mir157a/c* and *mir156a/c/d mir157a/c* mutants displayed a 10-to-20-fold increase in *SPL3*, depending on the leaf type. *SPL9* and *SPL15* transcripts increased very slightly in *miR156a/c* and *miR157a/c*, but increased up to 6-fold in *miR156a/c miR157a/c* quadruple and *miR156a/c/d miR157a/c* pentuple mutants. *SPL2*, *SPL10* and *SPL11* transcripts were relatively insensitive to a reduction in miR156/mir157, increasing only 2-fold or less in *mir156a/c* and *mir157a/c*, and about 3-fold in the quadruple and pentuple mutants. *SPL13* was the least responsive *SPL* transcript. *SPL13* transcript levels were approximately 1.8-fold higher than wild-type in *mir156a/c*, and were not significantly different in this genotype and the quadruple and pentuple mutants, implying that miR157 has no effect on the stability of this transcript. The expression of *SPL3*,

SPL4 and *SPL5* is regulated directly by miR156/miR157, and indirectly via the effect of SPL genes on the expression of miR172, which represses a group of *AP2-like* genes that regulate the transcription *SPL3*, *SPL4* and *SPL5* (Gandikota et al., 2007; Jung, Seo, Kang, & Park, 2011; Wu et al., 2009; Wu & Poethig, 2006). Consequently, the effect of variation in miR156/miR157 on *SPL3* transcripts is not necessarily attributable to miR156/miR157-induced transcript cleavage. However, the only way that miR156/miR157 are known to regulate the expression of other SPL genes is through a direct interaction with these transcripts. These findings therefore suggest that *SPL2*, *SPL9*, *SPL10*, *SPL11*, *SPL13* and *SPL15* are differentially sensitive to miR156/miR157-induced transcript cleavage. If we compare the SPL transcript levels in *miR156a/miR156c* vs in *miR157a/miR157c*, we can see that *SPL9*, *SPL10*, *SPL11* are more sensitive to miR156 reduction than miR157, which could contribute to the stronger precocious phenotypes of *miR156a/miR156c* compared to *miR157a/miR157c*. These findings suggest that different *SPL*s have various degree of sensitivity to miR156/miR157 in terms of transcript cleavage.

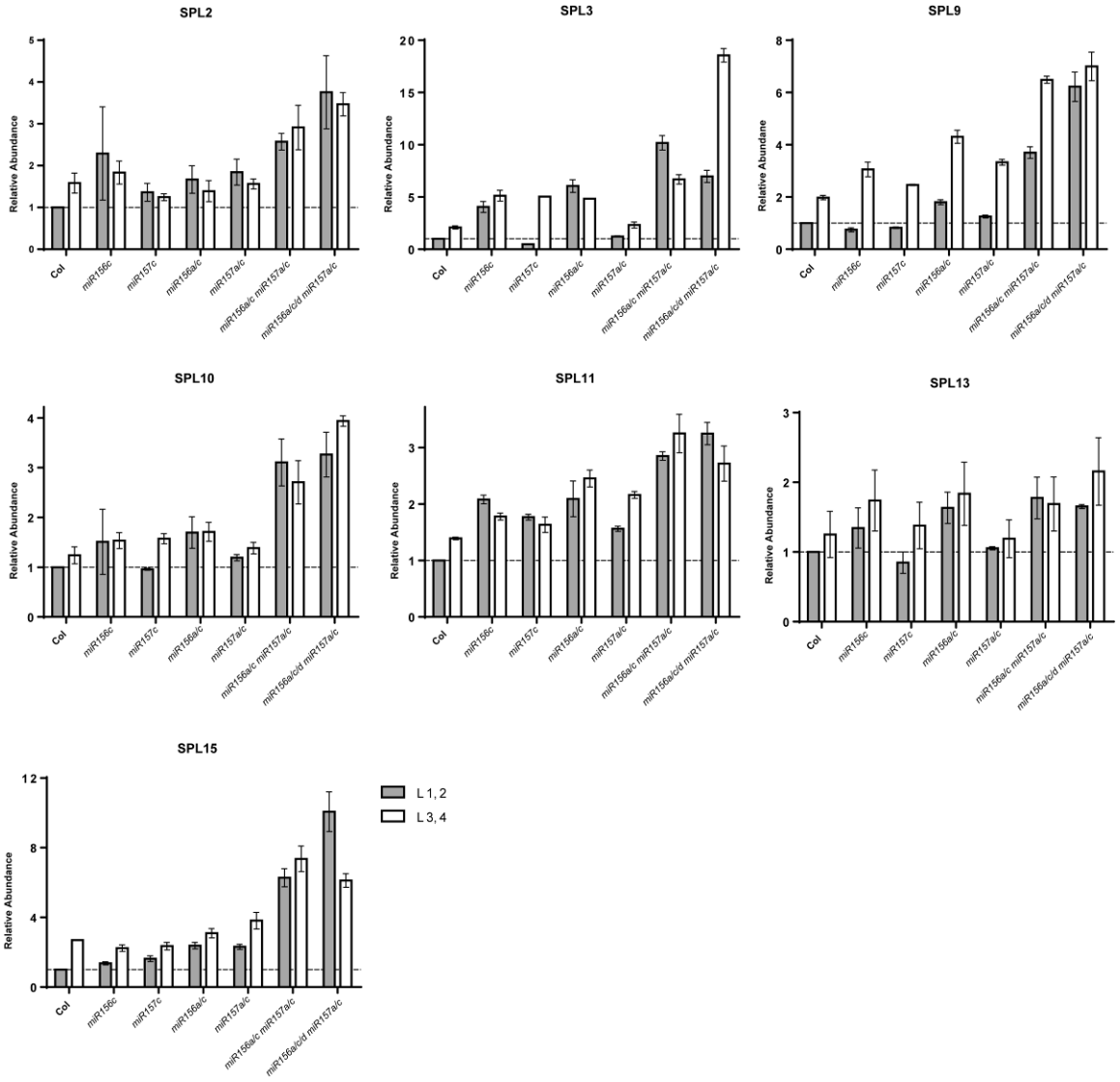

Figure 3.2 Different *SPL*s have various degree of sensitivity to reduction of miR156/miR157 at transcript level.

Young leaf primordia ~1mm in length were used in this analysis. Error bar showing ± standard deviation from 3 biological replicates.

3.3.2 *SPL9* and *SPL13* play important roles in promoting adult traits

The observation that *SPL* transcripts show different sensitivities to miR156/miR157 raises the question of whether this reflects their function in vegetative phase change. For example, *SPL13* is relatively insensitive to miR156/miR157 at the transcript level, but this does not necessarily mean that it is unimportant for vegetative phase change. To address this question, we asked whether *SPL13* and *SPL9* are required for the precocious phenotype of plants mutant for miR156 and miR157. For this purpose, the phenotype of the pentuple mutant *miR156a/miR156c miR157a/miR157c spl13-2* was compared to the phenotype of the quadruple mutant *miR156a/miR156c miR157a/miR157c*. We found that the loss of *SPL13* partially corrected the strong precocious phenotype of *miR156a/miR156c miR157a/miR157c* (Figure 3.3A). This result suggests that miR156 and miR157 regulate vegetative phase change in part through their effect on *SPL13*. We also introduced *spl9-4* into *miR156a/miR156c* and compared this triple mutant to *miR156a/miR156c*. As expected, the loss of *SPL9* rescued the precocious phenotype of *miR156a/miR156c*, resulting in rounded leaf 1&2, and delayed abaxial trichome production (Figure 3.3B). Taken together, these observations suggest that *SPL9* and *SPL13* both play important roles in promoting adult leaf identity, although their transcripts respond quite differently to variation in miR156/miR57.

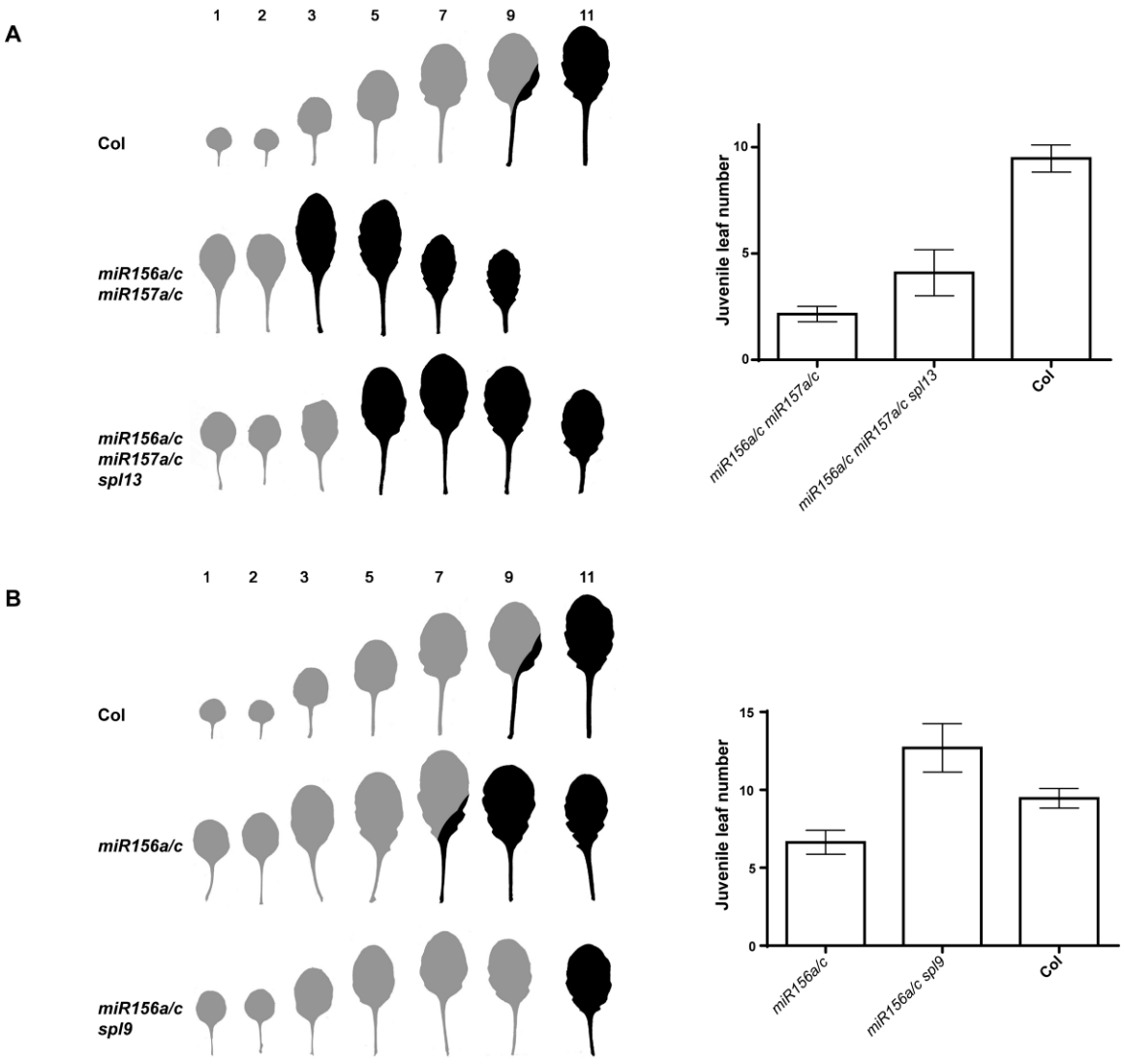

Figure 3.3 *SPL9* and *SPL13* are functionally important in promoting adult leaf traits.

(A) Heteroblasty and abaxial trichome phenotype demonstrate that the loss of *SPL13* can partially rescue the precocious phenotype of the *miR156a/miR156c miR157a/miR157c* quadruple mutant.

(B) Heteroblasty and abaxial trichome phenotype demonstrate that the loss of *SPL9* can rescue the precocious phenotype of the *miR156a/miR156c*.

Error bar showing ± standard deviation.

3.3.3 *SPL9* and *SPL13* are regulated by miR156/miR157 through different mechanisms

The observations that 1) *SPL13* transcript abundance shows small changes when miR156/miR157 change dramatically and 2) *SPL13* is essential for the strong adult phenotype of miR156/157 mutants suggest that translational repression is an important regulatory mechanism for phase change. To test this hypothesis, we decided to first measure the temporal pattern of *SPL13* transcripts and protein levels during vegetative development. With no antibody against SPL13 available, we used SPL13-GUS reporters to approximate SPL13 protein *in vivo*. The SPL13-GUS reporter has been described before, and is a translational fusion of GUS and SPL13 under the endogenous *SPL13* promoter (Xu, Hu, Zhao, et al., 2016). Young leaf primordia (LP), <1mm in length, were harvested at different time points during development. SPL13-GUS mRNA levels were measured by qRT-PCR and SPL13-GUS protein levels were measured as GUS activity by the MUG assay. Although the transcript level of SPL13-GUS showed very small changes from LP1&2 to LP7&8, there was dramatic increase in SPL13-GUS protein level as reflected by the MUG assay (Figure 3.4A). Similar measurements were made for an rSPL13-GUS reporter, which cannot be regulated by miR156 because it has a mutated target site. There was no significant change in both SPL13-GUS mRNA and protein between LP1&2 and LP3&4 (Figure 3.4B). Interestingly, we observed a two-fold increase of SPL13-GUS protein between LP3&4 and LP7&8, although miR156 declined by only 20% during this period. This non-linear response provides an explanation for why gradual changes in miR156 lead to qualitative changes in leaf identity.

To further test the hypothesis that *SPL13* is regulated by miR156 through translational repression, we took advantage of an estrogen-inducible miR156 mimicry line (IndMIM156), in which miR156 activity can be down-regulated by exogenous application of β-estrodiol. The SPL13-GUS transgene was crossed to IndMIM156 and these transgenes were then made homozygous. Young leaf primordia from mock-treated and β-estrodiol-treated plants were harvested and analyzed by qRT-PCR and the MUG assay. As shown in Figure 3.4C, down-regulation of miR156 by ~50%, produced a small increase in SPL13-GUS mRNA and a dramatic increase in SPL13-GUS protein. This again demonstrates that *SPL13* is repressed at a translational level, and that it responds non-linearly to changes in miR156. We were concerned about the ability of qRT-PCR to accurately measure the effective concentration of miR156 in this transgenic line. Because the SPL3 transcript level is highly correlated with the level of miR156, we used SPL3 expression as another measure of miR156 down-regulation. SPL3 transcripts increased over 4-fold in the induced plants, which is close to the increase in SPL3 transcripts in the *miR156c* mutant, which has ~50% of the wild-type level of miR156. Consequently, we believe the qRT-PCR measurement of miR156 in the IndMIM156 line is accurate.

Taken together, we conclude that *SPL13* is repressed by miR156 through translational repression. From LP 1&2 to LP 3&4, this translational repression is relieved, producing a dramatic increase in SPL13 protein but not its transcript; in later leaf primordia, a small reduction in the level of miR156 also produces a non-linear increase in the level of SPL13, although this increase is not as great as the one that occurs between LP1&2 and LP3&4.

As shown in Figure 3.2, the *SPL9* transcript is moderately sensitive to miR156/miR157 down-regulation. We were interested to see if transcript cleavage is the only way in which miR156/miR157 regulate *SPL9*. An SPL9-GUS reporter was introduced into the *miR156a/miR156c miR157a/miR157c* quadruple mutant background, this line was crossed to Col, and the resulting progeny were selfed to obtain stocks containing the SPL9-GUS reporter in wild-type, *miR156a/miR156c*, *miR157a/miR157c* and *miR156a/miR156c miR157a/miR157c* backgrounds. MUG assays and qRT-PCR measurements were performed on LP1&2 from SD-grown plants. We observed an over 2 -fold increase in SPL9-GUS transcript abundance in the *miR156a/miR156c* background, and an over 4-fold increase in the *miR156a/miR156c miR157a/miR157c* quadruple mutant background, when compared to WT (Figure 3.4D). The SPL9-GUS protein level increased even more dramatically, displaying a ~ 5 fold increase in *miR156a/miR156c* and ~36 fold increase in *miR56a/c miR157a/miR157c* (Figure 3.4D). This result suggests that *SPL9* is translationally repressed by miR156/miR157.

One way to characterize a miRNA's mode of action is to measure the ratio of un-cleaved/cleaved target transcripts in backgrounds with varying levels of the corresponding miRNA (J. Li, Reichel, & Millar, 2014). We used a modified 5' RNA Ligase Mediated Rapid Amplification of cDNA Ends (5' RLM-RACE) to quantify the un-cleaved/cleaved transcript ratio for *SPL9* and *SPL13* in Col, *miR156a/miR156c*, *miR157a/miR157c* and *miR156a/miR156c/miR157a/miR157c* genotypes. LP 1&2 from each genotype were harvested for total RNA extraction. Equal amounts of total RNA from each sample were then ligated to a 5'-end RNA adaptor. Purified RNA ligation products were then used in RT reactions using poly T primers. Relative expression levels of un-cleaved and cleaved SPL transcripts were then measured by qPCR using

primers specific for each type of transcripts, normalized to eif4A1. The un-cleaved/cleaved transcript ratio in each genotype was then calculated by dividing the two relative expression values. Since primers for un-cleaved and cleaved transcripts may have different efficiency, the un-cleaved/cleaved transcript ratio value by itself doesn't necessarily reflect the actual relative abundance of these transcripts. For this reason, we then normalized the un-cleaved/cleaved transcript ratio from different genotypes to the value in Col. The changes in un-cleaved/ cleaved transcript ratio from Col to *miR156a/miR156c*, *miR157a/miR157c* and *miR156a/miR156c/miR157a/miR157c* genotypes thus indicate the change in cleavage efficiency caused by a decrease in miR156/miR157.

As shown in Figure 3.4E, the un-cleaved *SPL13*/cleaved *SPL13* ratio increased very little in response to a dramatic decrease in miR156/miR157. In contrast, the un-cleaved *SPL9*/cleaved *SPL9* ratio increased quite significantly as the level of miR156/miR157 decreased. These results support the conclusion that transcript cleavage plays a more important role in the regulation of *SPL9* than *SPL13*.

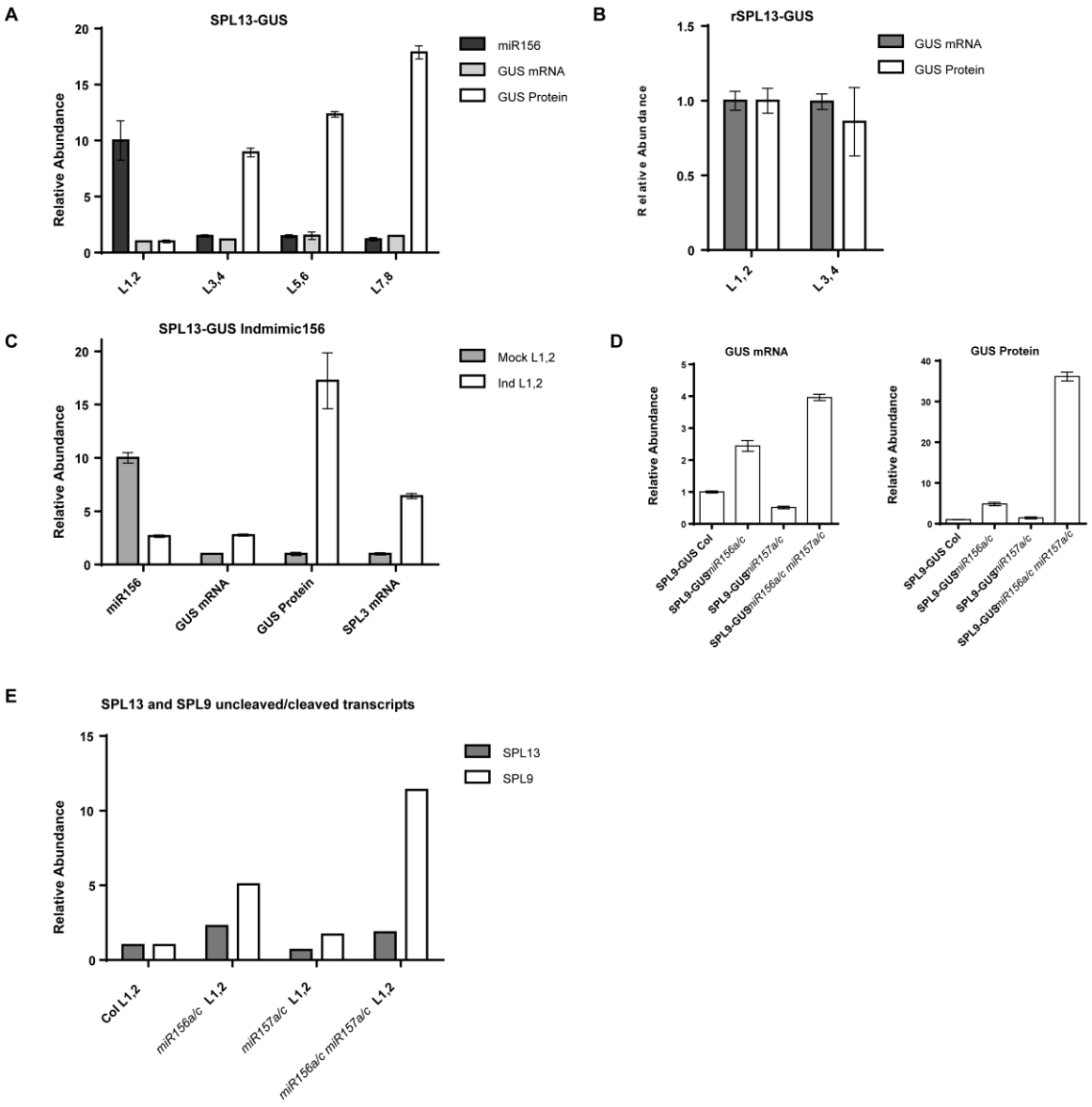

Figure 3.4 *SPL13* is regulated by miR156 through translational repression while both transcript cleavage and translational repression are important for *SPL9* regulation.

(A) Quantitative analysis of SPL13-GUS mRNA and protein level changes through development. Young leaf primordia <1mm in length were harvested at different time points. miR156 and SPL13-GUS mRNA levels were determined by qRT-PCR while SPL13-GUS protein levels were determined by MUG assay as GUS activity. For the ease of interpretation, SPL13-GUS mRNA and protein levels were normalized to the levels in LP1&2, and miR156 levels were normalized so that LP1&2 had the relative abundance of 10.

(B) Quantitative analysis of resistant SPL13-GUS mRNA and protein level changes through development. Resistant version of SPL13-GUS reporter where the miR156 recognition site were changed showed no temporal increase.

(C) Quantitative analysis of SPL13-GUS mRNA and protein level changes with inducible miR156 know-down. The SPL13-GUS line was crossed to Indmimic156 and made homozygous. Young leaf primordia from plants with mock and β-estrodiol treatment were harvested and analyzed with qRT-PCR and MUG assay. SPL3 transcript levels were measured as an indicator of miR156 knock-down.

(D) Quantitative analysis of SPL9-GUS mRNA and protein in different genetic background including WT, *miR156a/miR156c*, *miR157a/miR157c and miR156a/miR156c miR157a/miR157c*.

(E) Uncleaved/cleaved transcript quantification of *SPL9* and *SPL13*. For each *SPL*, relative abundance values were normalized to LP1&2. Results were from a single experiment with 3 technical replicates.

For (A) (B) (C) (D) error bars showing $\pm$ standard deviation from 3 biological replicates.

3.3.4 Translational repression or transcript cleavage: miRNA/target ratio does not determine the mode of action

The stoichiometry of a miRNA and its target can influence the mechanism of gene silencing (J. Li et al., 2014). To determine if the mode of action of miR156 is related to the relative abundance of miR156 and its targets, we measured the absolute quantity of several *SPL* transcripts and miR156 in LP3&4. This was done using known concentrations of *SPL* transcripts and miR156 as standards, and performing qRT-PCR on these standards in parallel with RNA from LP3&4. There was a 5-fold range in the abundance of different *SPL* transcripts, with *SPL5* and *SPL15* being the least abundant, and *SPL3* and *SPL13* being the most abundant (Figure 3.5). miR156 was 100 times more abundant than *SPL3* and *SPL13*, about 200 times more abundant than *SPL6* and *SPL9*, and about 500 times more abundant than *SPL5* and *SPL15*. As the translational reporters for *SPL3*, *SPL9*, and *SPL13* are expressed starting with leaves 3&4 (Xu et al, 2016), this result suggests that greater than a 200-fold excess of miR156 is required to completely repress these genes. Although the relative abundance of miR156 vs. SPL9 and SPL13 might suggest that translational repression is favored by a relatively low miR156:SPL transcript ratio (*SPL13*) whereas transcriptional cleavage is favored by a high miR156:SPL transcript ratio (*SPL9*), this seems unlikely because a 80% reduction in the level of miR156 produced only a slight increase in the level of most *SPL* transcripts, including *SPL9*. Indeed, we only observed a major increase in *SPL* transcripts when both miR156 and miR157 were reduced to very low levels (Figure 3.2), implying that transcript cleavage does not require high levels of these miRNAs. Thus the

miR156/SPL transcript ratio cannot explain the difference in the sensitivity of *SPL9* and *SPL13* to miR156-directed translational repression.

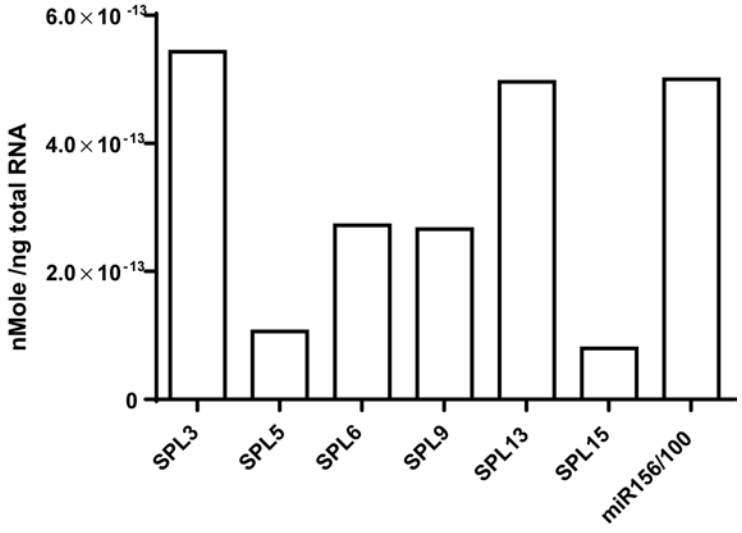

Figure 3.5 Absolute quantification of *SPL* transcripts in Col LP 3&4 reveals their relative abundance to miR156.

miR156 level is about 100 fold higher than the most abundant *SPL* transcript.

3.4 Discussion

3.4.1 Quantitative relationship between *SPL*s and miR156/miR157

When miR156/miR157 abundance is reduced below a critical level, as in *miR156a/miR156c miR157a/miR157c*, there is an increase in the transcript abundance of every *SPL* gene we measured. This increase in the total *SPL* transcript pool is expected to promote adult leaf identity. However different *SPL* transcripts display distinct response latitudes to a reduction in miR156/miR157, and adult leaf traits start to appear well before miR156/miR157 drop below this critical level. We hypothesized that some *SPL*s are regulated by miR156/miR157 through translational repression and used *SPL13* as an example to characterize its quantitative relationship to miR156. The response patterns of *SPL13* transcript and protein to miR156 reduction are different. *SPL13* transcript is insensitive to miR156 within a wide range of changes while *SPL13* protein shows a significant increase upon the reduction of miR156. A miR156-resistant version of the SPL13-GUS reporter, on the other hand, shows consistent high expression of both SPL13-GUS transcript and protein. These results suggest that *SPL13* is regulated by miR156 through translational repression. miR156 also cleaves *SPL13* transcripts, as demonstrated by the RLM-RACE results and by the observation that, in general, rSPL13-GUS reporters have much higher transcript levels than SPL13-GUS reporters. We believe the regulation *SPL13* occurs in two steps. Above a critical low level, miR156 cleaves *SPL13* constantly, keeping the *SPL13* transcript level within a relatively stable range. The fluctuation of miR156 causes changes in its translational

repression on *SPL13*, resulting in response at SPL13 protein level, which is responsible for adult leaf identity.

The stoichiometry of miRNA:target has been proposed to be important for miRNA function. Results from a large scale experiment assessing the repressive activity of miRNAs in cells showed that the degree of target repression did not directly correlate with miRNA abundance. Instead the miRNA:target ratio was correlated with the inhibition efficacy (Mullokandov et al., 2012). We measured the miR156:*SPL* ratio in leaf primordia 3,4 and found out that *SPL3* and *SPL13* were the most abundant transcripts; each was present at approximately 1% of the miR156 abundance. *SPL9* and *SPL6* were approximately 0.5% of miR156 level. If the level of repression on *SPL*s is determined mainly by the miRNA:target stoichiometry, we would expect higher *SPL3* and *SPL13* protein levels than *SPL9* and *SPL6*. However, GUS staining of SPL-GUS reporters showed different results. In L3,4 SPL9-GUS strength is on par with SPL13-GUS, both higher than SPL3-GUS while SPL6-GUS showed no expression (Xu, Hu, Zhao, et al., 2016). Therefore *SPL*s are not equal in their response to miR156 regulation and some unknown gene specific mechanisms could contribute to their interaction with the miRNA.

3.4.2 Mechanisms underlying the choice between transcript cleavage and translational repression

Plant miRNAs were initially suggested to function primarily through target cleavage because of their near-perfect complementarity to the target sequence. (Jones-Rhoades, Bartel, & Bartel, 2006; Tang, Reinhart, Bartel, & Zamore, 2003). 5'-RACE analysis was used in many cases to demonstrate the cleavage event. Sequencing of the miRNA degradome also indicated that a large number of miRNAs cleave their targets (Addo-

Quaye, Eshoo, Bartel, & Axtell, 2008). At the same time, there have been an increasing number of reports showing examples of translational repression in plants (Aukerman & Sakai, 2003; Chen, 2004; Gandikota et al., 2007; S. Li et al., 2013; L. Yang, Wu, & Poethig, 2012). Ribosomal profiling in *Arabidopsis* discovered widespread translational repression, in that the translation efficiency of miRNA targets was lower than that of non-miRNA targets (Liu et al., 2013). These results suggested that both transcript cleavage and translational repression play important roles in the silencing mechanisms of plant miRNAs. However, the relative contribution of transcript cleavage and translational repression is not well understood, either at a genomic scale or for particular genes. Here we showed that the mode of action is gene specific. miR156/miR157 target *SPL9* is regulated by both translational repression and transcript cleavage. *SPL13*, targeted by the same miRNAs as *SPL9*, is regulated primarily by translational repression in vegetative development when there is constant cleavage taking place. miR156-regulated *SPL* genes could serve as an excellent example to study the relative contribution of target cleavage and translational repression to a developmental program and how the choice between target cleavage and translational repression is made molecularly.

The mechanisms that determine the choice between translational repression and target cleavage is not well understood. Recent studies suggested that DOUBLE-STRANDED RNA-BINDING1 (DRB1) and DRB2 can direct miRNAs into either cleavage or translational repression fate (Reis, Hart-Smith, Eamens, Wilkins, & Waterhouse, 2015). However we observed different modes of actions on *SPL9* and *SPL13*, from the same miRNAs, which suggested the existence of more delicate regulatory mechanisms. We explored the possibility of miRNA: target stoichiometry in determining the silencing

mechanism and found that it could not explain the different modes of actions on different *SPL*s. It is possible that sequence properties specific to each *SPL* gene can lead to different regulatory modes from the same miRNAs. It is reported that nucleotides flanking the miR159 binding site of *MYB33* are critical for efficient silencing (J. Li et al., 2014). In *Arabidopsis*, miR156 targeted *SPL*s share the same target sequence but the flanking nucleotides are different (Figure 3.6). However for a particular *SPL*, such as *SPL13*, the two nucleotides flanking the target sequence are conserved across species (Figure 3.6). These flanking nucleotides may be responsible for the translational repression regulation of *SPL13* and will be investigated in the future.

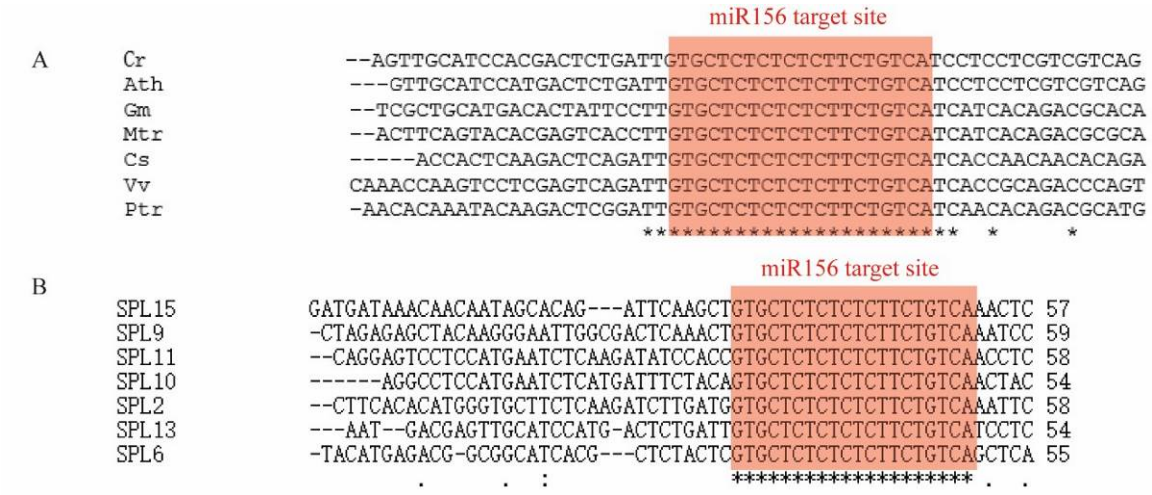

Figure 3.6 Figure 3.6 Flanking nucleotides of the miRNA target sites on *SPL*s

A. The two nucleotides flanking miR156 target site on *SPL13* is conserved across species. Colored box represents miR156 target site. (Cr: *Caspella rubella*; Ath: *Arabidopsis thaliana*; Gm: Glycine max; Mtr: *Medicago truncatula*; Cs: *Citrus sinensis*; Vv: *Vitis vinifera*; Ptr: *Populus trichocarpa*.)

B. *SPL*s in *Arabidopsis* have different flanking sequences of the miR156 target site.

4. Beyond embryonic development: the role of *VP1/ABI3-LIKE* (*VAL*) genes in regulating vegetative phase change

4.1 Abstract

Flowering plants undergo three major transitions (embryonic to vegetative, vegetative juvenile to vegetative adult, and vegetative to reproductive) in their life cycle. Embryonic to vegetative phase transition is regulated by the complex interaction network between the *AFL* (*ABI3, FUS3, LEC2*) and *VP1/ABI3-LIKE* (*VAL*) classes of the plant specific B3 domain transcription factors involving histone modifications by PcG repressive complexes (PRCs). Vegetative phase change is regulated by a decline in the level of miR156 and miR157. The down-regulation of the most important miR156-producing genes, *miR156A* and *miR156C*, is associated with an increase in PRC2 binding to these loci, resulting in higher H3K27me3 levles. Here we show that *VAL* genes also have important roles in promoting vegetative phase change. Loss-of-function *val1* mutants display moderate delay in phase change while *val1/val2* double mutants have severely prolonged juvenile phase which correlates with altered miR156 expression pattern resulting in higher miR156 abundance especially in leaf positions later than leaf 1&2. The increased abundance of miR156 comes from higher *Pri-miR156A* and *Pri-miR156C* transcript levels, accompanied by lower H3K27me3 in the genomic region. Inducible knock-down of *VAL1* in *val2* mutant background during seedling stage demonstrates that the effects of *VAL*s on vegetative development are not the residual outcome of arrested embryonic development.

Contributions: Jim Fouracre identified the *val1/atbmi1* double mutation from the EMS mutagenesis described in 4.3.1.

4.2 Background

Plants undergo three major developmental transitions in their life cycle. The first transition occurs when seeds germinate to become seedlings (embryonic to vegetative transition). The second major transition is the vegetative phase change, which refers to the transition from juvenile to adult phase of vegetative growth. This is followed by the reproductive transition marked by the production of floral organs. The molecular mechanisms underlying these developmental transitions have been extensively studied. As discussed in previous chapters, vegetative phase change is regulated by the decline of miR156 and miR157 and the subsequent increase of *SPL* abundance/activity. This regulatory module also defines an endogenous flowering pathway (Wang et al., 2009).

One of the central questions in vegetative phase change is how the stability of each phase is achieved. Chromatin modification, especially the repressive modification, histone H3 lysine 27 trimethylation (H3K27me3) was found to play important roles in controlling developmental transitions. A notable example is the regulation of flowering time by the floral repressor *FLOWERING LOCUS C (FLC)*, which is subjected to the repression by H3K27me3 deposition during vernalization (Sung & Amasino, 2004; Sung et al., 2006). Seed to seedling developmental transition is another example where the stability of phases is regulated by chromatin modifications. The LAFL network of transcription factors including the AFL clade of B3 domain proteins ABI3, FUS3 and LEC2, together with LEC1 and LEC1-LIKE (L1L), regulates seed development. During germination, this LAFL regulatory network must be repressed by a sister clade of transcription factors, the *VAL/HIS* B3 domain factors. These LAFL genes repressed by *VAL*s are also regulated by chromatin modifications, mainly from three types of

chromatin modification systems - polycomb repressive complex 1 (PRC1), polycomb repressive complex 2 (PRC2) and chromatin remodeling factors. The importance of *VAL*s and the chromatin modifications during the processes have been demonstrated by loss-of-function mutations in *VAL* genes and players of PCR1, PCR2 or chromatin remodeling complexes (Aichinger et al., 2009; Bratzel, López-Torrejón, Koch, Del Pozo, & Calonje, 2010; Kim, Lee, Eshed-Williams, Zilberman, & Sung, 2012; M. Suzuki, H. H. Y. Wang, & D. R. McCarty, 2007). It appears that H3K27me3 deposition at the LAFL genomic loci during and after the transition from embryonic stage to vegetative growth is crucial for the successful developmental progress. These findings open up questions on the possible roles of epigenetic regulation on vegetative phase change.

Recent studies in *Arabidopsis* revealed that the down-regulation of miR156 during vegetative phase change is correlated with increased levels of H3K27me3 in *miR156A* and *miR156C*, which is associated with increased PRC2 binding to these loci (Xu, Hu, Smith, et al., 2016). Loss-of-function mutations in the PRC2 component *SWINGER* (*SWN*) produced delayed phase change phenotypes especially when combined with the *PICKLE* (*PKL*) loss-of-function mutation. A question that has arisen following this discovery is the mechanism by which PCR2 localizes to miR156 loci in a temporal manner. *VAL*s are interesting candidates for this function. It has been reported that during embryonic to seedling transition, VALs and PRC1 function in the initial repression of their targeted LAFL genes which are then modified by H3K27me3 deposited by PRC2 (C. Yang et al., 2013). It would be interesting to test if *VAL*s have a regulatory role beyond embryonic development, and whether they participate in the epigenetic regulation of vegetative phase change by PRC2.

4.3 Results

4.3.1 *VAL1* loss-of-function mutation suppresses the early phase change phenotype of *miR157a/miR157c*

Vegetative phase change is regulated by the decline of miR156 and miR157, yet how the temporal expression patterns of these miRNAs are coordinated remains largely unknown. Forward genetics methods in search of mutations with altered phase change timing proved to be very powerful in unraveling the molecular mechanisms underlying vegetative phase change. The most frequently identified mutants, however, affect miRNA biogenesis or function in general, resulting in greatly reduced miR156 abundance or activity across all developmental stages, which leads to strong precocious phenotypes (Kurihara et al., 2006; M. Y. Park et al., 2005; Peragine et al., 2004; Telfer & Poethig, 1998; Li Yang et al., 2006). Detailed analysis of how miR156/miR157 quantitatively affect phase change phenotypes (Chapter 2) provided possible explanations to the rare emergence of mutations that specifically alter miR156 level or its temporal expression pattern. Since miR156/miR157 abundance correlates with phase change timing in a non-linear fashion, such that even a ~40% reduction of miR156 or miR157 barely produces recognizable phenotypes, it is extremely difficult to identify mutations that regulate either the temporal expression pattern or the abundance of one of the miR156/miR157 contributing genes. *miR157a/miR157c* double mutations are mildly precocious and represent a sensitized genetic background where moderate changes in miR156 abundance can create visible phase change phenotypes. It is

therefore a desirable genotype for mutagenesis, from which potential regulators of miR156 could be identified.

To identify regulators of miR156 in an unbiased way, we performed EMS mutagenesis in the sensitized genetic background *miR157a/miR157c* and then screened for enhancers as well as suppressors. Roughly 10,000 *miR157a/miR157c* seeds were mutagenized by EMS and grown under standard conditions. Self-fertilized seeds from approximately every 150 M1 plants were harvested in bulk. M2 seeds were planted and screened for precocious or late phase change phenotypes. Mutants of interest were then harvested individually. One of the mutants identified by my colleague, Jim Fouracre, suppressed the early phase change phenotypes of *miR157a/miR157c*, and was subsequently discovered to be a double mutant of *val1* and *AtBmi1*. This finding coincided with our previous assumptions that *VAL*s could function in vegetative phase change.

4.3.2 *VAL1* and *VAL2* regulate vegetative phase change

The phenotypes of loss-of-function *VAL* mutants during embryo development have been described (M. Suzuki, H. H. Wang, & D. R. McCarty, 2007; C. Yang et al., 2013). Here we examined the vegetative phenotypes of *val1-2(val1* here after*)*, *val2-1(val2)* and *val1-2/val2-1*. *val1* single mutation produced mild late phase change phenotypes under both LD and SD conditions. Abaxial trichome production was delayed in *val1* by about two leaves compared to Col. *val1* also displayed smoother leaf margins and less elongated leaf shapes (Figure 4.2). *val2* single mutations did not produce significant changes in phase change. *val1/val2* was reported to have arrested growth in seedling stage when

grown on MS plates. Under our growth conditions (in soil), a small fraction of *val1/val2* plants survived past the seedling stage, showing delayed growth and prolonged juvenile identity. Strikingly, in those *val1/val2* plants leaf 3 to leaf 6 or even leaf 7 share similar characteristics of leaf 1 & 2. This is very interesting because in WT, miR156 abundance reduces dramatically from leaf 1&2 to leaf 3&4, making the identity of leaf 1&2 distinct to leaf 3&4 or later leaves. The prolonged leaf 1&2 identity in *val1/val2* mutants suggested possible prolonged high expression of miR156, or very potent repression of its targeted *SPL* genes.

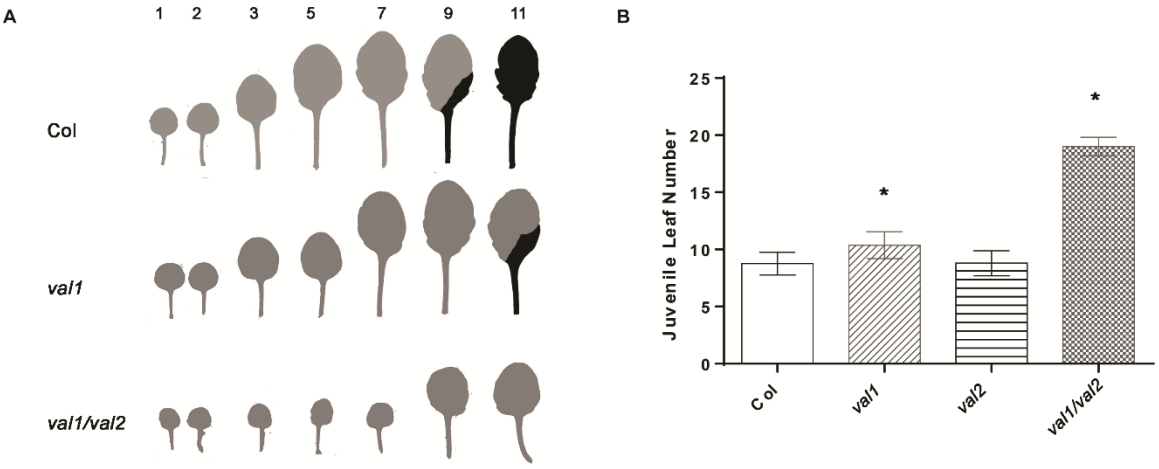

Figure 4.1 *VAL* mutants display delayed phase change phenotypes.

(A) Heteroblasty of *val1* and *val1/val2* compared to Col under SD 22C conditions.

(B) Juvenile leaf number as measured by the leaf number without abaxial trichome under SD 22C conditions. Error bars represents ± Standard Deviation. *: significantly greater than Col, t-test.

4.3.3 *VAL1* and *VAL2* regulate miR156 abundance in a temporal manner

The *val1/val2* mutant phenotypes indicated prolonged high abundance of miR156 thus we measured its miR156 levels in comparison to WT. It was also very important for us to determine if the overall abundance of miR156 abundance is increased in *val1/val2*, or if these mutations change the temporal expression pattern of these genes. Limited by the amount of tissue we could get from *val1/val2*, I harvested leaf 1&2, leaf 3&4, leaf 5&6 at the same time after planting (Day 19, SD conditions). The temporal expression pattern of miR156 in *val1/val2*, as revealed by Northern Blotting, was different to that in Col (Fig. 4.2). miR156 abundance in *val1/val2* leaf 1&2 was approximately the same as in Col but its decline rate was smaller therefore in leaf 3&4 and leaf 5&6, *val1/val2* produced more miR156 than Col. This elevated miR156 in leaf 3&4 and leaf 5&6 is consistent with the small and round leaf characteristics in *val1/val2*. qPCR measurements of miR156 recapitulated this observation except that there was slightly elevated miR156 in *val1/val2* leaf 1&2 compared to Col.

The loss of *VAL1* and *VAL2* thus leads to elevated miR156 abundance, and importantly, the change of temporal expression pattern of this miRNA. The decline rate of miR156 in *val1/val2* is lower than that in Col, resulting in higher miR156 abundance in *val1/val2* especially in later leaves.

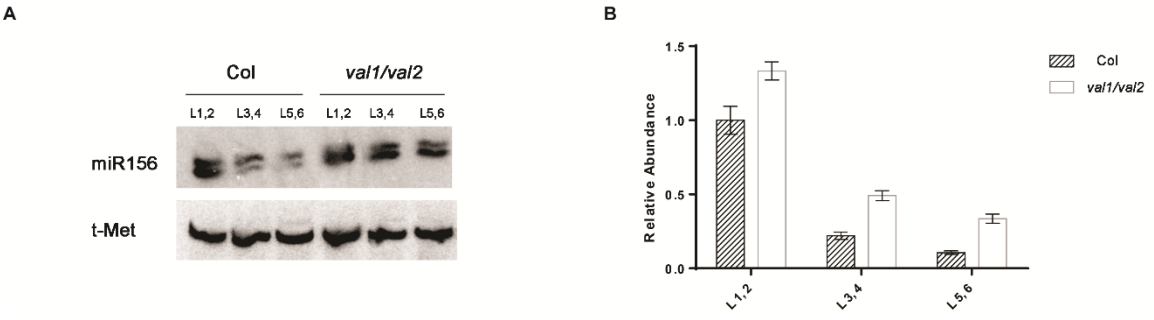

Figure 4.2 *val1/val2* double mutants produce prolonged high abundance of miR156

(A) Northern Blotting of miR156 in Col and *val1/val2* leaf tissues, 22C SD conditions. In Col, miR156 dropped dramatically from L1,2 to L3,4 while in *val1/val2* there was less degree of reduction.

(B) qRT-PCR of miR156 of miR156 in Col and *val1/val2* leaf tissues showing the similar results as in (A).

4.3.4 *VAL*s can function in vegetative development independent of their roles in embryonic development.

Since *val1/val2* mutants have strong defects in embryonic development, it is possible that the physiological or molecular consequences from the embryonic stage is carried over to vegetative development. To test if *VAL*s regulate vegetative phase change independent of their embryonic functions, I introduced an estradiol-inducible knock-down construct, IndamiRVal1, into a *val2* genetic background, which allowing me to eliminate the expression of both genes by exogenous application of β–estradiol. This was achieved by expressing an artificial miRNA within miR390a backbone to target *VAL1* coding sequence, under the control of the estradiol inducible module XVE (Carbonell et al., 2014). Homozygous transgenic plants were grown under normal growth conditions and allowed to germinate and develop green cotyledons. 10μM of estradiol spray was applied onto the experimental group of plants every three days. We observed delayed

growth and prolonged juvenile leaf identity in the induced plants compared to mock treated plants. Induced IndamiRVal1 plants generally have small round leaves and delayed abaxial trichome production by approximately two leaves (Figure 4.4). The small and round leaf characteristics resembled those of miR156 over-expression lines or multiple SPL loss-of-function mutants, but the abaxial trichome production delay was not as severe.

qRT-PCR quantification of the mature miR156 from both the induced and mock lines revealed that there was elevated abundance of miR156 at different time points in the induced plants. Noticeably, in the young leaf primordia at day 17 and day 21, induced plants showed 80% to 100% increase of miR156 compared to the mock group. We previously showed that phase change phenotypes are more sensitive to miR156 changes after miR156 abundance drops below the level in leaf primordia 3&4, which is consistent with the delayed phase change phenotypes in the induced lines. The elevated miR156 was possibly a result of increased levels of miR156A and miR156C primary transcripts, as shown in Figure 4.5C&D.

However, the late vegetative phase change phenotypes in induced IndamiRVal1 was weaker than what we observed in *val1/val2* double mutants. One explanation for this observation is that the knock-down of *VAL1* from the artificial miRNA is incomplete. As shown in Figure 4.5B, *VAL1* mRNA abundance in the induced lines is approximately 40%-50% of the mock group. Though we don't know if post-transcriptional regulation plays a role here in *VAL1*, we expect the overall knock-down of *VAL1* from the induction lines to be less effective than a null mutation.

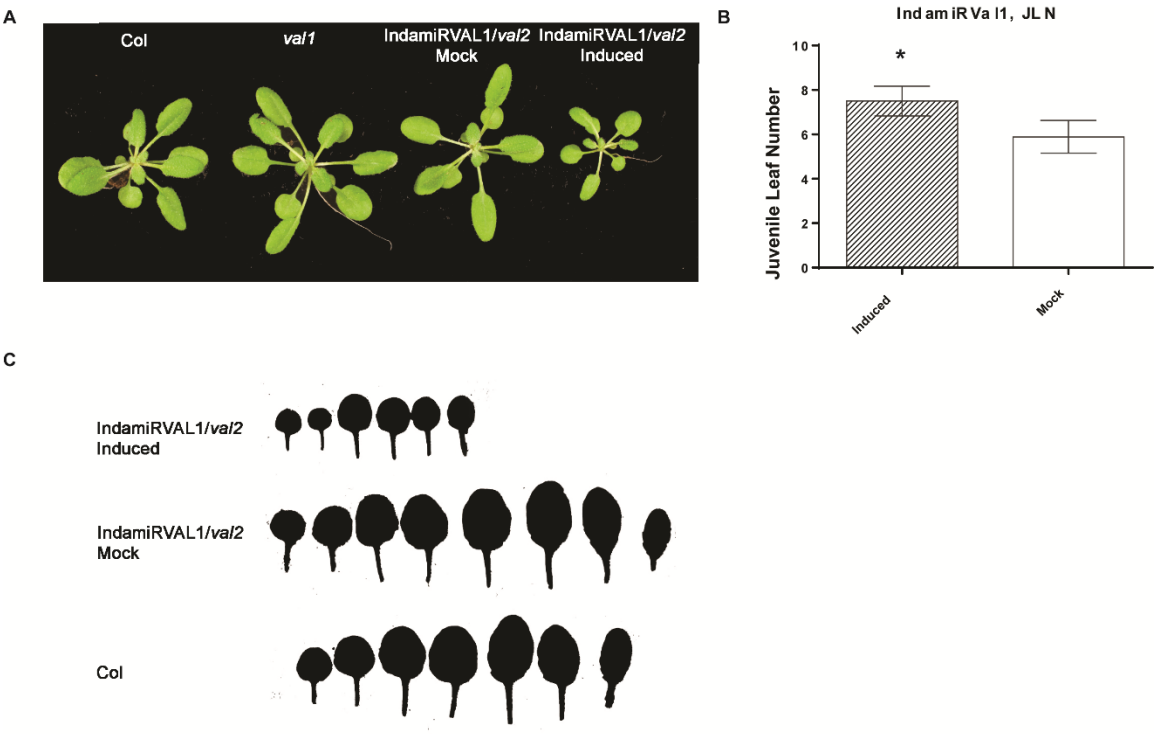

Figure 4.3 Induced knock-down of *VAL1* in *val2* background post-embryonically produces delayed phase change.

(A) An aerial view of the rosette leaves of Col, *val1*, IndamiRVal1 in *val2* both mock and induced.

(B) When induced with β-estradiol, IndamiRVal1 produces more leaves without abaxial trichome. *: significantly more than mock group, t-test, $p < 0.01$.

(C) Heteroblasty of Induced and mock IndamiRVal1 in *val2*. When induced with β-estradiol, IndamiRVal1 produces smaller and rounder leaves.

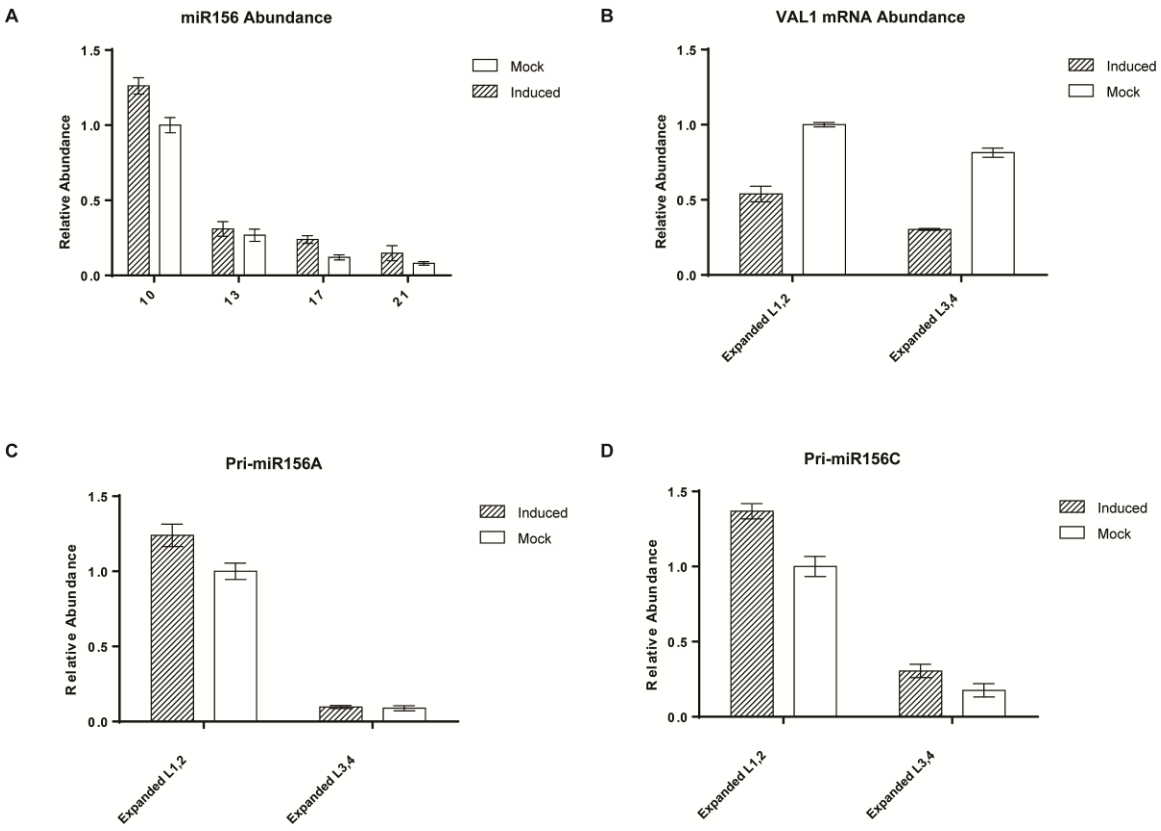

Figure 4.4 Induced IndamiRVal1 produces higher mature miR156 and *Pri-miR156A*, *Pri-miR156C*

(A) qRT-PCR measurement of mature miR156 abundance in leaf primordia samples harvested from different time point during vegetative development.

(B) qRT-PCR measurement of *VAL1* mRNA abundance in L1,2 and L3,4. Induced lines showed 50% to 65% reduction of *VAL1* transcript abundance.

(C) and (D) qRT-PCR measurements of Primary transcripts of *miR156A* and *miR156C*.

4.3.5 The elevated miR156 abundance in *val1/val2* during vegetative development is correlated with reduced H3K27me3 in *miR156A* and *miR156C*

During embryonic development, the loss of *VAL1* and *VAL2* results in dramatically increased LAFL gene expression and highly reduced H3K27me3 at these loci. We performed ChIP analysis to measure H3K27me3 levels at *miR156A* and *miR156C* genomic loci in WT and *val1/val2* to see whether the increased *miR156A* and *miR156C* transcript levels in *val1/val2* were associated with altered chromatin modification. As shown in Figure 4.6, in SD grown 3-week old rosette leaves, H3K27me3 levels at miR156A and miR156C promoter region as well as gene bodies are lower in *val1/val2* than in Col.

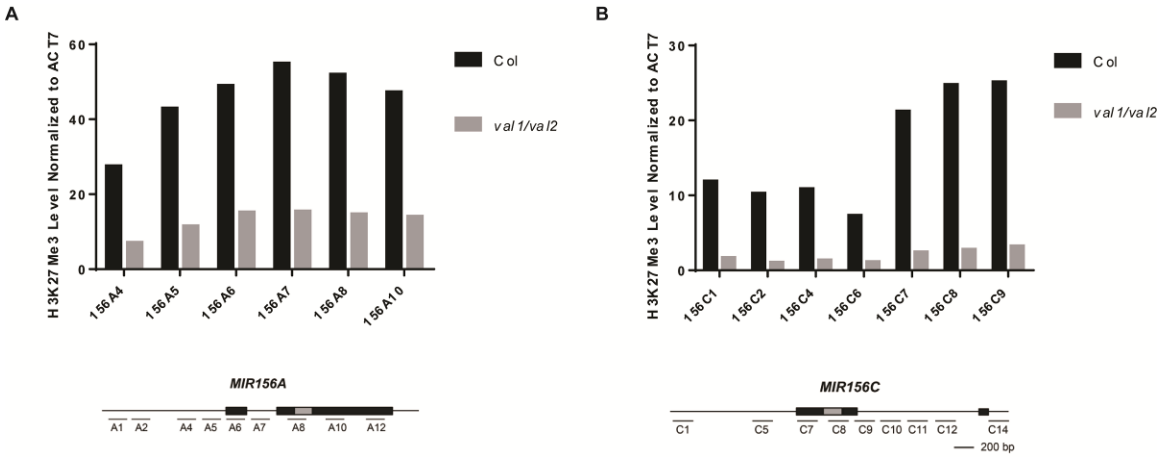

Figure 4.5 ChIP analysis revealed that *miR156A* and *miR156C* genomic loci have lower H3K27me3 than WT.

Illustration of primers used here is adopted from (Xu, Hu, Smith, et al., 2016). Black boxes represent exons and the gray box is the position of the miR156 hairpin. The direction of transcription is from left to right. The data is presented as the ratio of (H3K27me3 miR156A or C / H3) to (H3K27me3 ACT7/ H3).

4.4 Discussion

4.4.1 The variable phenotype of *val1/val2*

The *val1/val2* double mutants were shown to have strong embryonic developmental defects, in that the germinated seedlings have arrested development before they enter the vegetative phase (M. Suzuki et al., 2007; C. Yang et al., 2013). However in our grown conditions, a small percentage of the plants can overcome this barrier and grow into the vegetative phase. Similar observations were made by Yuan et.al. (Yuan et al., 2016) where strong and weak embryonic developmental phenotypes were present from the same *val1/val2* population. It appears that the embryonic phenotypes of *val1/val2* are not fully penetrant. However, it could also be due to the potential heterogeneous genetic background of the double mutant. *val1-2* is a T-DNA insertional mutation from the Salk lines which were generated from Columbia ecotype (Col-0) while *val2-1* derived from Wassilewskija (WS). Even with several rounds of backcrosses, the chromosomal landscape of the *val1/val2* double mutants could still be complicated. It is possible that the strong embryonic phenotype of *val1/val2* relies on other modifiers from a particular ecotype. I would be very helpful to obtain loss-of-function double mutants in both ecotypes and compare their phenotypes.

4.4.2 The source of temporal regulation of miR156 through *VAL1* and *VAL2*

We showed that in *val1/val2* mutants, the temporal expression pattern of miR156 is altered so that this miRNA declines not as fast as it does in WT. A direct consequence of the altered temporal expression pattern is the higher abundance of miR156 in *val1/val2*

mutants especially in leaf positions later than leaf 1&2, which correlates with reduced H3K27me3 at *miR156A* and *miR156C* genomic loci. One way that *VAL*s could change target gene expression is through the recruitment of PRC1, which is crucial for the initial repression, possibly by H2A ubiquitination mediated block of transcription. Subsequent recruitment of PRC2 incorporates H3K27me3 marks for the stable repression of such loci (Merini & Calonje, 2015; C. Yang et al., 2013). *miR156A* and *miR156C* genomic loci do bear RY/Sph DNA motifs that are potential B3 DNA binding domain targets. However, *VAL*s transcripts don't show a temporal expression pattern in leaf primordia series, which raises the question of how they regulate miR156 temporal expression. There are several possible directions for future research on this question. Firstly, it is possible that *VAL*s are under unknown post-transcriptional regulation that causes the VAL protein abundance or activity to change during shoot development. The temporal expression pattern of the VAL proteins could be approximated by GUS translational fusion reporters in future experiments. Secondly, VALs interact with PRC1 components such as AtBMI1, which was reported to be important in repression of the seed maturation genes during germination. It is possible that this mechanism is also involved in the regulation of miR156. While VAL abundance does not change temporally, PRC1 or its interaction with VALs could have a temporal pattern, resulting in the observed miR156 temporal expression. Also, VALs contain a plant homeodomain (PHD) and a CW domain that recognize H3K4me3 marks (Hoppmann et al., 2011; Sanchez & Zhou, 2011). So the H3K4me3 status in *miR156A* and *miR156C* might have some impact on the actual VALs functioning at *miR156A* or *miR156C*.

5. Natural variation of vegetative phase change in *Arabidopsis*

5.1 Abstract

The reference plant *Arabidopsis thaliana* grows naturally across wide range of locations throughout Europe and Asia. Distinct environmental conditions pose challenges to local populations and eventually lead to the formation of homozygous inbred lines referred as ecotypes or accessions. Vegetative phase change is regulated by miR156/miR157 and their targeted *SPL* genes, which represents a highly conserved regulatory module in plants. Ecotypes of *Arabidopsis* from different environments likely tuned this conserved pathway during evolution, and may contain tremendous amount of genetic variations that lead to phase change phenotypes. To determine the phenotypic variation of vegetative phase change among *Arabidopsis* natural accessions, we investigated a collection of ecotypes and found a wide range of phase change phenotypes. Voeran-1, Vessano-2 and Bozen-1 have significantly delayed phase change while Sha, Leb-3, Shigu-2 are precocious. These phenotypic variations in phase change showed no significant correlation to miR156 abundance. In Sha, while miR156 abundance showed little difference compared to Col, *SPL3* and *SPL15* transcripts were moderately elevated, possibly through a miR156-independent mechanism. Rough mapping located the causal polymorphism for the Sha phenotype on Chromosome 2. Traffic Lines were used to generate homozygous Sha recombinants and narrowed the polymorphism between 10.679mb and 10.78mb on Chromosome 2. Within the interval, *ARABIDOPSIS RESPONSE REGULATOR 12* (*ARR12*) has a one-nucleotide deletion in the promoter region of Sha, which may contribute to its increased transcript level compared to that in Col. While *arr12* loss-of-function mutations in Col did not show significant phenotypes, the triple mutant *arr1/10/12* displayed delayed phase change in Col.

Contributions: Scott Poethig did the cross between the Sha lines and the Traffic Lines, and participated in the phenotypic analysis of the recombinant lines. Gabrielle Rossidivito contributed to the genotyping of Sha recombinants.

5.2 Background

Genetic mutations have been the basis for modern genetics and molecular biology that shaped our understanding of biology. It has been a revelation to us that many important genetic, developmental or physiological pathways are shared among broad groups of organisms. Fine tune of these conserved pathways could account for phenotypic variations between and within species.

The major reference plant *Arabidopsis* is especially suitable for genetics and molecular biology, which tremendously facilitated our knowledge of plant biology in the past 30 years. *Arabidopsis* is native to Europe and central Asia and has been naturalized to other places in the world (Al-Shehbaz & O'Kane, 2002). It is a selfing species, therefore the plants collected from natural habitats are mostly homozygous inbred lines. These wild homozygous lines are often referred to as accessions of ecotypes. Genetic and phenotypic variations among different *Arabidopsis* accessions have been studied extensively and provided insights in basic plant biology. A notable example was the study of natural variation of flowering time in *Arabidopsis* ecotypes. *FRIGIDA* (*FRI*) was found to be a major determinant of natural variation in flowering time. Most of the early flowering accessions carry *FRI* alleles bearing deletions that disrupt its normal function (Johanson et al., 2000).

Vegetative phase change is a conserved developmental process regulated by the miR156-SPLs pathway (Michael J. Axtell, Snyder, & Bartel, 2007; Poethig, 2013). The understanding of the genetic basis of phase change is still far from complete. Natural genetic variation is an important resource for studying the genes involved in this process, and their roles in ecology and evolution. The study of natural variation in

Arabidopsis became more manageable with the sequencing of 80 accessions by the Genome 1001 project that revealed a large number of SNPs, small and large deletions, along with duplicated regions which could potentially support the adaptation of the species to its environment (Cao et al., 2011). Moreover, recent development of the Traffic Lines as genetic tools in *Arabidopsis* enables a researcher to visually identify seeds that have a recombinant chromosome based on seed fluorescence (Wu, Rossidivito, Hu, Berlyand, & Poethig, 2015). In this chapter I will determine the phenotypic variation of vegetative phase change among *Arabidopsis* natural accessions and demonstrate the use of Traffic Lines in creating introgressed lines for mapping natural variation.

5.3 Results

5.3.1 Phenotypic variation of vegetative phase change among *Arabidopsis* natural accessions

Vegetative phase change involves a suite of phenotypic variations including both qualitative and quantitative changes. An ecotype may possess a phase change related trait variation without having an altered phase change timing in general. In order to obtain a relatively comprehensive understanding of the variation of vegetative phase change among the ecotypes, we measured abaxial trichome appearance, leaf shape and leaf initiation rate of each ecotype. As shown in Figure 5.1A, under 22^{o}C SD conditions, abaxial trichome appearance has a huge variation among different ecotypes.

The latest ecotype Bozen-1 has 25.2 ± 2.5 leaves without abaxial trichomes compared to 9.8 ± 0.6 leaves in Col. There are also ecotypes with fewer juvenile leaves. Sha (6.8 ± 0.6), Leb-3 (6.3 ± 0.6) and Shigu-2 (5.5 ± 0.8) are some examples.

The leaf shape of ecotypes are shown as leaf scans in Figure 5.1B. In general, ecotypes that have fewer leaves without abaxial trichomes tend to display earlier adult leaf shape characteristics. At leaf 3, Sha, Leb-3 and Shigu-2 start to show much sharper leaf base angle, with elongated leaf shape and more prominent serrations at leaf margins. These features become more prominent in leaf position 5 and later leaves. On the other hand, Copac-1, Galdo-1, Bozen-1 and Voeran-1 have more leaves bearing round and smooth leaf characteristics.

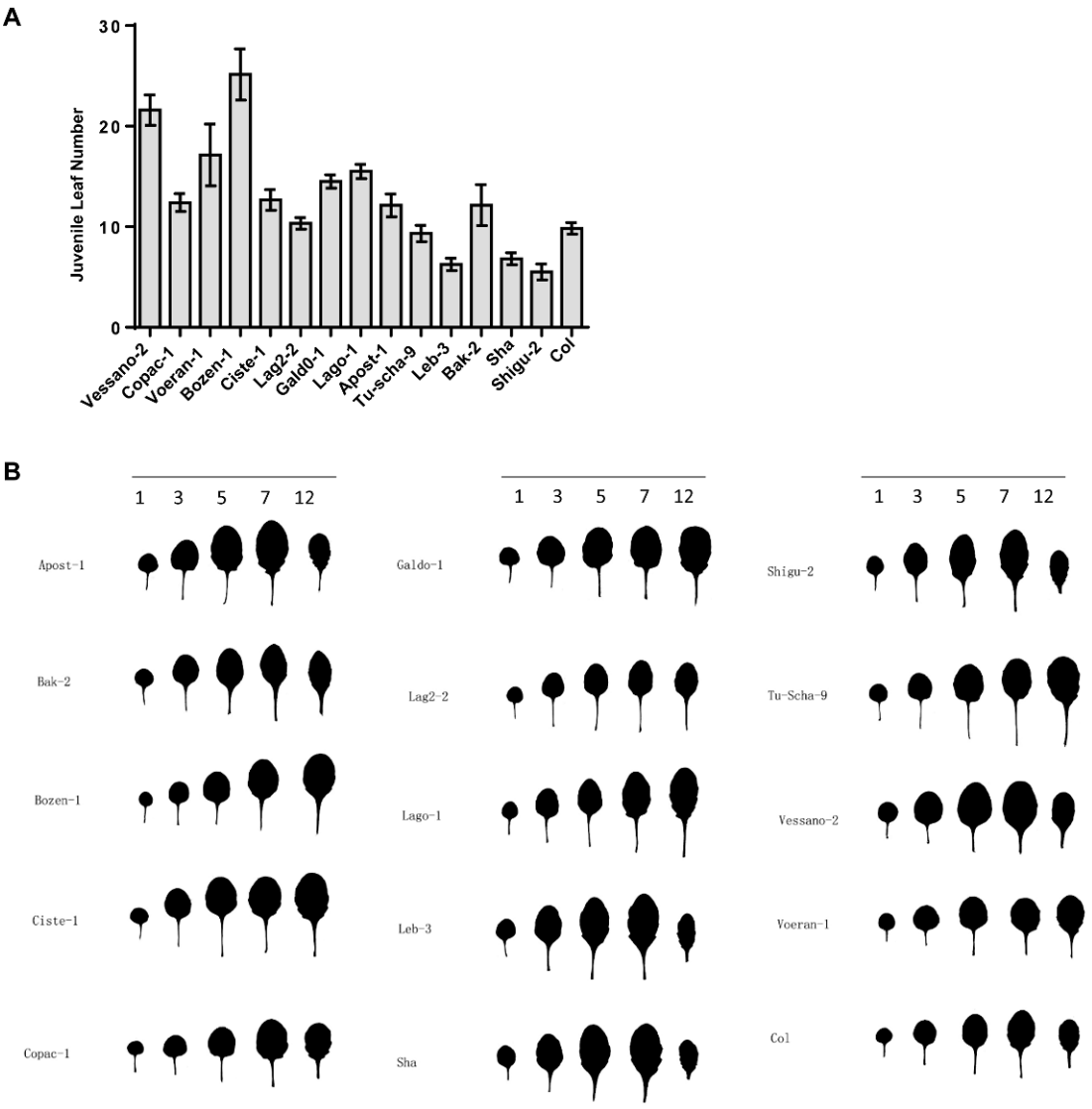

Figure 5.1 Abaxial trichome appearance and heteroblasty demonstrate the wide range of vegetative phase change phenotypes among selected ecotypes.

A. Juvenile leaf number measured as the number of leaves without abaxial trichome. Plants were grown under 22C SD conditions.

B. Leaf shape of selected ecotypes grown under 22C SD conditions, showing leaf 1, 3, 5, 7, 12.

Leaf initiation rate was measured as visible leaf primordia at given time point (days after planting), and we observed moderate variation among different ecotypes (Appendix 8.1). In early studies of phase change in *Arabidopsis*, it was found that leaf initiation rate was a trait independent of phase change (Telfer et al., 1997). Supporting evidence included the fact that three measured ecotypes Col, WS and Ler showed similar rate of leaf initiation. Also there were mutations such as *ALTERED MERISTEM PROGRAMMING1* (*AMP1*) and *PAUSED* (*PSD*) that altered leaf initiation rate but not the actual timing of other phase change related traits such as abaxial trichome appearance. However, there is emerging evidence suggesting a correlation between leaf initiation and phase change. Mutant screens using abaxial trichome as a marker for phase change yielded a large number of precocious mutations such as *SQUINT* (*SQN*), *HASTY* (*HST*) and they have slower leaf initiation rate than WT (Berardini, Bollman, Sun, & Poethig, 2001; Telfer & Poethig, 1998). More importantly, miR156 over-expression lines show faster leaf initiation rate than WT while miR156 deficient lines have slower leaf initiation rate. The general observation is, late phase change is often associated with faster leaf initiation while early phase change is correlated with slower leaf initiation. When assessing phase change with leaf number without abaxial trichomes, the leaf initiation rate differences may introduce certain degree of inaccuracy. However, since the leaf initiation rate differences among phase change mutants are usually not as dramatic, they would not offset the trichome differences in most cases. Figure 5.2A illustrates the leaf initiation rate and abaxial trichome relationship of the ecotype Voeran-1. Under SD conditions, Voeran-1 has faster leaf initiation rate than Col. At day 24, Voeran-1 has two more visible leaves than Col. When we plot the juvenile leaf number defined as the leaves without abaxial trichomes on the graph, we can determine that the juvenile phase of

Voeran-1 is ~29.5 days compared to 23.5 days in Col. Similar measurements of other ecotypes are included in Appendix 8.1.

After combing previous mentioned measurements, I sorted the ecotypes by their vegetative phase change phenotypes (Figure 5.2B). Bozen-1, Voeran-1 and Vessano-2 are the ecotypes with most prolonged phase change. Galgo-1, Apost-1 and Lago-1 are moderately late phase change. Bak-2, Copsc-1, Lag2-2, Ciste-1 are close to Col in phase change timing though there might be differences in a particular phase change related trait. For example, Bak-2 has slightly delayed abaxial trichome appearance but the leaf shape tends to be adult-like. Tu-scha-9 is slightly early phase change while Sha, Leb-3 and Shigu-2 are significantly precocious.

As a brief summary, vegetative phase change varies greatly among ecotypes. And the variation in most cases reflects overall change of phase change instead of just one sub-trait, which supports the idea that vegetative phase change is crucial for adaptation to different environment and is under selection.

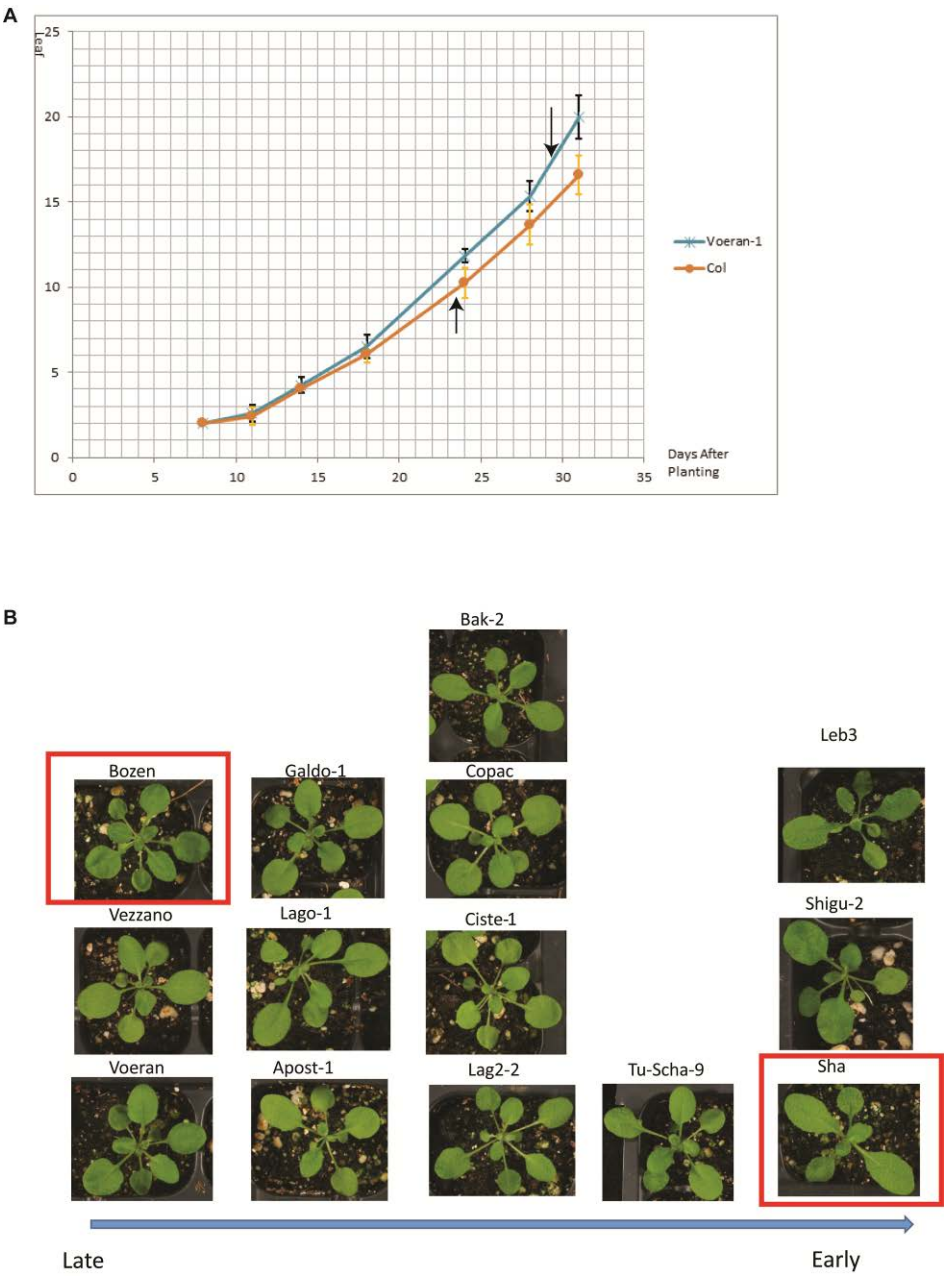

Figure 5.2 Sorting ecotypes according to their vegetative phase change phenotypes.

A. Example of leaf initiation measurement combined with abaxial trichome data.

B. Ecotypes are sorted by their vegetative phase change phenotypes.

5.3.2 miR156 abundance is not the cause of the phase change variations among ecotypes

A first step toward unraveling the genetic basis for the natural variation in phase change would be measuring the miR156 abundance in ecotypes with dramatic phase change phenotypes. 15-day old seedlings grown under 22C SD conditions were harvested for Northern Blotting analysis. As shown in Figure 5.3A, miR156 abundance only showed small fluctuations among ecotypes. These small differences are unlikely to produce the wide range of vegetative phase change phenotypes observed according to previous quantitative miR156 analysis. To further confirm this result, we measured the abundance of miR156, miR157 and miR172, which all regulate phase change, in Col, Bozen-1 and Sha leaf primordia harvested at different time points. There were very small variations of miRNA abundance among these ecotypes (Appendix 8.2), which could not explain the drastic vegetative phase change differences. We further looked at whether *SPL* transcript levels are altered in Sha compared to Col. Interestingly while miR156 abundance showed little changes, *SPL3* and *SPL15* transcripts were moderately elevated in Sha, possibly through a miR156-independent mechanism.

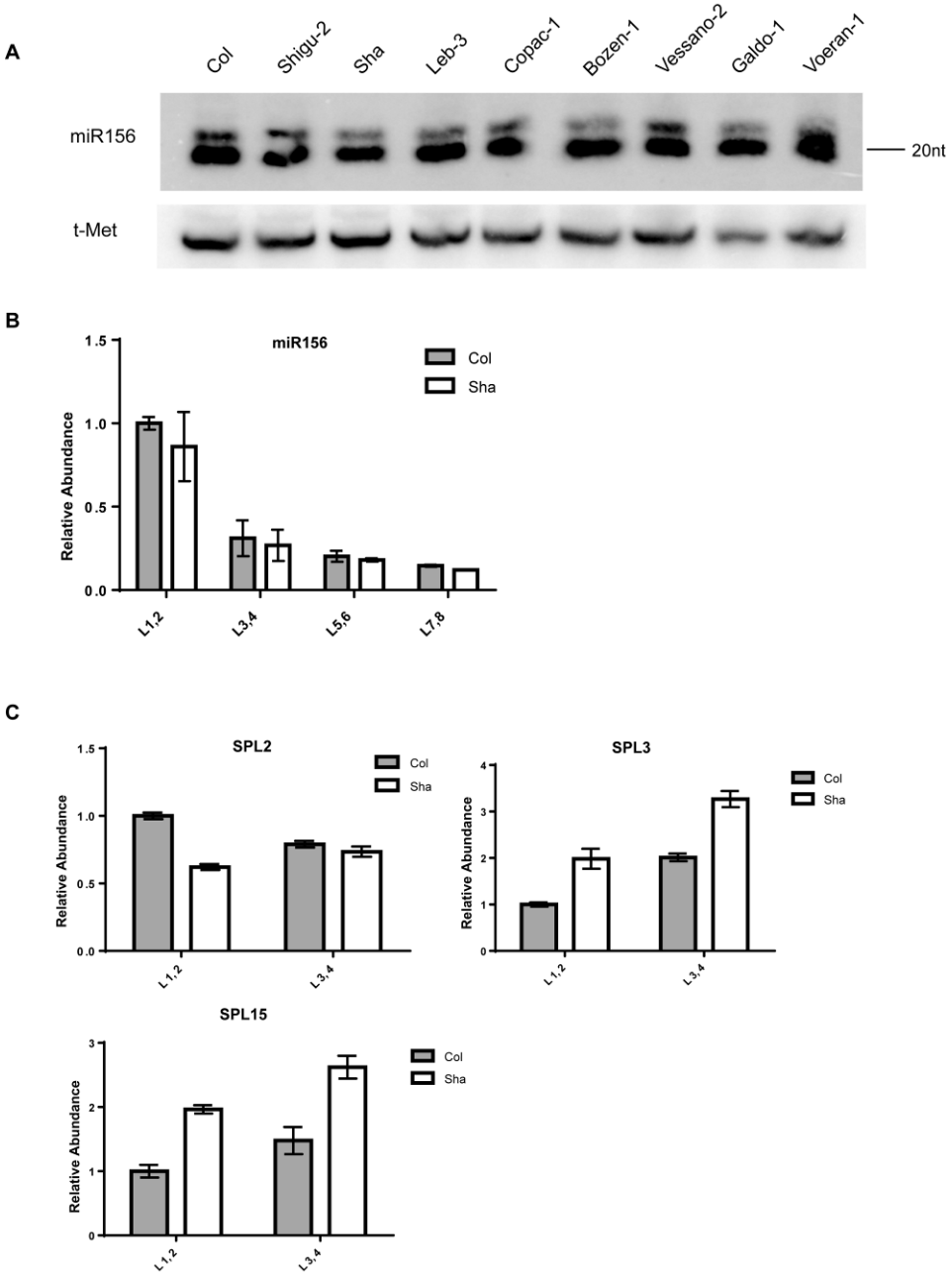

Figure 5.3 miR156 abundance and *SPL* transcript levels in ecotypes.

A. Northern Blotting of miR156 in 15 day old seedlings grown under 22C SD conditions.

B. qPCR of mature miR156 in Sha leaf primordia series in comparison to Col.

C. qPCR of *SPL2*, *SPL3*, *SPL15* in Sha leaf primordia compared to Col.

5.3.3 Mapping the genetic basis for the Sha phenotypes using Traffic Lines

Of the ecotypes we examined, we chose Sha to start mapping the genetic basis for its phase change phenotypes. Sha is a strongly precocious ecotype, with distinctive leaf shape characteristics compared to Col. F1 plants from the Sha to Col cross have very slightly precocious but close-to-Col phenotypes therefore the polymorphism(s) controlling the Sha phenotypes are incompletely recessive. Rough mapping was performed using the F2 segregating population from which DNA samples of strong Sha-like individuals (less than 25% of the whole population) were analyzed by SSLP markers. Linkage to several markers on Chr. 2 was observed, which placed the causative polymorphism from 10mb to 11.7mb. To confirm the rough mapping result, a strong Sha-like plant from the F2 population was backcrossed to Col and let self-pollinate in the next generation. The resulting backcross F2 population was then analyzed with SSLP markers on Chr.2. As shown in Figure 5.4A, when genotyped using SSLP marker F27A10 located at 10.57mb on Chr. 2, plants displaying early phase change phenotypes showed predominant Sha genetic background, and late phase change plants showed predominant Col background, while intermediate plants had heterogeneous genetic background.

However, further attempts to reduce the interval were unsuccessful because of difficulties in correctly assessing phenotypes. This was probably because multiple genes along the region contribute to the Sha phenotype, which at the same time regulated by multiple modifiers located on different chromosomes. When recombination occurred, there was no way to guarantee homozygous recombinant in between the desired interval. And the segregation of modifiers would make it even more difficult. The key to

solving the problem is to efficiently select lines with homozygous recombinant chromosomal regions in between the 10mb to 11.7mb interval.

This became possible with the newly introduced Traffic Lines (Wu et al., 2015). Traffic Lines are transgenic Col plants bearing seed-expressed GFP and RFP transgenes at given chromosomal locations. Figure 5.4B illustrates how a Traffic Line, specifically a line having RFP and GFP markers at 10mb and 11.7mb respectively, could be used to efficiently select homozygous recombinants. Sha or a Sha-like plants from the mapping population are crossed to the Traffic Line, followed by a backcross to Col. Seeds from this backcross are then selected under a fluorescent microscope for the presence of RFP but no GFP, which represents a recombinant having Sha genetic background from a random location south of the 10mb RFP marker. Similarly we also choose seeds with GFP but no RFP, which corresponds to Sha recombinants from a random location north of the 11.7mb GFP marker. Self-pollinated seeds from these two groups are then selected again by fluorescence. Strong RFP lines are homozygous Sha recombinants from random locations south of the 10mb RFP marker while strong GFP lines are homozygous Sha recombinants from the other direction.

Multiple homozygous recombinant lines were obtained using this method. The genetic background in between this chromosomal region was determined for each recombinant by dCAPs markers, and was analyzed along with plant phenotypes. Another advantage of using Traffic Lines in generating homozygous recombinant is accurate phenotyping even when the phenotypes are subtle. Rather than relying on a single plant, multiple progenies from the same homozygous recombinant were grown and analyzed, giving us statistical power to determine the phenotype. As shown in Figure 5.4C, several homozygous recombinant lines placed the polymorphism within 10.679mb and 10.78mb.

A

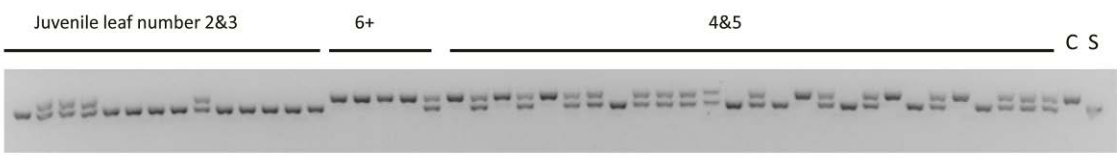

SSLP marker F27A10 (10.57mb)

B

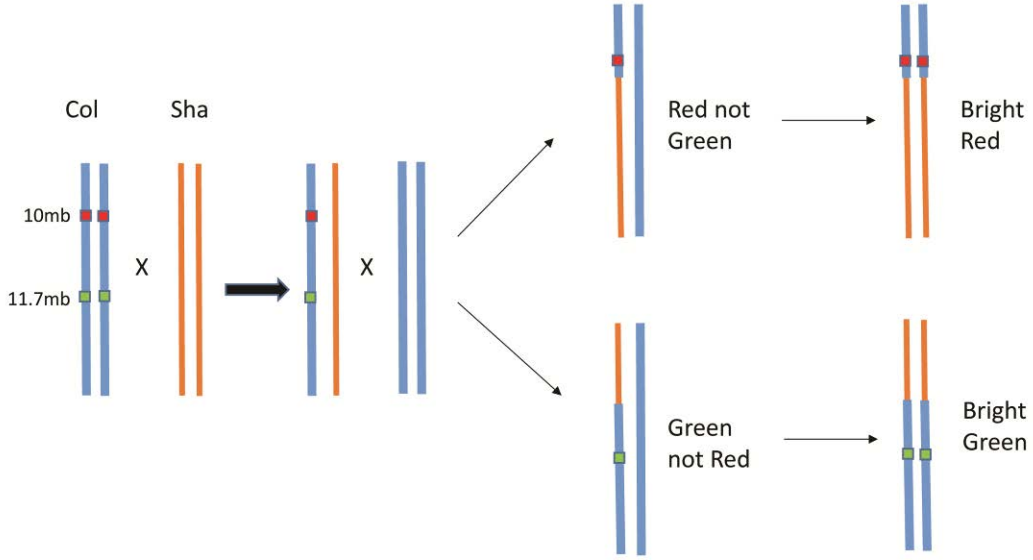

C

Line-10.0	CR640(10)	10.1	10.2	10.4	10.516	10.57	10.673	10.6792	10.78	10.906	11.19	CG515(11.7)	phenotype
1455G-1	sha	sha	sha	sha	sha	sha	sha	sha	sha	Sha	Col	col	sha
1455G-6	sha	sha	sha	sha	sha	sha	sha	col	Col	Col	Col	col	Col
1455G-9	sha	het	het	sha	sha	sha	sha	sha	sha	Col	Col	col	Sha
1455G-17	sha	sha		sha	sha	sha	sha	sha	Col	Col	Col	col	Col

Line		10.681	10.69	10.7	10.71	10.72	10.73	10.74	10.76	10.78	10.91	Phenotype
1609G		SHA	SHA	SHA	SHA	SHA	COL	COL	COL	COL	COL	Sha
1610R		COL	COL	COL	COL	COL	COL	SHA	SHA	SHA	SHA	Col

Figure 5.4 Mapping the polymorphism responsible for the Sha phenotypes.

A. SSLP marker F27A10 at 10.57mb on Chr. 2 demonstrate the co-segregation of Sha genetic background and early phase and the early abaxial trichome phenotype.

B. Strategy to obtain homozygous Sha recombinants between 10mb and 11.7mb interval, using Traffic Lines.

C. Genotypes and phenotypes of homozygous Sha recombinant lines.

5.4 Discussion

5.4.1 Candidate polymorphism for the Sha phenotype.

Within the small interval we identified, *ARABIDOPSIS* RESPONSE REGULATOR 12 (ARR12) appears to be a candidate for further analysis. ARR12 locates at 10.727mb on Chr.2, and is one of the 11 type-B response regulators that are involved in cytokinin responses (Mason et al., 2005). Although there were no reports suggesting a relationship between the cytokinin pathway and vegetative phase change, it was reported that enhanced cytokinin pathway led to early flowering and prolonged reproductive phase (Bartrina et al., 2017). Sha bears a one-nucleotide deletion in ARR12 promoter region compared to Col. Interestingly, this polymorphism is shared among several early phase change ecotypes from central Asia, but is not present in the late phase change ecotypes we analyzed. qPCR was performed to measure the transcript level of ARR12 in Sha compared to Col. In young leaf primordia at different leaf positions, ARR12 shows moderate increase of transcript abundance in Sha compared to Col (Figure 5.5A).

We next examined the phenotype of loss-of-function ARR12 mutations, but there was no significant differences to Col. Because of the high redundancy of ARRs as reported in cytokinin responses, we further analyzed the phenotypes of a triple loss-of-function mutant *arr1/10/12*. *arr1/10/12* displayed slower growth in the vegetative phase, and developed smaller and round leaves than WT. Abaxial trichome appearance was significantly delayed as well. Thus ARRs may act redundantly to promote adult phase identity. Over-expression lines of ARR12 have been made and will be analyzed in the future.

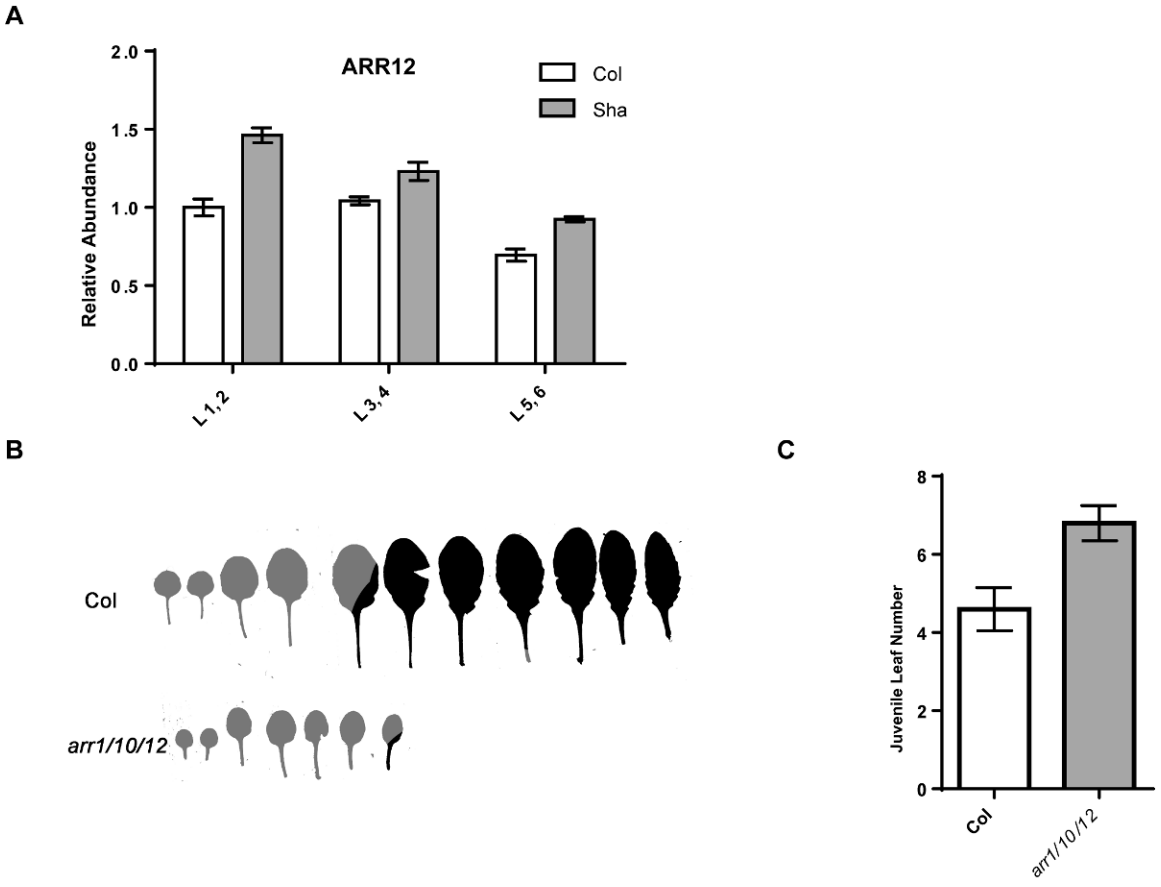

Figure 5.5 *ARR12* is a candidate for the Sha phenotype.

A. qPCR results show increased ARR12 transcript levels in Sha compared to Col.

B and C. Triple mutant *arr1/10/12* shows delayed phase change.

5.4.2 Traffic Lines as a tool for mapping natural variation

Mapping natural variation(s) among ecotypes can be difficult in some cases. A possible scenario is when the phenotype difference is controlled by multiple genes that are genetically linked. When using conventional mapping approaches, we can locate the causal polymorphism to the range containing these linked genes. However identifying homozygous recombinants in between the interval will required enormous amount of genotyping. The Traffic Lines hugely simplified the screening process by "visualizing" the homozygous recombinant with high accuracy without any molecular biology bench work. The process of making the desired recombinants using Traffic Lines also clears up genetic background of the other chromosomes, which is always helpful for increasing our confidence of the identified polymorphism.

Traffic Lines are also useful in the initial identification of the causal polymorphism region. There are collections of Traffic Lines where each line bears RFP and GFP markers flanking approximately one third of a particular chromosome. 15 such traffic lines could encompass all five chromosomes in the *Arabidopsis* genome. The ecotype of interest is crossed to all 15 traffic lines and the F2 seeds of each cross will be planted depending on the fluorescence. For each F2 population, plants from non-fluorescent seeds are compared against those from fluorescent seeds. If the polymorphism controlling the phenotype of interest lies in between the GFP and RFP markers of one traffic line, we would expect uniform phenotypes from non-fluorescent seeds, while a uniformly different phenotype from all fluorescent seeds.

We believe the Traffic Lines will become an extremely useful tool in future studies of natural variation, and also in *Arabidopsis* genetics in general.

6. Conclusions and Future directions

6.1 Conclusions

In Chapter 2, we performed detailed genetic analysis of miR156 and miR157 in *Arabidopsis* and demonstrated that *miR156A*, *miR156C*, *miR157A* and *miR157C* are the major contributors to the mature miR156/miR157 pool. The abundance of miR156/miR157 changes in a non-linear fashion during shoot development, and that the morphological consequences of variation in miR156/miR157 depends on the absolute amount of these transcripts. Major changes (e.g. a 50% reduction) in the level of miR156/miR157 have relatively little effect on leaf morphogenesis when these transcripts are abundant, as is the case early in shoot development. The morphological transitions associated with vegetative phase change require a relatively low level of miR156/miR157; once the abundance of these miRNAs has declined sufficiently, small changes in their abundance can have major effects on leaf size and shape. Although miR156 is less abundant than miR157, it has a more significant impact on early vegetative morphology than miR157, which can be partially explained by miR156's higher loading efficiency onto AGO1 than miR157.

In Chapter 3, we examined how *SPL* genes responded to changes in miR156/miR157 abundance. *SPL2*, *SPL9*, *SPL10*, *SPL11*, *SPL13* and *SPL15* transcripts are differentially sensitive to miR156/miR157-induced cleavage. *SPL9* and *SPL13* both play important roles in miR156-mediated developmental transitions although miR156/miR157 have different effects on the stability of their transcripts. Quantitative analysis of the effect of miR156 on the RNA and protein levels of *SPL9* and *SPL13* indicates that miR156 regulates *SPL13* mainly by promoting its translational repression, but regulates *SPL9* via both transcript cleavage and translational repression. The non-linear response of SPL

gene expression to variation in the abundance of miR156/miR157 provides a molecular mechanism for the rapid, qualitative changes in shoot morphology that occur during vegetative phase change.

In Chapter 4, we demonstrated that *VAL*s are required for the down-regulation of miR156 during vegetative phase change. Loss-of-function *val1* mutants display moderate delay in phase change while *val1/val2* double mutants have severely prolonged juvenile phase which correlates with elevated miR156 abundance. The increased abundance of miR156 is the result of increased *Pri-miR156A* and *Pri-miR156C* transcript levels, accompanied by reduced H3K27me3 in the genomic region. Inducible knock-down of *VAL1* in *val2* mutant background during seedling stage demonstrates that the effects of *VAL*s on vegetative development are not the residual outcome of arrested embryonic development.

In Chapter 5, we explored natural variation of vegetative phase change among ecotypes of *Arabidopsis* and found a wide range of phenotypic variations that were not directly related to miR156 abundance. Rough mapping of the polymorphism(s) responsible for the early phase change phenotypes of Sha indicated a candidate region on Chr. 2. Subsequent mapping utilizing the Traffic Lines narrowed the polymorphism between 10.679mb and 10.78mb on Chromosome 2. Within the interval, *ARABIDOPSIS RESPONSE REGULATOR 12* (*ARR12*) has a one-nucleotide deletion in the promoter region of Sha, which may contribute to its increased transcript level compared to that in Col. While *arr12* loss-of-function mutations in Col did not show significant phenotypes, the triple mutant *arr1/10/12* displayed delayed phase change in Col.

6.2 Generating miR156 and miR157 loss-of-function mutations using the CRISPR-Cas9 genome editing systems

The use of T-DNA insertional mutations in our previous genetic analysis of miR156 and miR157 provided valuable information on how these miRNAs regulate vegetative phase change. However there are some caveats when working with T-DNA insertional mutations. Firstly, T-DNA mutants don't always work well with transgenic reporter lines as the transgenes are prone to silencing. When SPL-GUS reporters were crossed to *miR156a/c* or *miR157a/c* mutants, we observed frequent occurrence of silencing. This might have been due to the increased SPL-GUS expression, or the common components on the SPL-GUS construct and the T-DNA insertion causing RNAi. Using an *rdr6* genetic background may help reduce the chance of silencing but will increase the difficulty of genetic analysis. The second complication brought by the T-DNA mutants is the fact that some T-DNA insertional mutations are from an ecotype other than Col. Even after several generations of introgression to Col, it is inevitable to have random chromosomal segments from another ecotype remaining in the line which could affect phase change phenotypes. Thirdly, the current T-DNA mutation library cannot guarantee a knock-out mutation in a given gene. In fact, when we were trying to identify *miR156f* loss-of-function mutations, the T-DNA insertional mutation in *miR156F* resulted in increased transcript level of *Pri-miR156F*. Last but not least, T-DNA insertional mutations can cause chromosomal rearrangement such as translocations (Clark & Krysan, 2010), making certain lines harder to work with, and also increasing the difficulty establishing causal relationships between genes and phenotypes.

In recent years, CRISPR (Clustered Regularly Interspaced Short Palindromic Repeats)/Cas (CRISPR-associated) system brought significant advancement in targeted genome editing (Cong et al., 2013). The application of CRISPR-Cas9 system in *Arabidopsis* for efficient genome editing has been successful (Yanfei Mao et al., 2013; Y. Mao et al., 2016). This system generates double-strand breaks (DSBs) at target sites mediated by the short guide RNA (sgRNA). DNA sequence modifications including insertion, deletion or point mutations are then achieved via the error-prone non-homologous end joining (NHEJ) pathway or sequence replacement through the error-free homologous recombination (HR) pathway. After stable mutations at the target loci are obtained, the CRISPR-Cas9 transgene can be removed by backcrossing.

CRISPR-Cas9 systems appear to be ideal for generating loss-of-function mutations in miR156 and miR157. There is a canonical PAM sequence (5'-NGG-3') 4 nucleotides away from the 3' of mature miR156 and miR157 in the *Arabidopsis* genome. When we design a guide RNA targeting this site, multiple miR156 or miR157 loci in the genome can be edited by this same CRISPR-Cas9 transgene. Since our goal is to find loss-of-function mutations, we can focus on screening deletion mutations resulting in the loss of mature miR156 or miR157 sequences in each locus. After a mutation in one of the miR156 or miR157 genes has been identified, we can cross it to WT to remove the CRISPR-Cas9 transgene, or harvest the seeds to allow mutations in other miR156/miR157 loci to be induced. The ability to continuously induce loss-of-function mutations in different miR156/miR157 loci over generations is very helpful for generating double, triple or higher order mutants especially when some of the genes are linked.

With this rationale, we constructed CRISPR-Cas9 targeting miR156 or miR157 loci in *Arabidopsis* genome in the pCAM-NAP:eGPF vector, where selection of plant

transformants is achieved by seed fluorescence (Wu et al., 2015). Individual T2 plants were genotyped using primers flanking the miR156 mature sequences in different miR156 genomic loci. Seeds from mutant candidates were harvested individually and further screened/confirmed in the next generation. From the preliminary screening, we were able to identify mutations that resulted in the deletion of miR156 mature sequence in different miR156 loci, including a double mutant *miR156e-1/miR156f-1*. This is of particular interest since *miR156E* and *miR156F* are both located on chromosome 5. Figure 6.1 shows the nature of the miR156E and miR156F mutations. *miR156e-1* is a mutation causing a 18-nucleotide deletion in miR156E genomic locus, which includes 15 nucleotides of the miR156 mature sequence and another 3 nucleotides right at the 3' of it. *miR156f-1* is a mutation causing a 79-nucleotide deletion in miR156F genomic locus, which includes the full miR156 mature sequence.

These preliminary results demonstrated that our CRISPR-Cas9 system is suitable for generating loss-of-function miR156/miR157 mutations in Col background. With additional work in future screening, we are likely to have a collection of high quality miR156/miR157 loss-of-function mutations.

Figure 6.1 CRISPR-Cas9 induced miR156 mutations.

Shown here are examples of CRISPR induced stable mutations in *miR156E* and *miR156F*. WT *miR156E* and *miR156F* sequences are aligned with homozygous mutations identified. Dashed lines represent deletions. Red colored nucleotides are mature miR156 sequences.

6.3 Phase change mutant screen using sensitized genetic background

Our understanding of vegetative phase change has been greatly facilitated by genetic screens for altered phase change timing using abaxial trichome as a phenotypic marker. The mutations resulted from previous screens were mostly precocious mutants with strong phenotypes. In fact, a large percentage of these mutations involved the general miRNA biogenesis pathway. Mutations in specific miR156 regulators or miR156 regulatory elements have not been identified. The genetic analysis of miR156 and miR157 from previous chapters provided explanation to this observation. The phase change phenotypes correlate with miR156/miR157 levels in a non-linear fashion therefore in a WT genetic background, significant phenotypes would not appear until miR156 abundance shows ~80% decline. Since each of miR156A and miR156C contributes to 40%-50% of the total mature miR156, down-regulation of one of them would not produce visible phenotypes. To have the ability to identify mutations that affect miR156 abundance, possibly in a temporal manner, it is necessary to use a sensitized genetic background where moderate changes in miR156 produce visible phenotypes. As shown in Chapter 2, when miR156A or miR156C was mutated in the *miR157a/miR157c* background, we observed much stronger precocious phenotypes, thus *miR157a/miR157c* is a suitable genotype to perform such screening. Moreover, since

miR157a/miR157c by itself is moderately precocious, screening for late phase change mutations can be easier than in WT.

We performed an EMS mutagenesis using *miR157a/miR157c* as the genetic background. Roughly 10,000 *miR157a/miR157c* seeds were mutagenized by EMS and grew under standard conditions. Seeds from approximately every 150 M1 plants were harvested in bulk. M2 seeds were planted and screened for precocious or late phase change phenotypes. Mutants of interest were then harvested individually. To determine whether miR156 was specifically affected in those mutants, qPCR was performed to quantify the fold change of miR156 and other miRNAs (miR159, miR166 or miR167). According to the miRNA level patterns, mutants could be sorted into four categories. 1) miRNA level in general is not changed. 2) miR156 and other miRNAs are reduced. 3) miR156 and other miRNAs are elevated. 4) miR156 abundance is affected while other miRNAs remain unchanged.

Table 6.1 shows a brief summary of some mutants from the screen. The quantification of miRNAs in those mutations is shown in Appendix 8.3. There are several mutants of particular interest. 1561 is a mutation with an early phase change phenotype. There is ~50% reduction of miR156 abundance while other miRNAs are not affected. This mutation would not have been identified without using the sensitized genetic background since 50% reduction of miR156 in WT generally produces weak phenotypes that hardly stand out in mutant screens. This mutation could possibly be a regulatory element in miR156A or miR156C, which is responsible for its normal expression. It could also be an important regulator promoting the expression of miR156. 10-4 is another interesting mutation which has moderate delay in phase change and increased abundance of miR156 and other miRNAs.

Individual mutants were backcrossed to *miR157a/miR157c*. F2 seeds were harvested and ready for bulk segregation mapping analysis using the map-by-sequencing methods (James et al., 2013).

	Phenotypes	miRNA abundance
1410	3 juvenile leaves (early)	Slightly increased miR156, no changes in other miRNAs
1411	2 juvenile leaves (early), sqn like	Reduced miR156 and other miRNAs
1412	3 juvenile leaves, (early) large leaf 1&2	Slightly increased miR156, Slightly reduced or no changes in other miRNAs
1418	5 juvenile leaves, (late, close to WT), samll&round leaves	Reduced miR156, no changes in other miRNAs
1421	2 juvenile leaves (early)	Reduced miR156, no changes in other miRNAs
1423	2 juvenile leaves (early)	Reduced miR156, no changes in other miRNAs
8-1	2 juvenile leaves (early)	Reduced miR156 and other miRNAs
9-1	2 juvenile leaves (early)	Reduced miR156, slightly reduced or no change in other miRNAs
9-2	2 juvenile leaves (early)	Slightly increased miR156, no changes in other miRNAs
10-4	7 juvenile leaves (late)	Increased miR156 and other miRNAs
10-5	2 juvenile leaves (early)	No changes in miR156 and other miRNAs
11-1	2 juvenile leaves (early)	Reduced miR156 and other miRNAs
11-3	2 juvenile leaves (early)	No changes in miR156 and other miRNAs
1553	Late phase change JL=9	No/little change in miRNAs
1554	Late phase change JL=8	No change in miR156, high miR166
1555	Late phase change JL=7	No change in miR156, high miR166
1556	Late phase change JL=7	No/little change in miRNAs
1558	Late phase change JL=8	No/little change in miRNAs
1559	early phase change JL=3	slightly reduced miR156, slightly increased miR166
1560	Probably KANADI	slightly reduced miR156, slightly increased miR166
1561	early phase change JL=2	~50% reduction in miR156, small changes in other miRNAs
1562	early phase change JL=2	No/little change in miRNAs
1563	early phase change JL=2	No/little change in miRNAs
1676	early phase change JL=3	No change in miR156, increased miR166

Table 6.1 Mutants identified from EMS mutagenesis of *miR157a/miR157c* plants.

The phenotypes of mutants in *miR157a/miR157c* background were characterized under 22C LD conditions where *miR157a/miR157c* had 4.8 ± 0.6 juvenile leaves.

7. Materials and methods

Plant materials and growth conditions

miR156a and *miR156c* mutants were described in a previous study (L. Yang et al., 2013). *miR156d* (SALK_40772), *miR157a* (Flag_375C03), *miR157c* (SALK_039809) were obtained from the *Arabidopsis* Biological Resource Center (Ohio State University, Columbus, OH) and crossed to Col-0 multiple times before further analysis. *VAL* mutants were as described in (M. Suzuki et al., 2007) and were obtained from Dr. Suzuki. Seeds were sowed on watered Farfard #2 Mix soil and put under 4C conditions for 3 days before moving to the growth chamber.

Transgenic lines

miR156 sensitive and resistant versions of SPL13-GUS reporters have been described before (Xu, Hu, Zhao, et al., 2016). The SPL9-GUS reporter construct used in this study was modified from the previously described SPL9-GUS by putting the whole pSPL9:SPL9-GUS into the Napin:eGFP vector with restriction enzymes XmaI and SbfI. SPL9-GUS lines were generated by first transforming the SPL9-GUS construct into *miR156a/miR156c miR157a/miR157c* plants. Homozygous single insertion lines were then crossed to Col and further genotyped to obtain SPL9-GUS lines in different genetic background.

The IndamiRVal1 construct was made by Golden Gate assembly of three main parts. The first part was an artificial miRNA from miR390a backbone targeting *VAL1*, under the

control of a minimum 35S promoter with LexA binding site. The second part consisted of 35S driven XVE module for inducible control of the first part. The third part is pFAST-R which is a selection marker (GFP) under the control of a seed specific promoter.

miR156 and miR157 CRISPR-Cas9 constructs were made according to the methods from Mao et.al. (Yanfei Mao et al., 2013). Briefly speaking, DNA duplexes corresponding to the guide RNAs targeting miR156 or miR157 were synthesized from IDT and hybridized. The hybridized DNAs were then cloned into psgR-Cas9-At using type II restriction enzyme mediated digestion-ligation reactions. Confirmed clones were then cloned into the Napin:eGFP binary construct for plant transformation via EcoRI and HindIII restriction sites.

The estradiol-inducible MIM156 line was constructed using a gateway compatible version of the XVE system as described (Brand et al., 2006). The MIM156 as described in (Franco-Zorrilla et al., 2007) was cloned into pMDC160 by standard gateway cloning method using primers in Table S1 (referred to as pMDC160-MIM156). Plants containing pMDC150-35S (Brand et al., 2006) were crossed to transgenic pMDC160-MIM156 plants and made homozygous. Induction of gene expression was performed by spraying 10μM 17-ß-estradiol (0.01% Silwet 77) on seedlings at the desired time point. Tissues were harvested at 24hr after induction.

RNA sequencing

Sequencing libraries were generated from small RNAs isolated from shoot apices of *FRI FLC* and *FRI flc-3* seedlings grown in the conditions described by Willmann and

colleagues (Willmann & Poethig, 2011). The shoot apex samples consisted of the shoot apical meristem and leaf primordia 1 mm or less in length. Libraries were generated using a lab-assembled version of Illumina's 2007 small RNA library sample preparation protocol, followed by high-throughput sequencing with Illumina's Genome Analyzer II platform. These sequence data are available in the NCBI Gene Expression Omnibus database under series accession number GSE72303.

MUG assay

Tissue samples were harvested into 2ml tubes submerged in liquid nitrogen, and then homogenized using a bead-beater. 300µl of extraction buffer (10 mM EDTA pH 8.0, 0.1% SDS, 50 mM sodium phosphate pH 7.0, 0.1% Triton X-100; 10 mM ß-mercaptoethanol and 25 µg/ml PMSF added fresh before experiment) was then added to each tube. Samples were mixed well and incubated on ice for 10 mins, after which they were centrifuged at 4^{o}C (13000 rpm) for 15 mins to remove cell debris. 96ul of supernatant was removed and incubated with 4ul of 25mM 4-MUG at 37^{o}CIncubation time varied among reporters to ensure the end fluorescence readings fall within the linear range. The reaction was terminated by adding 100ul of 1M sodium carbonate to each tube, and fluorescence was measured using a Modulus fluorometer (E6072 filter kit). The amount of MU in each sample was then calculated by comparing this reading to a standard curve constructed by plotting the fluorescence readings from serial dilutions (100nM, 250nM, 500nM, 1000n) of 4-MU. The 4-MU equivalent was divided by the incubation time andthis value was then normalized to the amount of protein in the sample, which was determined by performing a Bradford assay on the supernatant

remaining in the original tube. For each sample, GUS activity was expressed as 4-MU equivalent/min/mg protein. Values were then normalized to the control sample of each experiment.

qPCR analysis of miRNA and transcript level

RNA was extracted from young leaf primordia no larger than 1mm in length using Trizol (Invitrogen), and then treated with DNase (Ambion) following manufacture's protocols. For miRNAs, 600ng RNA was used in the reverse transcription reaction with SnoR101 reverse primer and the miRNA specific RT primer. For SPL transcripts quantification, 600ng RNA was used in the reverse transcription with Oligo(dT). qPCR reactions were then run with primers listed in Table S1 in triplicate to generate the result of one biological replicate.

Northern Blotting of miRNAs

Total RNAs were extracted from plant tissues homogenized in liquid nitrogen using Trizol (Invitrogen). The total RNAs were then incubated on ice with 500mM NaCl and 5% PEG8000 for 2 hours and then centrifuged at 13,000 rpm for 10min. Supernatants were collected and incubated with 10% volume of 3M NaOAc and 2 volumes of 100% ethanol at -20C for 2 hours. Small RNAs were then precipitated by centrifugation at 13,000 rpm for 10min, followed by cold 75% ethanol twice. RNA blotting was then performed as

described (Wu & Poethig, 2006). For mixed probe measurements, 1:1 ratio of miR156 and miR157 probes were used.

Absolute quantification of *SPL* transcripts and miRNAs

The mature miR156 and miR157 used as references were synthesized by IDT. The reference transcripts for *SPL* genes were synthesized by *in vitro* transcription. The template for each *SPL* in vitro transcription was generated by PCR using primers in Table S1 and cDNA from Col. Denaturing gel electrophoresis on each purified *SPL* transcript was performed to confirm that the *in vitro* transcription products were single species RNAs with the expected sizes. For each *SPL* quantification, the reference mRNA generated from in vitro transcription was diluted to 1.00E-8 M. Series of 10x dilutions were made in 600ng/µl E.coli. total RNA background and then ran along with RNA samples from Col leaf 3, 4 in qRT-PCR reactions to estimate the approximate concentration of the experimental samples. Then series of 2x dilutions of the reference mRNA near the experimental sample concentration range were made and ran along with the experimental sample in qRT-PCR reactions again. The 2^{-CT} values of the reference samples were plotted against the concentrations. The CT value of the unknown sample was then fitted into the graph to calculate its concentration.

Modified 5' –RACE quantification of cleaved *SPL* transcripts

5 µg of total RNA was used in the ligation reaction with 1 µg of GeneRacer (Invitrogen) RNA adapter following manufacture's protocol without carrying out the de-capping procedure. After 2 hours incubation at 37C, dilute the reaction mixture with nuclease free water and proceed with standard phenol: chloroform extraction. Purified RNA ligation products pellet were then dissolved with 10µl nuclease free water. 5µl of the RNA was used in the reverse transcription reaction with Oligo(dT) primer. qPCR was then performed using primers in Table S1 to quantify cleaved and un-cleaved *SPL* transcripts.

Immunoprecipitation of AGO1-FLAG

Tissues were harvested in liquid nitrogen and homogenized with cold molar and pestle. For each sample, approximately 1mL ground powder was mixed and dissolved in 2mL lysis buffer (50mM Tris HCl, pH 7.4, with 150mM NaCl, 1mM EDTA, 1% Triton X-100, 1mM PMSF, 1% Protease Inhibitor) followed by 15min incubation on ice. 20% homogenized samples were saved for RNA extraction and the rest were centrifuged at 13,000 rpm at 4C for 20min to remove dell debris. The resulting clear supernatants were then filtered through 45µm filters. Immunoprecipitations were then performed using Anti-FLAG® M2 Magnetic Beads (Sigma) following the manufacturer's protocol. After the IP, RNAs were extracted from the beads using Trizol (Invitrogen).

8. Appendix

8.1 Leaf initiation measurements of ecotypes.

The leaf initiation rate of selected ecotypes were measured as visible leaf number plotted against the time of measurement (day after planting). Ecotypes display a wide range of leaf initiation rate. By incorporating abaxial trichome into the graph (as indicated by arrows), we can approximate the duration of the juvenile vegetative phase of each ecotype.

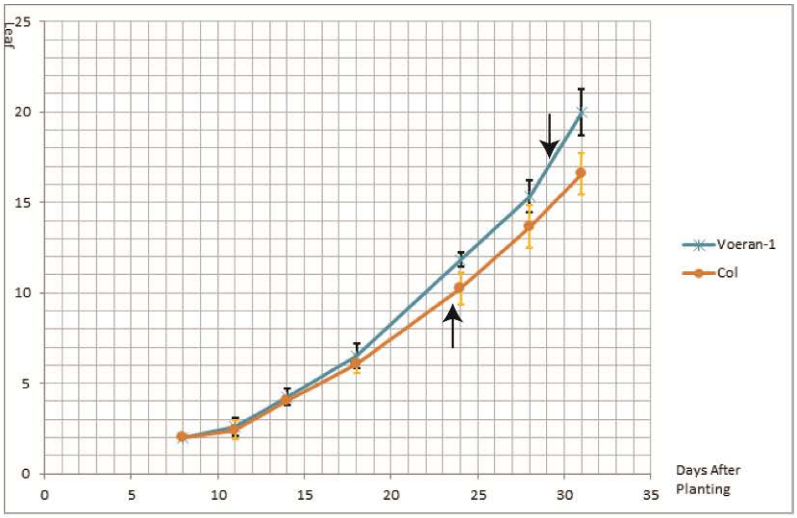
Leaf
25
20
15
10
5
0
0
5
10
15
20
25
30
35
Days After Planting
Voeran-1
Col

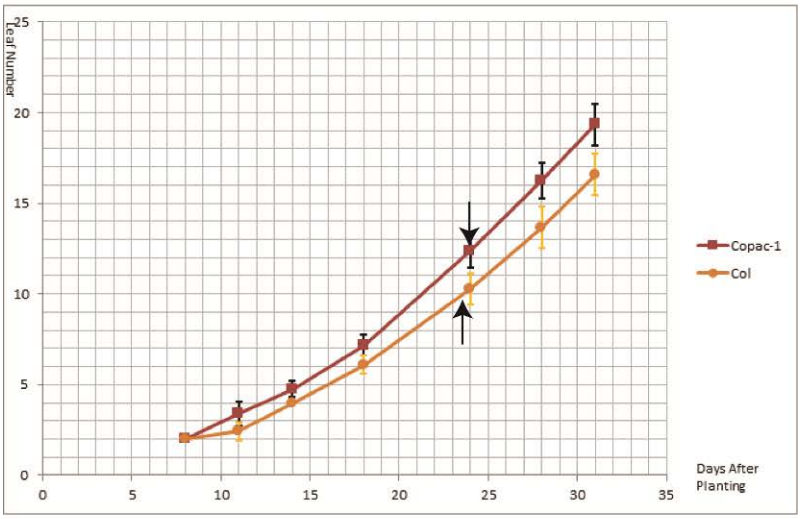
Leaf Number
25
20
15
10
5
0
0
5
10
15
20
25
30
35
Days After Planting
Copac-1
Col

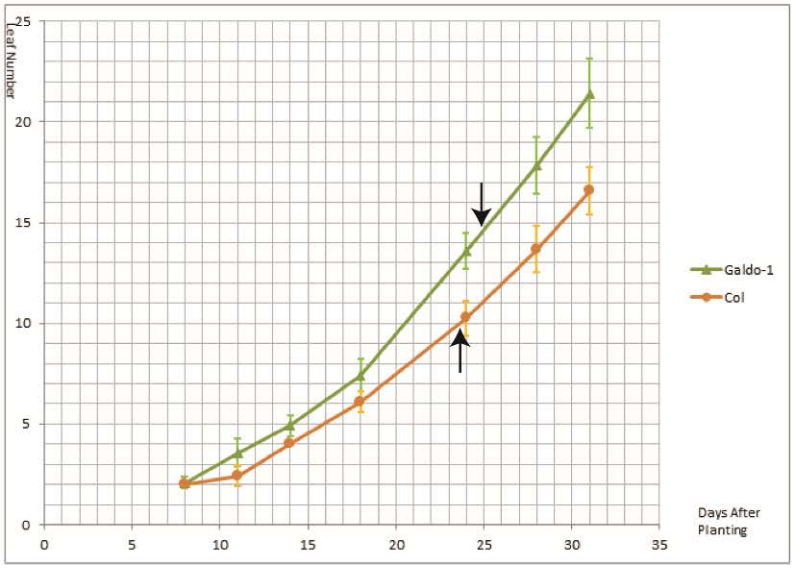
Leaf Number
25
20
15
10
5
0
0
5
10
15
20
25
30
35
Days After Planting
Galdo-1
Col

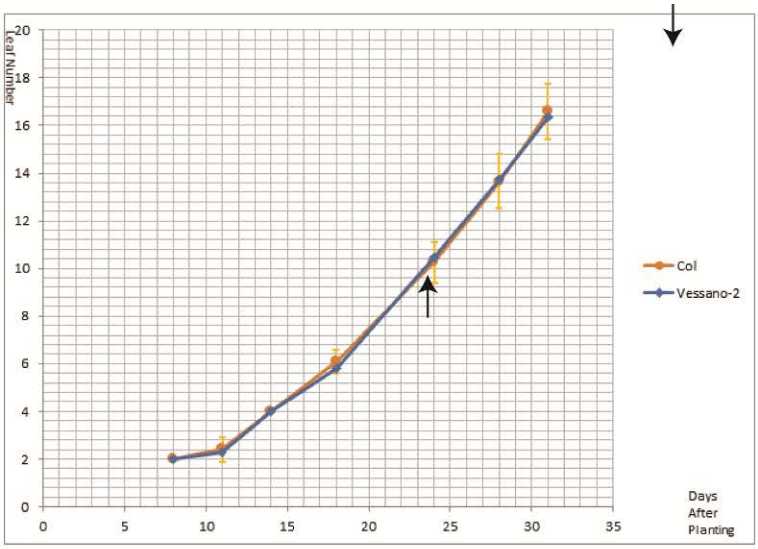
Leaf Number
0
2
4
6
8
10
12
14
16
18
20
0
5
10
15
20
25
30
35
Col
Vessano-2
Days After Planting

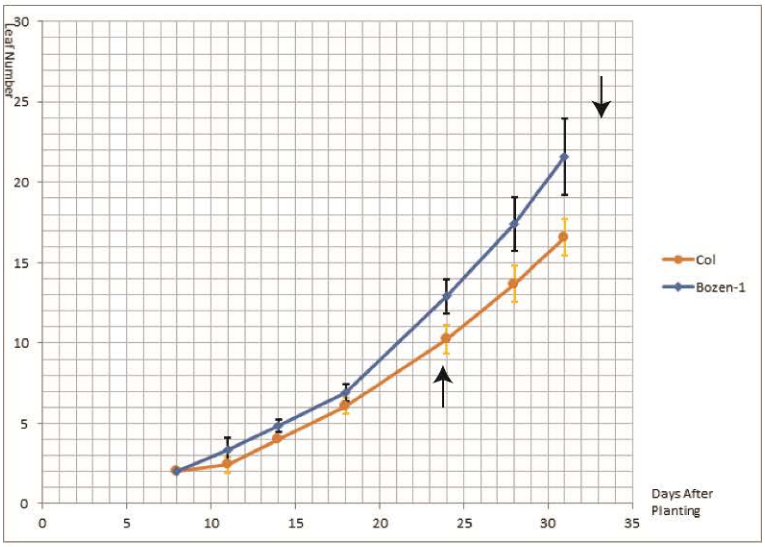
Leaf Number
0
5
10
15
20
25
30
0
5
10
15
20
25
30
35
Col
Bozen-1
Days After Planting

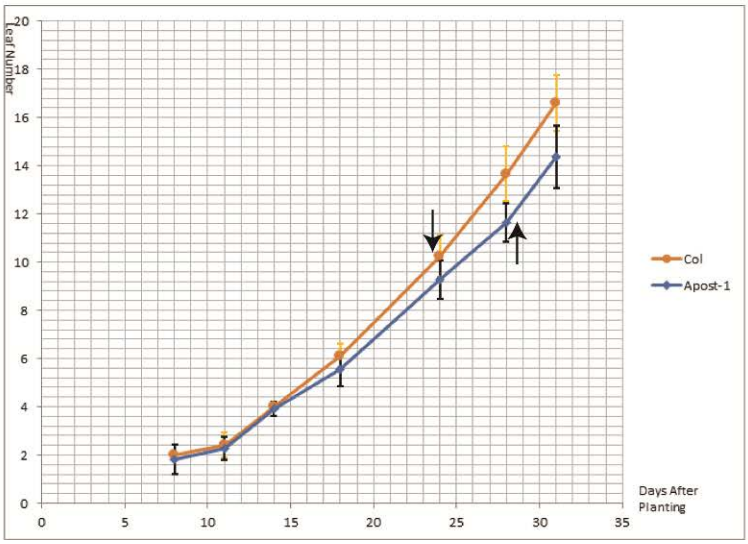
Leaf Number
0
2
4
6
8
10
12
14
16
18
20
0
5
10
15
20
25
30
35
Col
Apost-1
Days After Planting

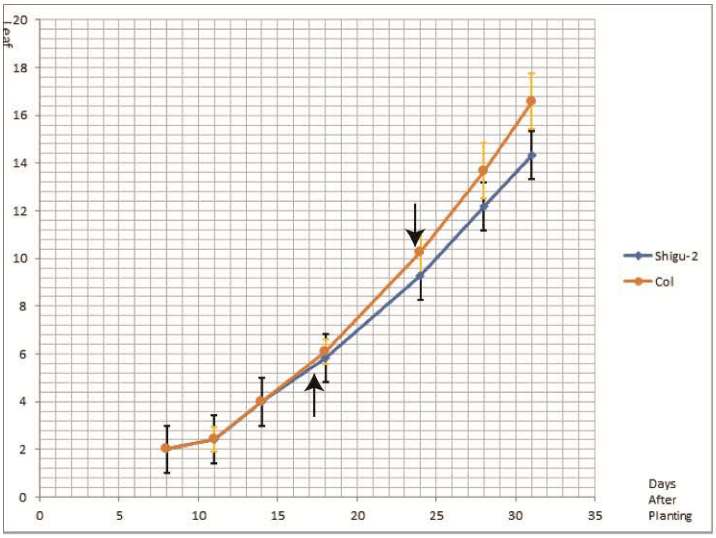
Leaf
Shigu-2
Col
Days
After
Planting

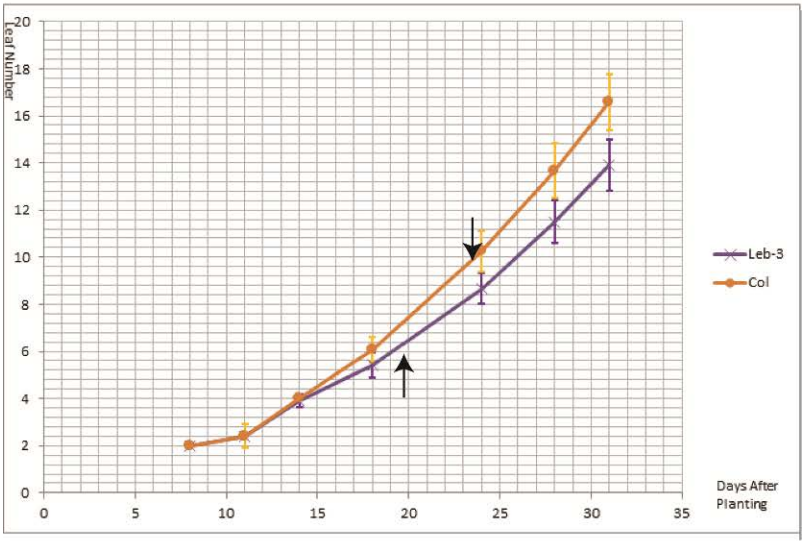
Leaf Number
Leb-3
Col
Days After
Planting

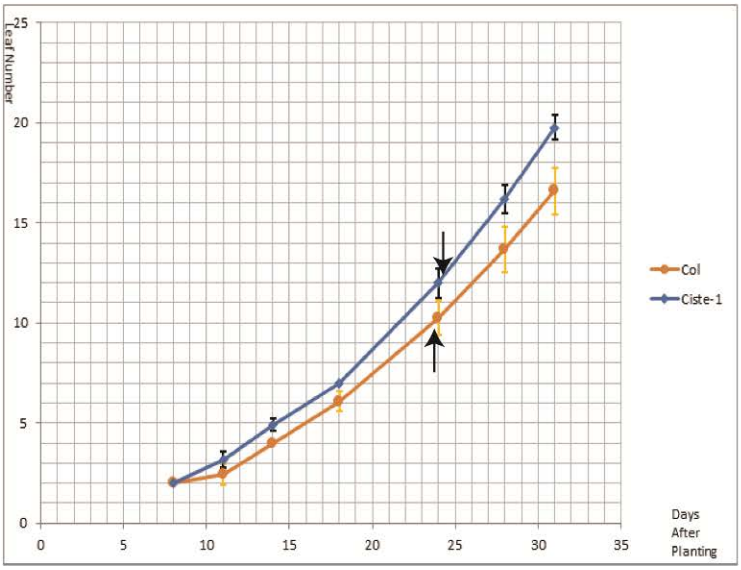
Leaf Number
Col
Ciste-1
Days
After
Planting

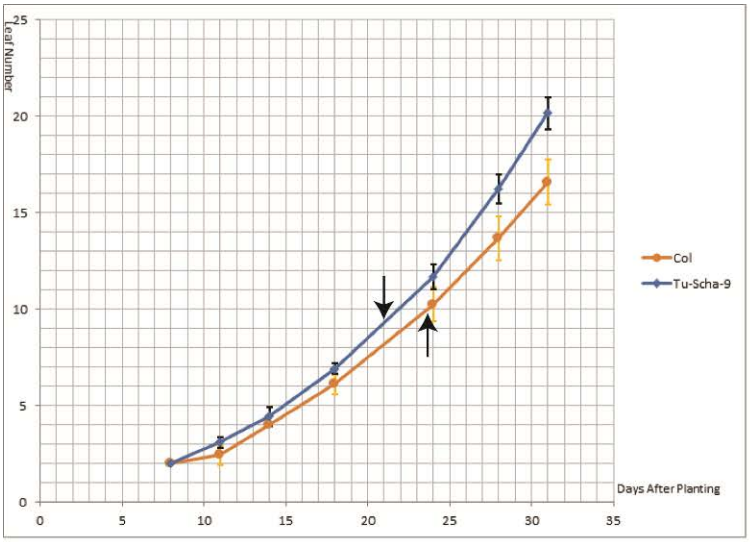
Leaf Number
Days After Planting
Col
Tu-Scha-9

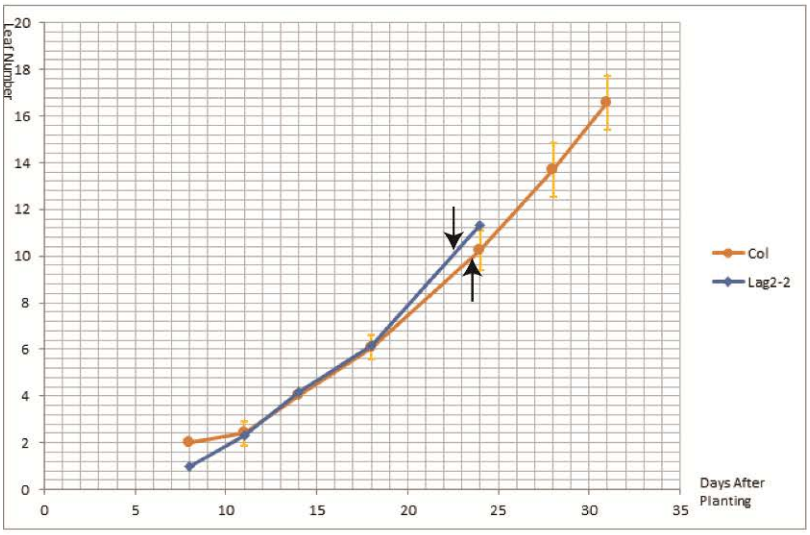
Leaf Number
Days After Planting
Col
Lag2-2

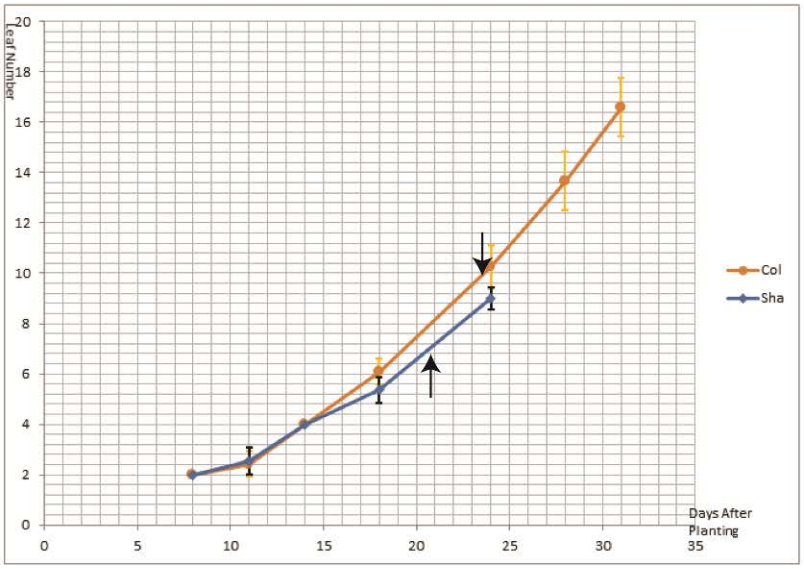
Leaf Number
Days After Planting
Col
Sha

8.2 miRNA abundance in Col, Bozen-1, Sha leaf primordia at different time points.

These important phase change related miRNAs are not differentially regulated in ecotypes.

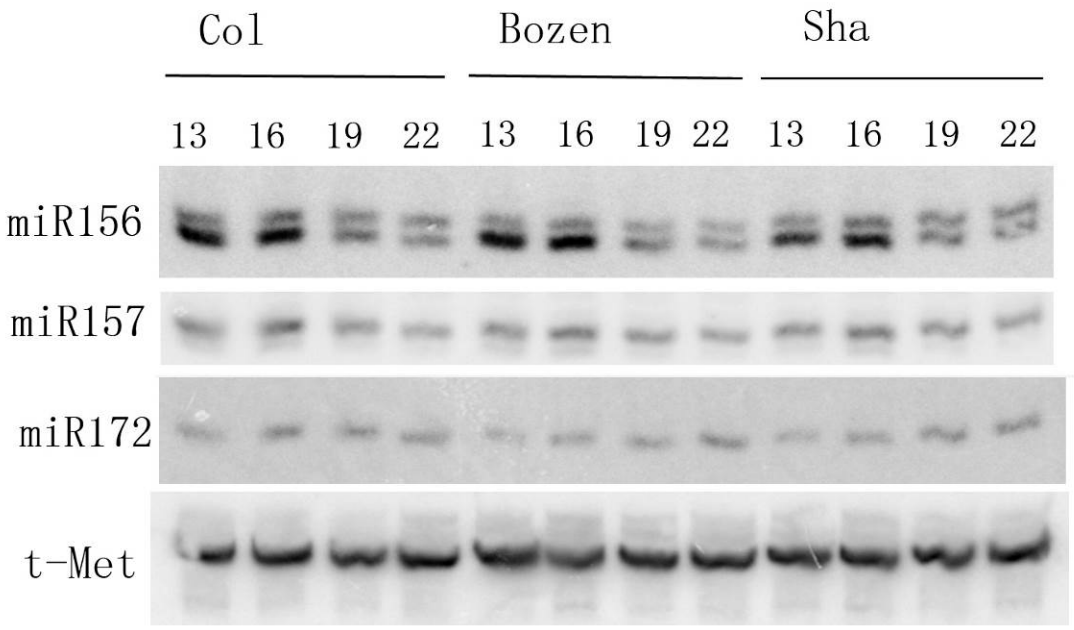

8.3 qPCR analysis of miR156 and other miRNAs in EMS induced mutants from *miR157a/miR157c* background.

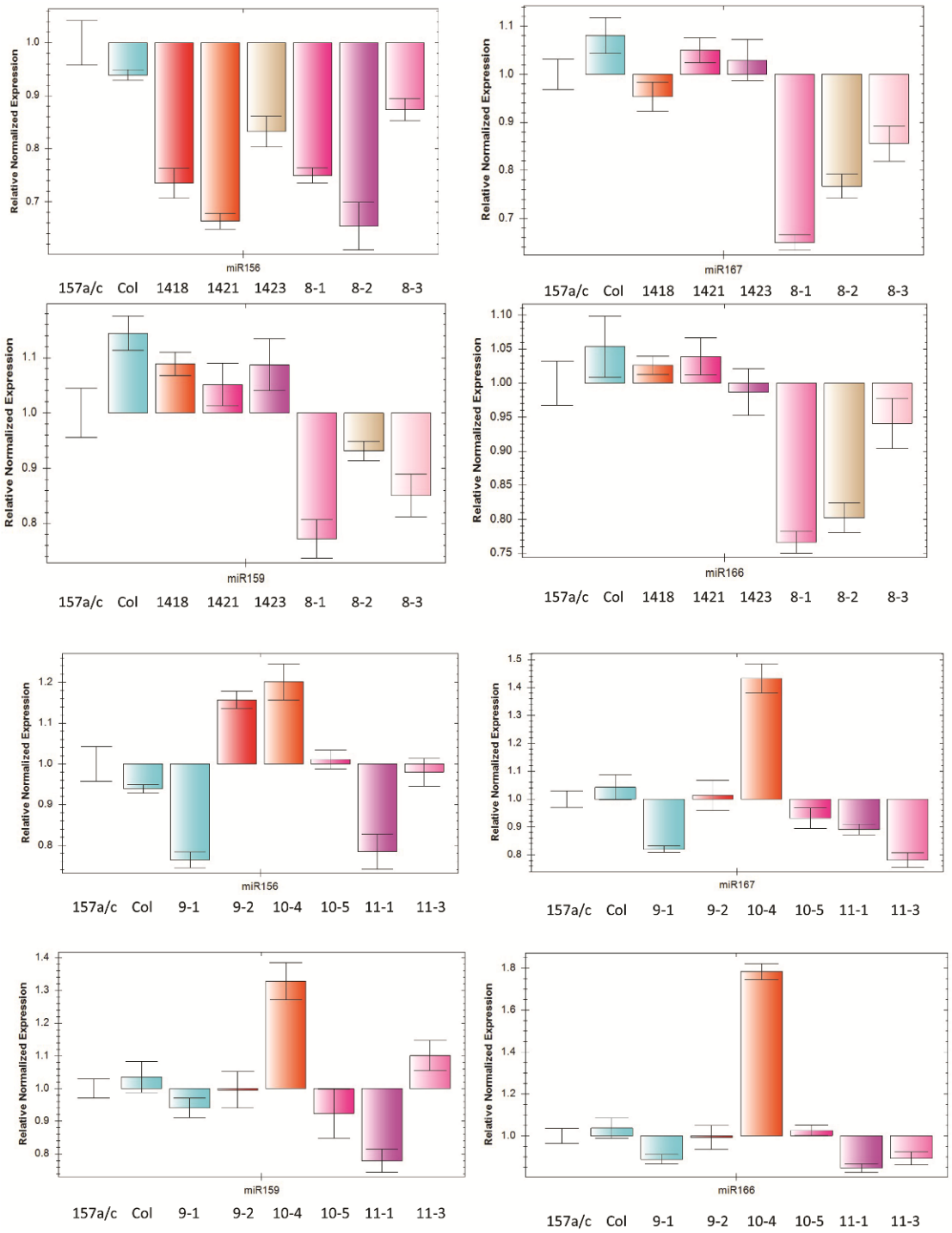

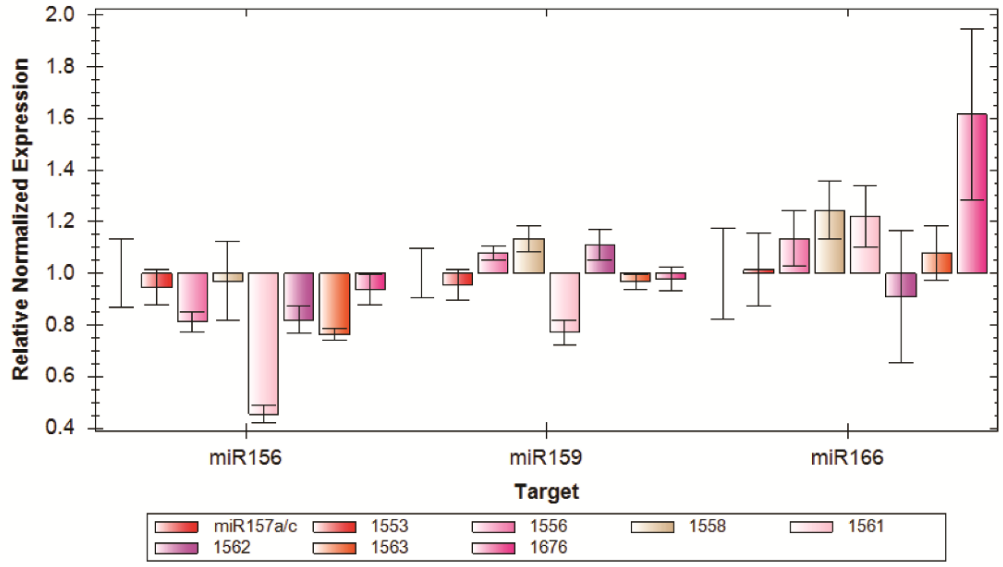
Relative Normalized Expression
2.0
1.8
1.6
1.4
1.2
1.0
0.8
0.6
0.4
miR156
miR159
miR166
Target
miR157a/c
1553
1556
1558
1561
1562
1563
1676

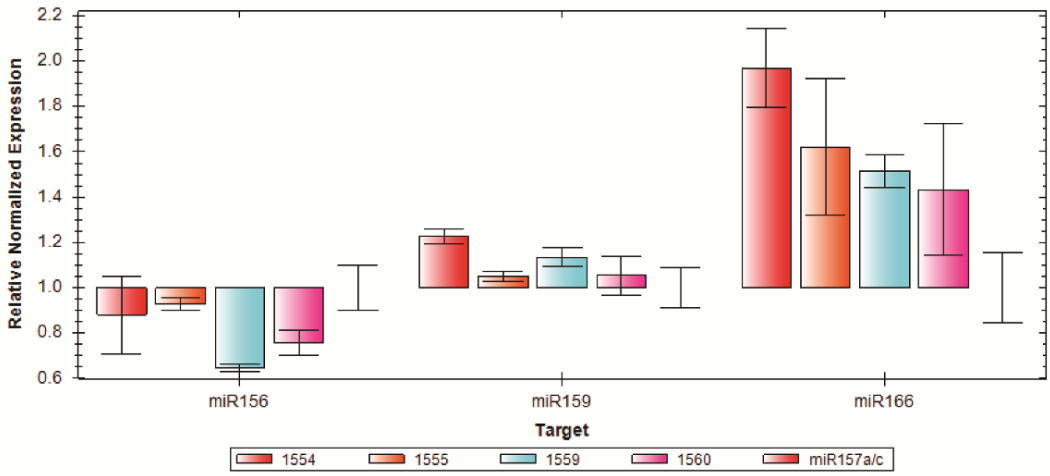
Relative Normalized Expression
2.2
2.0
1.8
1.6
1.4
1.2
1.0
0.8
0.6
miR156
miR159
miR166
Target
1554
1555
1559
1560
miR157a/c

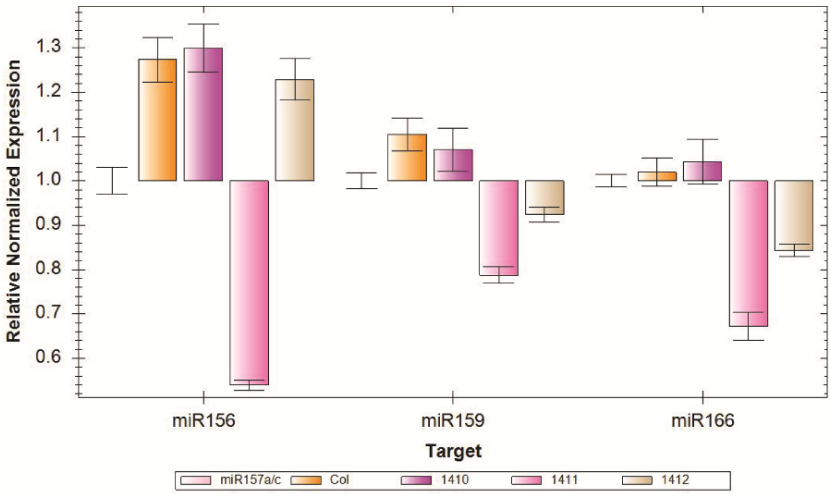
Relative Normalized Expression
1.3
1.2
1.1
1.0
0.9
0.8
0.7
0.6
miR156
miR159
miR166
Target
miR157a/c
Col
1410
1411
1412

8.4 List of primers used.

qPCR

At snoR101-F	CTTCACAGGTAAGTTCGCTTG
At snoR101-R	AGCATCAGCAGACCAGTAGTT
qmiR156-F	GCGGCGGTGACAGAAGAGAGT
qmiR156-R	GTGCAGGGTCCGAGGT
qmiR157-F	GCGGCGGTTGACAGAAGATAG
qmiR157-R	GTGCAGGGTCCGAGGT
qSPL2-F	TTTCCGATACCGAGCACAATAG
qSPL2-R	TACGGGTTGGAGGTTGCTTGAGG
qSPL3-F	ATGAGTATGAGAAGAAGCAAAGCG
qSPL3-R	TCCACTACTACTTGTAGCTTTACCT
qSPL4-F	TCAAGGGTAGAGATGACACTTCCTAT
qSPL4-R	TCTCCTTCGTGGCTCTGAAACTTC
qSPL5-F	CGATAGGTGCACTGTTAATTTGACT
qSPL5-R	TCTGGTAGCTCATGAAACCTGCTGCA
qSPL6-F	ACAGTGCAGCAGGTTTCATTTCCTC
qSPL6-R	CTCCAGAAACTTGTTGCCTACTAC
qSPL9-F	AATTGGCGACTCAAACTGTG
qSPL9-R	CTGAAGAAGCTCGCCATGTA
qSPL10-F	CAGACAAAGGTGTGGGAGAATGCTC
qSPL10-R	TAGGGAAAGTGCCAAATATTGGCG
qSPL11-F	AGTCCAAGTTTCAACTTCATGGCG
qSPL11-R	GAACAGAGTAGAGAAAATGGCTGC
qSPL13-F	GCTCGAGAACCGCATCGTT
qSPL13-R	CCCGTAAAAAACTGTCTCAACTGCT
qSPL15-F	TGAATGTTTTATCACATGGAAGCTC
qSPL15-R	TCATCGAGTCGAAACCAGAAGATG
qSPL-Cleaved-F	GGACTGAAGGAGTAGAAATCTTCTG
qGUS-F	CGTCCAAGGAAACAAGAAGGG
qGUS-R	AGCGTTCTTGTAGCCGAAATC
q-ARR12-F	GGATGCTATGGCTCTGTTGAG
q-ARR12-R	TCTGTTCCTGCTTCATCGTG
qVal1-F2	TGGGATGTGAGTAGGTGTTCA
qVal1-R2	CTTCTCTTCTTGTGCTCTCTTCC
qVal2-F2	CAAAGTGGTCGTGCTCTGAT
qVal2-R2	CTCTGCCGGACAAGTGTATC
qPri-miR156A-F	CTTCGTTCTCTATGTCTCAATCTCTC
qPri-miR156A-R	TGATTAAAGGCTAAAGGTCTCCTC
qPri-miR156C-F	AAAAGCCTCAGATCTAACTCCAACAC
qPri-miR156C-R	GCGTTTCTCTTAAAATTTGTCCCAAAACT

Genotyping	
miR156a-2LP	AAAGAGATCAGCACCGGAATC
miR156a-2RP	CGCGCTTCACTTAAAATTACG
miR156c-1LP	aacagattcttcctctcttctcc
miR156c-1RP	AAAGAGATCACGACTAGAAATCACG
miR157a-1LP	TTTATCATCCACATGCGGTG
miR157a-1RP	TTTTGGTCATCATATAAACGAATTG
miR157c-1LP	TGCAAAATAGGTAGATAGGGCC
miR157c-1RP	TCTCTCCAGTTACAAAACATGACC
miR156d-1LP	cggtttctggactaattggaatttcc
miR156d-1RP	GACTCATCTTTTGAAGCTAGGAGTTGG
156B-TALEN-F	AGAGGGAGAGATGGTGATTGA
156B-TALEN-R	TGTCTAAGCCAAATTTGAGAGAG
Wiscseq_DsLoxHs063_11D.2_LP	ACCAGTCGACCAATACGACC
Wiscseq_DsLoxHs063_11D.2_RP	TCGCAACACTTCTGCGATAG
SALK_059568_LP	TACAGTCCATGCAGTTGCAAG
SALK_059568_RP	ACATGCAACCTCGTTTACCTG
SALK_100053_LP	TATGCAAGGAGTCACACCCTC
SALK_100053_RP	TGACGAAAATCCATGGCTTAC

Sha mapping

Sha-10.513-NcoI-F	TGAATTAATGATGATTTAAACG**C**CAT**G**
Sha-10.513-NcoI-R	AATGGTGTTGAGATGAATGAGTC
Sha-10.516-HindIII-F	ACGTTTTGTATTTTTAACAATGTAAAAG**CT**
Sha-10.516-HindIII-R	GAGAAATGTTGCTTACATTGAAGA
Sha-10.673-EcoRI-R	TTCTCTTATGATCATTGCATCG**G**AA**T**T
Sha-10.673-EcoRI-F	GATTCGCGAATTGAACTAAATC
Sha-10.6792-BglII-F	CTAAATTATTTAAAATAGGAATTAAG**AG**ATC
Sha-10.6792-BglII-R	AATATGCCCCGTCCAATGCA
Sha-10.906-EcoRI-F	GAATATTGTTTCGCCATTAGA**G**A**A**TT
Sha-10.906-EcoRI-R	TGAATAACAACGTACACGTATCAC
Sha-10.824-SalI-F	CAACGGGATGGGACCGCCGTC
Sha-10.824-SalI-R	AAGATGGAATCGTTTTACGACAA
Sha-10.85-HindIII-R	GGATTGGAATACATCAGTTTGAAA**GC**T
Sha-10.85-HindIII-F	CCCACTTTATCACGTCCC
Sha-10.80-SalI-R	TACCTCAGTGTCAGACTTCTCTGTC**GA**

Sha-10.80-SalI-F	GAAATGGATGCCACAAAACAG
Sha-10.875-SmaI-F	AGAAAGGTTATGGAAAATGCAGT**CC**C
Sha-10.875-SmaI-R	GGTGCATAACTCTGGCAGG
Sha-12.0-EcoRI-F	CTGTGGATCACTGGATCACTTT**G**AA**T**
Sha-12.0-EcoRI-R	CATCACTAGAATAGAAATTAGAGCCC
Sha-12.3-HindIII-F	ACGTCTTCAGAATCGCGAA**G**C**T**
Sha-12.3-HindIII-R	AATTGACGGAACTAGCCAGAC
Sha-10.45-HindIII-F	GACCCTTCTGAGGCGGCCAA**AG**CT
Sha-10.45-HindIII-R	AGTTGAGACCATCAGTCACTGG
Sha-10.5-XbaI-F	CCTAAATGATTATCAAAAACGAAAT**C**T**A**
Sha-10.5-XbaI-R	ACCACTCTTGTTTTGTATCCCAT
Sha-10.53-BglII-F	TCCAGATTGCATAACCAGGAGGT**A**G**A**
Sha-10.53-BglII-R	GAATGAAGTAAGAGTCATAAGAGGGG
Sha-10.4827-HindIII-F	CTTCTTGAAGGAAAGAGTGTGATAA**GC**
Sha-10.4827-HindIII-R	ATCTGAACCGAACCAGACCGTTT
Sha-10.4881-BglII-F	TAGTGTCTCGAAAAGAGAACTTAAG**AT**C
Sha-10.4881-BglII-R	AGGAATGGTCGGCATATCTGTT
Sha-10.8-EcoRI-F	AATGGAAAAGGAACTGACTCGA**AT**
Sha-10.8-EcoRI-R	TTTCTGAAAAAATTAAACATGTTTC
Sha-10.69 SmaI-F	ATTAGGCGAAGTGAGTAAGGTT**C**C**C**GG
Sha-10.69 SmaI-R	CCACATATATAGGTTTGTGTATTTTG
Sha-10.70 XbaI-F	ACATCTTTAATAGCATCCTTTAGC**T**CT**A**G
Sha-10.70 XbaI-R	CAAAGAGGCATAAGAAAGATATGT
Sha-10.71 XbaI-F	gttTTCACCAAAGTATCTCTTCC**T**C**T**
Sha-10.71 XbaI-R	CATGGTTAGTAGAGCACGTGA
Sha-10.72 SmaI-F	CCTATCAACTGGTTTGACAGATCT**CC**
Sha-10.72 SmaI-R	GACCAAACCAATGTATATTGTCAG
Sha-10.73 XbaI-R	AATCTAGTTATCGCTTAGGTGCTC**T**CTA**G**
Sha-10.73 XbaI-F	ATCGACCAGGTTAGCATCCA
Sha-10.681 EcoRI-F	AATATCAACAGAATTGAATCAGA**A**T**T**
Sha-10.681 EcoRI-R	GGAATGGAATCTGAATGTTTGA
Sha-10.71 SalI-F	TTCACCAAAGTATCTCTTCCC**GT**
Sha-10.71 SalI-R	TGATATGCACATGGTTAGTAGAG
Sha-10.74 XbaI-F	gtttAGTTATCTTGAGGTTTAAGAAGTT**C**T**A**
Sha-10.74 XbaI-R	ATCAATAGAAATTGTGTTGCCA
Sha-10.76 XbaI-F	GATTCGTCTCTTTTCAGCTTCT**AG**
Sha-10.76 XbaI-R	CTATATGTTCTTTGAGCAGCTAAAG

SPL transcript template Amplification	
	TAATACGACTCACTATAGGGcaaCCACAAAATAAACCGG
T7-SPL3-R	ttttttttttttttttttttttGGCTTGAAATAAC
T7-SPL5-F	TAATACGACTCACTATAGGGatgGAGGGTCAGAGAACACA
T7-SPL5-R	ttttttttttttttttttttGTAAAAAACACATTAC
T7-SPL6-F	TAATACGACTCACTATAGGGatgGATTCTTGGAGCTACG
T7-SPL6-R	ttttttttttttttttttttAGGCATAGATATC
T7-SPL9-F	TAATACGACTCACTATAGGGatgGAGATGGGTTCCAACT
T7-SPL9-R	ttttttttttttttttttttAATCTGATCTCA
T7-SPL13-F	TAATACGACTCACTATAGGGATGGACTGGAATTTCAAACTTAGC
T7-SPL13-R	ttttttttttttttttttttCAAAAAGAGGTTTC
T7-SPL15-F	TAATACGACTCACTATAGGGatgGAGTTGTTAATGTGTTCGG
T7-SPL15-R	ttttttttttttttttttttGAAAAAAACATCC

Cloning

MIM156-F	CACCAAGAAAAATGGCCATCCCCTAGC
MIM156-R	GAGGAATTCACTATAAAGAGAATCG
CRISPR-156AC-1	GATTGAGAAGAGAGTGAGCACACAA
CRISPR-156AC-2	aaacTTGTGTGCTCACTCTCTTCTc
156B Oligo-1	GATTGAGAAGAGAGTGAGCACATGC
156B Oligo-2	aaacGCATGTGCTCACTCTCTTCTc
miR156 Oligo-1	GATTGCAGAAGAGAGTGAGCACACA
miR156 Oligo-2	aaacTGTGTGCTCACTCTCTTCTGc
miR157CD Oligo-1	gattgACAGAAGATAGAGAGCACTA
miR157CD Oligo-2	aaacTAGTGCTCTCTATCTTCTGTc
Val1 amiR Oligo F1	TGTATGACTATAGTCCTCTTTCCATATGATGATCACATTCGTTAT CTATTTTTTATGGAAAGAGTACTATAGTCA
Val1 amiR Oligo R1	AATGTGACTATAGTACTCTTTCCATAAAAAATAGATAACGAATG TGATCATCATATGGAAAGAGGACTATAGTCA
Val1 amiR Oligo F2	TGTATACCGCGGAAGCAAGTGGCCAATGATGATCACATTCGTT ATCTATTTTTTTGGCCACTTGATTCCGCGGTA
Val1 amiR Oligo R2	AATGTACCGCGGAATCAAGTGGCCAAAAAAATAGATAACGAAT GTGATCATCATTGGCCACTTGCTTCCGCGGTA
Val2 amiR Oligo F1	TGTATTTCCGCTCGGTGGTTGGCTCATGATGATCACATTCGTTA TCTATTTTTTGAGCCAACCAACGAGCGGAAA
Val2 amiR Oligo R1	AATGTTTCCGCTCGTTGGTTGGCTCAAAAAATAGATAACGAATG TGATCATCATGAGCCAACCACCGAGCGGAAA

BIBLIOGRAPHY

Achard, P., Herr, A., Baulcombe, D. C., & Harberd, N. P. (2004). Modulation of floral development by a gibberellin-regulated microRNA. *Development, 131*(14), 3357-3365. doi:10.1242/dev.01206

Addo-Quaye, C., Eshoo, T. W., Bartel, D. P., & Axtell, M. J. (2008). Endogenous siRNA and miRNA Targets Identified by Sequencing of the *Arabidopsis* Degradome. *Current Biology, 18*(10), 758-762. doi:http://dx.doi.org/10.1016/j.cub.2008.04.042

Aichinger, E., Villar, C. B., Farrona, S., Reyes, J. C., Hennig, L., & Kohler, C. (2009). CHD3 proteins and polycomb group proteins antagonistically determine cell identity in *Arabidopsis*. *PLoS Genet, 5*(8), e1000605. doi:10.1371/journal.pgen.1000605

Al-Shehbaz, I. A., & O'Kane, S. L. (2002). Taxonomy and Phylogeny of *Arabidopsis* (Brassicaceae). *The Arabidopsis Book / American Society of Plant Biologists, 1*, e0001. doi:10.1199/tab.0001

Aukerman, M. J., & Sakai, H. (2003). Regulation of Flowering Time and Floral Organ Identity by a MicroRNA and Its APETALA2-Like Target Genes. *The Plant Cell, 15*(11), 2730-2741. doi:10.1105/tpc.016238

Axtell, M. J., & Bowman, J. L. (2008). Evolution of plant microRNAs and their targets. *Trends Plant Sci, 13*(7), 343-349. doi:10.1016/j.tplants.2008.03.009

Axtell, M. J., Snyder, J. A., & Bartel, D. P. (2007). Common Functions for Diverse Small RNAs of Land Plants. *The Plant Cell, 19*(6), 1750-1769. doi:10.1105/tpc.107.051706

Bartrina, I., Jensen, H., Novák, O., Strnad, M., Werner, T., & Schmülling, T. (2017). Gain-of-Function Mutants of the Cytokinin Receptors AHK2 and AHK3 Regulate Plant Organ Size,

Flowering Time and Plant Longevity. *Plant Physiology, 173*(3), 1783-1797. doi:10.1104/pp.16.01903

Berardini, T. Z., Bollman, K., Sun, H., & Poethig, R. S. (2001). Regulation of vegetative phase change in *Arabidopsis* thaliana by cyclophilin 40. *Science, 291*(5512), 2405-2407. doi:10.1126/science.1057144

Bollman, K. M., Aukerman, M. J., Park, M. Y., Hunter, C., Berardini, T. Z., & Poethig, R. S. (2003). HASTY, the *Arabidopsis* ortholog of exportin 5/MSN5, regulates phase change and morphogenesis. *Development, 130*(8), 1493-1504.

Brand, L., Hörler, M., Nüesch, E., Vassalli, S., Barrell, P., Yang, W., . . . Curtis, M. D. (2006). A Versatile and Reliable Two-Component System for Tissue-Specific Gene Induction in *Arabidopsis*. *Plant Physiology, 141*(4), 1194-1204. doi:10.1104/pp.106.081299

Bratzel, F., López-Torrejón, G., Koch, M., Del Pozo, J. C., & Calonje, M. (2010). Keeping Cell Identity in *Arabidopsis* Requires PRC1 RING-Finger Homologs that Catalyze H2A Monoubiquitination. *Current Biology, 20*(20), 1853-1859. doi:https://doi.org/10.1016/j.cub.2010.09.046

Cao, J., Schneeberger, K., Ossowski, S., Gunther, T., Bender, S., Fitz, J., . . . Weigel, D. (2011). Whole-genome sequencing of multiple *Arabidopsis* thaliana populations. *Nat Genet, 43*(10), 956-963. doi:http://www.nature.com/ng/journal/v43/n10/abs/ng.911.html#supplementary-information

Carbonell, A., Takeda, A., Fahlgren, N., Johnson, S. C., Cuperus, J. T., & Carrington, J. C. (2014). New Generation of Artificial MicroRNA and Synthetic Trans-Acting Small Interfering RNA

Vectors for Efficient Gene Silencing in *Arabidopsis*. *Plant Physiology, 165*(1), 15-29. doi:10.1104/pp.113.234989

Chen, X. (2004). A MicroRNA as a Translational Repressor of APETALA2 in *Arabidopsis* Flower Development. *Science, 303*(5666), 2022-2025. doi:10.1126/science.1088060

Chuck, G., Cigan, A. M., Saeteurn, K., & Hake, S. (2007). The heterochronic maize mutant Corngrass1 results from overexpression of a tandem microRNA. *Nat Genet, 39*(4), 544-549. doi:10.1038/ng2001

Clark, K. A., & Krysan, P. J. (2010). Chromosomal translocations are a common phenomenon in *Arabidopsis* thaliana T-DNA insertion lines. *The Plant journal : for cell and molecular biology, 64*(6), 990-1001. doi:10.1111/j.1365-313X.2010.04386.x

Clarke, J. H., Tack, D., Findlay, K., Van Montagu, M., & Van Lijsebettens, M. (1999). The SERRATE locus controls the formation of the early juvenile leaves and phase length in *Arabidopsis*. *The Plant Journal, 20*(4), 493-501. doi:10.1046/j.1365-313x.1999.00623.x

Cong, L., Ran, F. A., Cox, D., Lin, S., Barretto, R., Habib, N., . . . Zhang, F. (2013). Multiplex Genome Engineering Using CRISPR/Cas Systems. *Science (New York, N.Y.), 339*(6121), 819-823. doi:10.1126/science.1231143

Cui, L. G., Shan, J. X., Shi, M., Gao, J. P., & Lin, H. X. (2014). The miR156-SPL9-DFR pathway coordinates the relationship between development and abiotic stress tolerance in plants. *Plant J, 80*(6), 1108-1117. doi:10.1111/tpj.12712

Evans, M. M., Passas, H. J., & Poethig, R. S. (1994). Heterochronic effects of glossy15 mutations on epidermal cell identity in maize. *Development, 120*(7), 1971-1981.

Franco-Zorrilla, J. M., Valli, A., Todesco, M., Mateos, I., Puga, M. I., Rubio-Somoza, I., . . . Paz-Ares, J. (2007). Target mimicry provides a new mechanism for regulation of microRNA activity. *Nat Genet, 39*(8), 1033-1037. doi:10.1038/ng2079

Fu, C., Sunkar, R., Zhou, C., Shen, H., Zhang, J. Y., Matts, J., . . . Wang, Z. Y. (2012). Overexpression of miR156 in switchgrass (Panicum virgatum L.) results in various morphological alterations and leads to improved biomass production. *Plant Biotechnol J, 10*(4), 443-452. doi:10.1111/j.1467-7652.2011.00677.x

Gandikota, M., Birkenbihl, R. P., Hohmann, S., Cardon, G. H., Saedler, H., & Huijser, P. (2007). The miRNA156/157 recognition element in the 3' UTR of the *Arabidopsis* SBP box gene SPL3 prevents early flowering by translational inhibition in seedlings. *Plant J, 49*(4), 683-693. doi:10.1111/j.1365-313X.2006.02983.x

Gregory, B. D., O'Malley, R. C., Lister, R., Urich, M. A., Tonti-Filippini, J., Chen, H., . . . Ecker, J. R. (2008). A link between RNA metabolism and silencing affecting *Arabidopsis* development. *Dev Cell, 14*(6), 854-866. doi:10.1016/j.devcel.2008.04.005

Grigg, S. P., Canales, C., Hay, A., & Tsiantis, M. (2005). SERRATE coordinates shoot meristem function and leaf axial patterning in *Arabidopsis*. *Nature, 437*(7061), 1022-1026. doi:10.1038/nature04052

Hildebrand, F. (1875). Ueber die Jungendzustände solcher Pflanzen, welche im Alter vom vegetativen Charakter ihrer Verwandten abweichen. *Flora, 21*, 321-330.

Hoppmann, V., Thorstensen, T., Kristiansen, P. E., Veiseth, S. V., Rahman, M. A., Finne, K., . . . Aasland, R. (2011). The CW domain, a new histone recognition module in chromatin proteins. *EMBO J, 30*(10), 1939-1952. doi:10.1038/emboj.2011.108

Hsieh, L.-C., Lin, S.-I., Shih, A. C.-C., Chen, J.-W., Lin, W.-Y., Tseng, C.-Y., . . . Chiou, T.-J. (2009). Uncovering Small RNA-Mediated Responses to Phosphate Deficiency in *Arabidopsis* by Deep Sequencing. *Plant Physiology, 151*(4), 2120-2132. doi:10.1104/pp.109.147280

Huijser, P., & Schmid, M. (2011). The control of developmental phase transitions in plants. *Development, 138*(19), 4117-4129. doi:10.1242/dev.063511

Hyun, Y., Richter, R., Vincent, C., Martinez-Gallegos, R., Porri, A., & Coupland, G. (2016). Multi-layered Regulation of SPL15 and Cooperation with SOC1 Integrate Endogenous Flowering Pathways at the *Arabidopsis* Shoot Meristem. *Developmental Cell, 37*(3), 254-266. doi:http://dx.doi.org/10.1016/j.devcel.2016.04.001

Iki, T., Yoshikawa, M., Meshi, T., & Ishikawa, M. (2012). Cyclophilin 40 facilitates HSP90-mediated RISC assembly in plants. *The EMBO Journal, 31*(2), 267-278. doi:10.1038/emboj.2011.395

Irish, E. E., & Karlen, S. (1998). Restoration of Juvenility in Maize Shoots by Meristem Culture. *International Journal of Plant Sciences, 159*(5), 695-701. doi:doi:10.1086/297587

Iwakawa, H.-o., & Tomari, Y. Molecular Insights into microRNA-Mediated Translational Repression in Plants. *Molecular Cell, 52*(4), 591-601. doi:10.1016/j.molcel.2013.10.033

James, G. V., Patel, V., Nordström, K. J., Klasen, J. R., Salomé, P. A., Weigel, D., & Schneeberger, K. (2013). User guide for mapping-by-sequencing in *Arabidopsis*. *Genome Biology, 14*(6), R61. doi:10.1186/gb-2013-14-6-r61

Johanson, U., West, J., Lister, C., Michaels, S., Amasino, R., & Dean, C. (2000). Molecular Analysis of FRIGIDA, a Major Determinant of Natural Variation in *Arabidopsis* Flowering Time. *Science, 290*(5490), 344-347. doi:10.1126/science.290.5490.344

Jones-Rhoades, M. W., Bartel, D. P., & Bartel, B. (2006). MicroRNAS and their regulatory roles in plants. *Annu Rev Plant Biol, 57*, 19-53. doi:10.1146/annurev.arplant.57.032905.105218

Jung, J. H., Seo, P. J., Kang, S. K., & Park, C. M. (2011). miR172 signals are incorporated into the miR156 signaling pathway at the SPL3/4/5 genes in *Arabidopsis* developmental transitions. *Plant Mol Biol, 76*, 35-45. doi:10.1007/s11103-011-9759-z

Kim, S. Y., Lee, J., Eshed-Williams, L., Zilberman, D., & Sung, Z. R. (2012). EMF1 and PRC2 cooperate to repress key regulators of *Arabidopsis* development. *PLoS Genet, 8*(3), e1002512. doi:10.1371/journal.pgen.1002512

Kurihara, Y., Takashi, Y., & Watanabe, Y. (2006). The interaction between DCL1 and HYL1 is important for efficient and precise processing of pri-miRNA in plant microRNA biogenesis. *RNA, 12*(2), 206-212. doi:10.1261/rna.2146906

Lauter, N., Kampani, A., Carlson, S., Goebel, M., & Moose, S. P. (2005). microRNA172 down-regulates glossy15 to promote vegetative phase change in maize. *Proc Natl Acad Sci U S A, 102*(26), 9412-9417. doi:10.1073/pnas.0503927102

Lee, R. C., Feinbaum, R. L., & Ambros, V. (1993). The C. elegans heterochronic gene lin-4 encodes small RNAs with antisense complementarity to lin-14. *Cell, 75*(5), 843-854.

Li, J., Reichel, M., & Millar, A. A. (2014). Determinants beyond both complementarity and cleavage govern microR159 efficacy in *Arabidopsis*. *PLoS Genet, 10*(3), e1004232. doi:10.1371/journal.pgen.1004232

Li, S., Liu, L., Zhuang, X., Yu, Y., Liu, X., Cui, X., . . . Chen, X. (2013). microRNAs inhibit the translation of target mRNAs on the endoplasmic reticulum in *Arabidopsis*. *Cell, 153*(3), 562-574. doi:10.1016/j.cell.2013.04.005

Liu, M.-J., Wu, S.-H., Wu, J.-F., Lin, W.-D., Wu, Y.-C., Tsai, T.-Y., . . . Wu, S.-H. (2013). Translational Landscape of Photomorphogenic *Arabidopsis*. *The Plant Cell, 25*(10), 3699-3710. doi:10.1105/tpc.113.114769

Mao, Y., Zhang, H., Xu, N., Zhang, B., Gou, F., & Zhu, J.-K. (2013). Application of the CRISPR–Cas System for Efficient Genome Engineering in Plants. *Molecular Plant, 6*(6), 2008-2011. doi:10.1093/mp/sst121

Mao, Y., Zhang, Z., Feng, Z., Wei, P., Zhang, H., Botella, J. R., & Zhu, J. K. (2016). Development of germ-line-specific CRISPR-Cas9 systems to improve the production of heritable gene modifications in *Arabidopsis*. *Plant Biotechnol J, 14*(2), 519-532. doi:10.1111/pbi.12468

Mason, M. G., Mathews, D. E., Argyros, D. A., Maxwell, B. B., Kieber, J. J., Alonso, J. M., . . . Schaller, G. E. (2005). Multiple Type-B Response Regulators Mediate Cytokinin Signal Transduction in *Arabidopsis*. *The Plant Cell, 17*(11), 3007-3018. doi:10.1105/tpc.105.035451

Merini, W., & Calonje, M. (2015). PRC1 is taking the lead in PcG repression. *Plant J, 83*(1), 110-120. doi:10.1111/tpj.12818

Mi, S., Cai, T., Hu, Y., Chen, Y., Hodges, E., Ni, F., . . . Qi, Y. (2008). Sorting of small RNAs into *Arabidopsis* argonaute complexes is directed by the 5' terminal nucleotide. *Cell, 133*(1), 116-127. doi:10.1016/j.cell.2008.02.034

Mi, S., Cai, T., Hu, Y., Chen, Y., Hodges, E., Ni, F., . . . Qi, Y. (2008). Sorting of Small RNAs into *Arabidopsis* Argonaute Complexes Is Directed by the 5′ Terminal Nucleotide. *Cell, 133*(1), 116-127. doi:http://dx.doi.org/10.1016/j.cell.2008.02.034

Moose, S. P., & Sisco, P. H. (1994). Glossy15 Controls the Epidermal Juvenile-to-Adult Phase Transition in Maize. *The Plant Cell, 6*(10), 1343-1355. doi:10.1105/tpc.6.10.1343

Morel, J.-B., Godon, C., Mourrain, P., Béclin, C., Boutet, S., Feuerbach, F., . . . Vaucheret, H. (2002). Fertile Hypomorphic ARGONAUTE (ago1) Mutants Impaired in Post-Transcriptional Gene Silencing and Virus Resistance. *The Plant Cell, 14*(3), 629-639. doi:10.1105/tpc.010358

Mullokandov, G., Baccarini, A., Ruzo, A., Jayaprakash, A. D., Tung, N., Israelow, B., . . . Brown, B. D. (2012). High-throughput assessment of microRNA activity and function using microRNA sensor and decoy libraries. *Nature methods, 9*(8), 840-846. doi:10.1038/nmeth.2078

Orkwiszewski, J. A., & Poethig, R. S. (2000). Phase identity of the maize leaf is determined after leaf initiation. *Proc Natl Acad Sci U S A, 97*(19), 10631-10636. doi:10.1073/pnas.180301597

Park, M. Y., Wu, G., Gonzalez-Sulser, A., Vaucheret, H., & Poethig, R. S. (2005). Nuclear processing and export of microRNAs in *Arabidopsis*. *Proc Natl Acad Sci U S A, 102*(10), 3691-3696. doi:10.1073/pnas.0405570102

Park, W., Li, J., Song, R., Messing, J., & Chen, X. (2002). CARPEL FACTORY, a Dicer Homolog, and HEN1, a Novel Protein, Act in microRNA Metabolism in *Arabidopsis* thaliana. *Current Biology, 12*(17), 1484-1495. doi:http://dx.doi.org/10.1016/S0960-9822(02)01017-5

Pasquinelli, A. E., & Ruvkun, G. (2002). Control of developmental timing by micrornas and their targets. *Annu Rev Cell Dev Biol, 18*, 495-513. doi:10.1146/annurev.cellbio.18.012502.105832

Peragine, A., Yoshikawa, M., Wu, G., Albrecht, H. L., & Poethig, R. S. (2004). SGS3 and SGS2/SDE1/RDR6 are required for juvenile development and the production of trans-acting siRNAs in *Arabidopsis*. *Genes Dev, 18*(19), 2368-2379. doi:10.1101/gad.1231804

Poethig, R. S. (1988). Heterochronic mutations affecting shoot development in maize. *Genetics, 119*(4), 959-973.

Poethig, R. S. (1990). Phase change and the regulation of shoot morphogenesis in plants. *Science, 250*(4983), 923-930. doi:10.1126/science.250.4983.923

Poethig, R. S. (2013). Vegetative phase change and shoot maturation in plants. *Curr Top Dev Biol, 105*, 125-152. doi:10.1016/B978-0-12-396968-2.00005-1

Reinhart, B. J., Slack, F. J., Basson, M., Pasquinelli, A. E., Bettinger, J. C., Rougvie, A. E., . . . Ruvkun, G. (2000). The 21-nucleotide let-7 RNA regulates developmental timing in Caenorhabditis elegans. *Nature, 403*(6772), 901-906. doi:10.1038/35002607

Reinhart, B. J., Weinstein, E. G., Rhoades, M. W., Bartel, B., & Bartel, D. P. (2002). MicroRNAs in plants. *Genes Dev, 16*(13), 1616-1626. doi:10.1101/gad.1004402

Reis, R. S., Hart-Smith, G., Eamens, A. L., Wilkins, M. R., & Waterhouse, P. M. (2015). Gene regulation by translational inhibition is determined by Dicer partnering proteins. *Nat Plants, 1*, 14027. doi:10.1038/nplants.2014.27

Rhoades, M. W., Reinhart, B. J., Lim, L. P., Burge, C. B., Bartel, B., & Bartel, D. P. (2002). Prediction of plant microRNA targets. *Cell, 110*(4), 513-520.

Riese, M., Hohmann, S., Saedler, H., Munster, T., & Huijser, P. (2007). Comparative analysis of the SBP-box gene families in P. patens and seed plants. *Gene, 401*(1-2), 28-37. doi:10.1016/j.gene.2007.06.018

Rogers, K., & Chen, X. (2013). Biogenesis, Turnover, and Mode of Action of Plant MicroRNAs. *The Plant Cell, 25*(7), 2383-2399. doi:10.1105/tpc.113.113159

Sanchez, R., & Zhou, M. M. (2011). The PHD finger: a versatile epigenome reader. *Trends Biochem Sci, 36*(7), 364-372. doi:10.1016/j.tibs.2011.03.005

Schwab, R., Palatnik, J. F., Riester, M., Schommer, C., Schmid, M., & Weigel, D. (2005). Specific effects of microRNAs on the plant transcriptome. *Dev Cell, 8*(4), 517-527. doi:10.1016/j.devcel.2005.01.018

Shikata, M., Yamaguchi, H., Sasaki, K., & Ohtsubo, N. (2012). Overexpression of *Arabidopsis* miR157b induces bushy architecture and delayed phase transition in Torenia fournieri. *Planta, 236*(4), 1027-1035. doi:10.1007/s00425-012-1649-3

Smith, M. R., Willmann, M. R., Wu, G., Berardini, T. Z., Moller, B., Weijers, D., & Poethig, R. S. (2009). Cyclophilin 40 is required for microRNA activity in *Arabidopsis*. *Proc Natl Acad Sci U S A, 106*(13), 5424-5429. doi:10.1073/pnas.0812729106

Stief, A., Altmann, S., Hoffmann, K., Pant, B. D., Scheible, W.-R., & Bäurle, I. (2014). *Arabidopsis* miR156 Regulates Tolerance to Recurring Environmental Stress through SPL Transcription Factors. *The Plant Cell, 26*(4), 1792-1807. doi:10.1105/tpc.114.123851

Sung, S., & Amasino, R. M. (2004). Vernalization in *Arabidopsis* thaliana is mediated by the PHD finger protein VIN3. *Nature, 427*(6970), 159-164.

Sung, S., He, Y., Eshoo, T. W., Tamada, Y., Johnson, L., Nakahigashi, K., . . . Amasino, R. M. (2006). Epigenetic maintenance of the vernalized state in *Arabidopsis* thaliana requires LIKE HETEROCHROMATIN PROTEIN 1. *Nat Genet, 38*(6), 706-710. doi:http://www.nature.com/ng/journal/v38/n6/suppinfo/ng1795_S1.html

Suzuki, M., Wang, H. H., & McCarty, D. R. (2007). Repression of the LEAFY COTYLEDON 1/B3 regulatory network in plant embryo development by VP1/ABSCISIC ACID INSENSITIVE 3-LIKE B3 genes. *Plant Physiol, 143*(2), 902-911. doi:10.1104/pp.106.092320

Suzuki, M., Wang, H. H. Y., & McCarty, D. R. (2007). Repression of the LEAFY COTYLEDON 1/B3 Regulatory Network in Plant Embryo Development by VP1/ABSCISIC ACID INSENSITIVE 3-LIKE B3 Genes. *Plant Physiology, 143*(2), 902-911. doi:10.1104/pp.106.092320

Tang, G., Reinhart, B. J., Bartel, D. P., & Zamore, P. D. (2003). A biochemical framework for RNA silencing in plants. *Genes & Development, 17*(1), 49-63. doi:10.1101/gad.1048103

Telfer, A., Bollman, K. M., & Poethig, R. S. (1997). Phase change and the regulation of trichome distribution in *Arabidopsis* thaliana. *Development, 124*(3), 645-654.

Telfer, A., & Poethig, R. S. (1998). HASTY: a gene that regulates the timing of shoot maturation in *Arabidopsis* thaliana. *Development, 125*(10), 1889-1898.

Usami, T., Horiguchi, G., Yano, S., & Tsukaya, H. (2009). The more and smaller cells mutants of *Arabidopsis* thaliana identify novel roles for SQUAMOSA PROMOTER BINDING PROTEIN-LIKE genes in the control of heteroblasty. *Development, 136*(6), 955-964. doi:10.1242/dev.028613

Vazquez, F., Gasciolli, V., Crete, P., & Vaucheret, H. (2004). The nuclear dsRNA binding protein HYL1 is required for microRNA accumulation and plant development, but not posttranscriptional transgene silencing. *Curr Biol, 14*(4), 346-351. doi:10.1016/j.cub.2004.01.035

Wang, J. W., Czech, B., & Weigel, D. (2009). miR156-regulated SPL transcription factors define an endogenous flowering pathway in *Arabidopsis* thaliana. *Cell, 138*(4), 738-749. doi:10.1016/j.cell.2009.06.014

Wang, J. W., Park, M. Y., Wang, L. J., Koo, Y., Chen, X. Y., Weigel, D., & Poethig, R. S. (2011). miRNA control of vegetative phase change in trees. *PLoS Genet, 7*(2), e1002012. doi:10.1371/journal.pgen.1002012

Whaley, W. G., & Leech, J. H. (1950). The Developmental Morphology of the Mutant "Corn Grass". *Bulletin of the Torrey Botanical Club, 77*(4), 274-286. doi:10.2307/2481899

Wightman, B., Ha, I., & Ruvkun, G. (1993). Posttranscriptional regulation of the heterochronic gene lin-14 by lin-4 mediates temporal pattern formation in C. elegans. *Cell, 75*(5), 855-862.

Willmann, M. R., & Poethig, R. S. (2011). The effect of the floral repressor FLC on the timing and progression of vegetative phase change in *Arabidopsis*. *Development, 138*(4), 677-685. doi:10.1242/dev.057448

Wu, G., Park, M. Y., Conway, S. R., Wang, J. W., Weigel, D., & Poethig, R. S. (2009). The sequential action of miR156 and miR172 regulates developmental timing in *Arabidopsis*. *Cell, 138*(4), 750-759. doi:10.1016/j.cell.2009.06.031

Wu, G., & Poethig, R. S. (2006). Temporal regulation of shoot development in *Arabidopsis* thaliana by miR156 and its target SPL3. *Development, 133*(18), 3539-3547. doi:10.1242/dev.02521

Wu, G., Rossidivito, G., Hu, T., Berlyand, Y., & Poethig, R. S. (2015). Traffic lines: new tools for genetic analysis in *Arabidopsis* thaliana. *Genetics, 200*(1), 35-45. doi:10.1534/genetics.114.173435

Xie, K., Wu, C., & Xiong, L. (2006). Genomic Organization, Differential Expression, and Interaction of SQUAMOSA Promoter-Binding-Like Transcription Factors and microRNA156 in Rice. *Plant Physiology, 142*(1), 280-293. doi:10.1104/pp.106.084475

Xie, Z., Allen, E., Fahlgren, N., Calamar, A., Givan, S. A., & Carrington, J. C. (2005). Expression of *Arabidopsis* MIRNA Genes. *Plant Physiology, 138*(4), 2145-2154. doi:10.1104/pp.105.062943

Xie, Z., Johansen, L. K., Gustafson, A. M., Kasschau, K. D., Lellis, A. D., Zilberman, D., . . . Carrington, J. C. (2004). Genetic and Functional Diversification of Small RNA Pathways in Plants. *PLOS Biology, 2*(5), e104. doi:10.1371/journal.pbio.0020104

Xu, M., Hu, T., Smith, M. R., & Poethig, R. S. (2016). Epigenetic Regulation of Vegetative Phase Change in *Arabidopsis*. *Plant Cell, 28*(1), 28-41. doi:10.1105/tpc.15.00854

Xu, M., Hu, T., Zhao, J., Park, M. Y., Earley, K. W., Wu, G., . . . Poethig, R. S. (2016). Developmental Functions of miR156-Regulated SQUAMOSA PROMOTER BINDING PROTEIN-LIKE (SPL) Genes in *Arabidopsis* thaliana. *PLoS Genet, 12*(8), e1006263. doi:10.1371/journal.pgen.1006263

Yamaguchi, A., Wu, M. F., Yang, L., Wu, G., Poethig, R. S., & Wagner, D. (2009). The microRNA-regulated SBP-Box transcription factor SPL3 is a direct upstream activator of LEAFY, FRUITFULL, and APETALA1. *Dev Cell, 17*(2), 268-278. doi:10.1016/j.devcel.2009.06.007

Yang, C., Bratzel, F., Hohmann, N., Koch, M., Turck, F., & Calonje, M. (2013). VAL- and AtBMI1-Mediated H2Aub Initiate the Switch from Embryonic to Postgerminative Growth in *Arabidopsis*. *Current Biology, 23*(14), 1324-1329. doi:http://dx.doi.org/10.1016/j.cub.2013.05.050

Yang, L., Conway, S. R., & Poethig, R. S. (2011). Vegetative phase change is mediated by a leaf-derived signal that represses the transcription of miR156. *Development, 138*(2), 245-249. doi:10.1242/dev.058578

Yang, L., Liu, Z., Lu, F., Dong, A., & Huang, H. (2006). SERRATE is a novel nuclear regulator in primary microRNA processing in *Arabidopsis*. *The Plant Journal, 47*(6), 841-850. doi:10.1111/j.1365-313X.2006.02835.x

Yang, L., Wu, G., & Poethig, R. S. (2012). Mutations in the GW-repeat protein SUO reveal a developmental function for microRNA-mediated translational repression in *Arabidopsis*. *Proc Natl Acad Sci U S A, 109*(1), 315-320. doi:10.1073/pnas.1114673109

Yang, L., Xu, M., Koo, Y., He, J., & Poethig, R. S. (2013). Sugar promotes vegetative phase change in *Arabidopsis* thaliana by repressing the expression of MIR156A and MIR156C. *Elife, 2*, e00260. doi:10.7554/eLife.00260

Yu, B., Yang, Z., Li, J., Minakhina, S., Yang, M., Padgett, R. W., . . . Chen, X. (2005). Methylation as a Crucial Step in Plant microRNA Biogenesis. *Science, 307*(5711), 932-935. doi:10.1126/science.1107130

Yu, S., Cao, L., Zhou, C. M., Zhang, T. Q., Lian, H., Sun, Y., . . . Wang, J. W. (2013). Sugar is an endogenous cue for juvenile-to-adult phase transition in plants. *Elife, 2*, e00269. doi:10.7554/eLife.00269

Yuan, W., Luo, X., Li, Z., Yang, W., Wang, Y., Liu, R., . . . He, Y. (2016). A cis cold memory element and a trans epigenome reader mediate Polycomb silencing of FLC by vernalization in *Arabidopsis*. *Nat Genet, 48*(12), 1527-1534. doi:10.1038/ng.3712

http://www.nature.com/ng/journal/v48/n12/abs/ng.3712.html#supplementary-information

Zhao, J. P., Jiang, X. L., Zhang, B. Y., & Su, X. H. (2012). Involvement of microRNA-mediated gene expression regulation in the pathological development of stem canker disease in Populus trichocarpa. *PLoS One, 7*(9), e44968. doi:10.1371/journal.pone.0044968

Zimmerman, R. H., Hackett, W. P., & Pharis, R. P. (1985). Hormonal Aspects of Phase Change and Precocious Flowering. In R. P. Pharis & D. M. Reid (Eds.), *Hormonal Regulation of Development III: Role of Environmental Factors* (pp. 79-115). Berlin, Heidelberg: Springer Berlin Heidelberg.

Zotz, G., Wilhelm, K., & Becker, A. (2011). Heteroblasty—A Review. *The Botanical Review, 77*(2), 109-151. doi:10.1007/s12229-010-9062-8